

AL AZHAR UNIVERSITY.
FACULTY OF MEDICINE.
RADIOLOGY DEPARTEMENT.

HEPATOBIILIARY IMAGING

ESSAY

Submitted in partial fulfillment of master degree in (Radiology)

By

EL SAID MAHMOUD M. EL KATERY
M.B.,B.Ch

SUPERVISORS

Prof. Dr. **MOSTAFA FADEL SONBOL**
Prof. of radiology.
Faculty of medicine.
AL AZHAR university.

Dr. **HATEM HAFEZ SHERIF**
Ass. Prof. of radiology.
Faculty of medicine.
AL AZHAR university.

Dr. **MOHAMED FAROUK AGAG**
Ass. Prof. of radiology.
Faculty of medicine.
AL AZHAR university.

Acknowledgment

Acknowledgment

First & foremost, my deep Gratefulness & indebtedness to Allah.

I would like to express my appreciation & deep gratitude to Prof. Dr. *Mostafa Fadel Sonbol*, Professor of Radiology, Faculty of medicine, Al-Azhar University, who give me a lot of his great guidance and valuable advice. His continous encouragement and marvelous support have made this work possible. I wish to express to him my unlimited grate-fulness.

I would like to express my deep gratitude to Dr. *Hatem M. Hafez Sherif*, Assistant Professor of Radiology, Faculty of medicine, Al-Azhar university, and also to Dr. *Mohamed Farouk Agag*, Assistant Professor of Radiology, Faculty of medicine, Al-Azhar university, for there valuable advice, sincere help and continuous support throughout this work.

Also, I wish to extend my thanks to all members & staff of Radiology Department, Faculty of Medicine, and Al-Azhar University.

Finally, I'm grateful to every one who extended me a kind hand in my work.

El-Said Mahmoud El-Katery
2002

Contents

	Page
Aim of the work.....	1
Introduction.....	2
Review of the literature:-.....	4
-Embryology of hepatobiliary system. -Anatomy of hepatobiliary system. -Ultrasound examination. -Power Doppler examination. -Spiral CT examination. -MRI examination. -Percutaneous Transhepatic Cholangiography (PTC). -Endoscopic Retrograde Cholangiopancreatography (ERCP). -Biliary Scintigraphy. -Angiography of the liver and gallbladder. -Pathology of hepatic focal disease. -Disorders of the gallbladder.	
Illustrative Cases.....	111
Summary and Conclusion.....	136
References.....	138
Arabic summary.....	

Aim Of The Work

AIM OF THE WORK

The aim of this work is to access different radiological methods for diagnoses of different lesions at hepatobiliary system as:-

1- US

- Real time.
- Intraoperative US of the liver.
- Labaroscopic US of the liver.

2- Power Doppler.

3- CT

- Spiral CT.
- 3D imaging.
- CT arterial portography.
- CT hepatic arteriography.

4- MRI.

5- Percutaneous Transhepatic Colangiography. (PTC)

6- Endoscopic Retrograde Cholangiopancreatography. (ERCP)

7- Biliary scintigraphy.

8- Angiography of the liver and gallbladder.

INTRODUCTION

The revolution in imaging techniques over the past few years has created a bewildering array of choices for clinicians investigating patients with suspected hepatobiliary disease. In particular, advances in ultrasound (US), CT scan, MR imaging and scintigraphy have led to improved detection and characterization of liver lesions such that a definitive diagnosis can often be achieved non-invasively. *(Helena, 1998)*

The radiologists also have been the contributors to as well as recipients of noteworthy interventional techniques such as endoscopic retrograde cholangiopancreatography (ERCP) and, to a less extent, percutaneous transhepatic cholangiography for direct visualization of the ductal system. *(Claire, 1998)*

US are the primary imaging modality for hepatic and biliary system. It is convenient, quick, and inexpensive and therefore continues to play a valuable role in the screening of patients with suspected hepatobiliary disease. Colour Doppler and particularly power Doppler enable the sonographer to assess the vascularity of focal hepatic lesions aiding in the characterization of these lesions. US unquestionably a useful modality for guidance of biopsy and drainage procedures due to its portability and the real-time capabilities and multiplanar views possible with scanning probes. *(Helena, 1998)*

At present, the sensitivity of conventional transabdominal US for the detection of some hepatic lesions is low, only 20% for liver metastasis of gastrointestinal carcinomas less than 1 cm in diameter. US diagnosis can be particularly difficult because of tissue attenuation in patients with cirrhosis. Recently Intermittent Second-Harmonic Gray-Scale US (ISHGS US) may be useful method to increase the sensitivity of US while maintaining its advantages in terms of availability and noninvasiveness. *(Rolf, 2000)*

CT is the first line imaging studies in the radiologic work up of patients with suspected hepatic disease and enables a number of useful distinctions to be made. Shortly before the advent of multislice CT, CT cholangiography is proposed as non-invasive method for study of the biliary ducts. The quality of bile duct system imaging is expected to improve further with implementation of multislice CT. *(Prassopoulos, 1998)*

Contrast enhanced helical CT scans in the portal phase has a sensitivity of 91% for detection of hepatic metastases greater than 1 cm in size. An advantage of CT scan is the ability to image extrahepatic disease, an important prognostic indicator in patients considered for hepatic resection for metastatic large bowel cancer. Inherent disadvantage of CT scan include the radiation burden and use of iodinated contrast medium, but overall CT scan remains an excellent modality in the investigation of hepatic lesions in view of its good contrast resolution and speed of acquisition. *(Helena, 1998)*

Obtaining CT cholangiograms using an oral biliary contrast agent is a feasible, noninvasive, method for revealing biliary anatomy. However, visualization of the biliary tree was suboptimal in 36% of the patient. *(Elaine, 2000)*

Magnetic Resonance Cholangiopancreatography (MRCP) is a noninvasive diagnostic technique that visualizes the anatomy and pathology of biliary ducts. This application of MR, which provides both cross sectional imaging of ductal structures and projectional images of biliary ducts, is based on a heavily T2-weighted sequence. As a result, MRCP show stationary fluid, including bile and pancreatic juice, with high signal intensity. *(Joe, 2001)*

2D single-shot turbo spine-echo MRCP can be performed as a complement to ERCP and can replace ERCP in high-risk patient and in case of unsuccessful cannulation. *(A.Arslan, 2000)*

The gold standard for biliary imaging is direct contrast opacification by either ERCP or Percutaneous Transhepatic Cholangiography (PTC). Although these techniques provide excellent delineation of biliary anatomy and pathology, both are physician intensive and costly. Furthermore because these procedures are invasive, they are associated with risks and complications -PTC has a complication rate of 3.4% whereas ERCP has a complication rate that ranges from 0.5% to 5%. *(Elaine, 2000)*

Several amino-diacetic acid compounds labelled with Tc^{99m} have been used to investigate biliary excretion and the pathway from liver to small intestine. Tribromo methyl HIDA is generally available. It is cleared from the circulation by the hepatic cells and secreted into the bile by carrier mechanisms identical to bilirubin, when liver function is poor there is proportionally increase kidney excretion. HIDA compounds accumulate into the gallbladder and are excreted into the small bowel. Hepatobiliary scintigraphy is also used to assess the hepatic uptake, bile duct patency, cystic duct patency, gallbladder function, gallstones, common bile duct patency and sphincter of oddi dysfunction. *(Peter, 1999)*

EMBRYOLOGY OF HEPATOBILLIARY STSTEM:-

Early in the fourth week of fetal development, the liver, gall bladder, and bile duct system develop from an endodermal outgrowth, or hepatic diverticulum. (*William, et al 1989*)

During the 5th week, the diverticulum differentiates into the origin of the cystic duct and the gall bladder in the caudal portion, and in cephalic portion, two endodermal cellular buds begin forming the right and left lobes. (*Netter, 1964*).

These solid cell buds grow into columns or cylinders that branch and form anastomoses forming a network, and invade the vitelline and the umbilical veins. The capillary like vessels of the plexus eventually differentiate into liver sinusoids. The endothelial cells of the plexus become the Kupffer cells. (*England, 1983*)

The columns of the endodermal cells and the liver parenchyma grow out into the surrounding mesoderm. The mesoderm provides the haemopoietic tissue and the connective tissue for the fibrous liver capsule (Glisson's capsule) and the portal tracts. (*England, 1983*)

As the terminal branches of the right and left lobes canalize the bile system is formed. (*William, et al 1989*)

Both lobes are equal in size until the beginning of the 6th week, at which time right lobe becomes larger, the caudate and quadrate lobes develop from the right lobe, and the left lobe actually undergoes some degeneration. (*William, et al 1989*)

At the 6th week, the liver fills most of the abdominal cavity and the relative development of the liver becomes less active. (*William, et al 1989*)

The yolk sac regresses as the liver enlarges. When the yolk sac disappears, haemopoiesis takes place in the liver at 6th week, peaks at 12-24 weeks, and ceases at birth. (*Guyton, 1986, Tortara, et al 1998*)

Oxygenated blood and nutrients are delivered to the fetus through the umbilical vein. Which ascends and divides into two branches. (*Marieb, 1989, Stephens, et al 1989*)

The left branch joins the portal vein and enters the liver, the right branch, ductus venosus, flows directly into the Inferior Vena Cava (IVC), by passing the liver. (*Graif, et al 1983, Cicio, et al 1983*)

Normally both of these vessels deteriorate into fibrous cords sometimes after birth. (*Abbitt, 1995*)

The left umbilical vein becomes the ligamentum teres, or round ligament and the ductus venosus becomes the ligamentum venosum. In some persons the left umbilical vein persists, and both ligamentum teres and ligamentum venosum become canalized as collateral vessels with certain diseases such as portal hypertension. (*Glazer, et al 1980*)

ANATOMY OF HEPATOBILLIARY SYSTEM:-

Gross Anatomy:

The liver (hepar), the largest gland, lies in the upper right part of the abdominal cavity, occupying most of the right hypochondrium and epigastrium and extending into the left hypochondrium as far as the left lateral line. (*William, et al 1989*)

The normal liver measures 17 to 18 cm in an anterior projection. The shape of the liver is complex, superiorly it is dome shaped conforming to the under of the diaphragm. Inferiorly, the under surface of the liver is concave and slopes downward to a sharp border. Considerable individual variants exist in the normal size and shape. (*Bismuth, 1988*)

In males it weights 1.4 –1.8 Kg, and in females 1.2- 1.4Kg. It is somewhat cuneiform, reddish brownie colour. Despite its weight , it is widely believed that , like various other viscera , its position is not maintained by peritoneal or fibrous attachment , but mainly by intra abdominal pressure due to tonus in the abdominal muscles . The

continuity of the hepatic veins with the inferior vena Cava may provide some support. (*William, et al 1989*)

Borders of the Liver:

Accessible to the superior, anterior and right surfaces are continuous as rounded borders, but a sharp Inferior border separates the right and anterior surfaces, from the inferior surface. This inferior border is rounded between the right and inferior surfaces but becomes thin and angular at the lower limit of the anterior surface and is notched along this edge by ligamentum teres, to the right of the midline. Lateral to the fundus of gall bladder, which often correspond to second notch 4-5 cm to the right of midline. The inferior border largely follows the costal margin ; left to the fundus it ascends less obliquely than the costal margin ; crossing the infrasternal angle to pass behind the left costal margin near the tip of eighth costal cartilage . It then ascends sharply to merge with the thin margin of the left lobe. At the infrasternal angle the inferior border adjoins the anterior abdominal wall and is examination by percussion , but is not usually palpable . In the mid line the inferior border is about one handbreadth below the xiphisternal joint . In women and children the border often projects a little below the right costal margin. (*William, et al 1989*)

Hepatic Lobes:

Lobular division of the liver can be described as:

- ***Anatomic*** based on external landmarks
- ***Segmental*** based on hepatic function

Anatomic Division:

A broad division that uses the falciform ligament to divide the liver into the right and left lobes . Classifies the caudate and quadrate lobes as a part of right lobe. A more accurate approach dividing the liver in to right , left , caudate , quadrate lobes using a simulated H configuration on the visceral surface. (*Kane,1980-1981*)

The Right Lobe:

It is six times larger than the left, (William, et al 1989). Occupies the right hypochondrium and separated from the left lobe by the falciform ligament on the diaphragmatic surface and by the left inter segmental fissure (left saggital fossa) on its visceral surface. It is somewhat quadrilateral. The falciform ligament marks the anterior surface, and the visceral, posterior surfaces are marked by three fossae: the porta, the gallbladder, and the IVC. (Hagen-Ansert S, et al 1995)

The Caudate Lobe:

The caudate lobe, anatomically distinct from the left and right hepatic lobes, it is interposed between the IVC posteriorly, the left hepatic lobe anteriorly and superiorly, the main portal vein inferiorly. (Brown, et al 1982)

The caudate process is small elevation extending obliquely and laterally of the caudate lobe right margin, as tongue like projection, coursing between the IVC and the portal vein and extending to the visceral surface of the right lobe. (Donoso, et al 1989)

The Quadrate Lobe:

It is situated on the visceral surface; it is bounded posteriorly by the porta hepatis; anteriorly by the inferior margin of the liver and laterally by the gall bladder fossa on the right fissure of ligamentum teres on the left.

The Left Lobe:

Lies in the epigastrium and left hypochonderium. Anatomically, it is separated from the right hepatic lobe by the falciform ligament separates it from the quadrate lobe, and the fissure ligamentum venosum separates it from the caudate lobe. The left lobe is flatter and smaller in size than the right lobe but varies in size its superior surface is slightly convex, and molded to the diaphragm, and tapers off to the left about the left mammary line. (Brown, et al 1982)

Segmental Anatomy:

It is based on two of the liver's most important functions, as a gland with bile ducts, and as a vascular and storage organ supplied by blood from portal veins and hepatic arteries. (*William, et al 1989*)

Using the functional and the segmental method , the liver is divided into three lobes and four segments based on blood supply and biliary drainage :

- 1) The right lobe containing anterior and posterior segment.
- 2) The left lobe containing medial and lateral segment.
- 3) The caudate lobe.

So the previously described quadrate lobe is now the medial segment of the left lobe .

The anatomical left lobe is now the left lateral segment .

The caudate is considered as a separate lobe.

The hepatic veins demarcate the anatomic landmarks for the lobes and segments of the liver. The middle hepatic vein delineates the separation between the right and the left lobes. The right lobe is comprised of an anterior and posterior segment with the boundary depicted by the right hepatic vein. The left lobe is comprised of a medial and lateral segment by the left hepatic vein. (*Baron et al, 1992*)

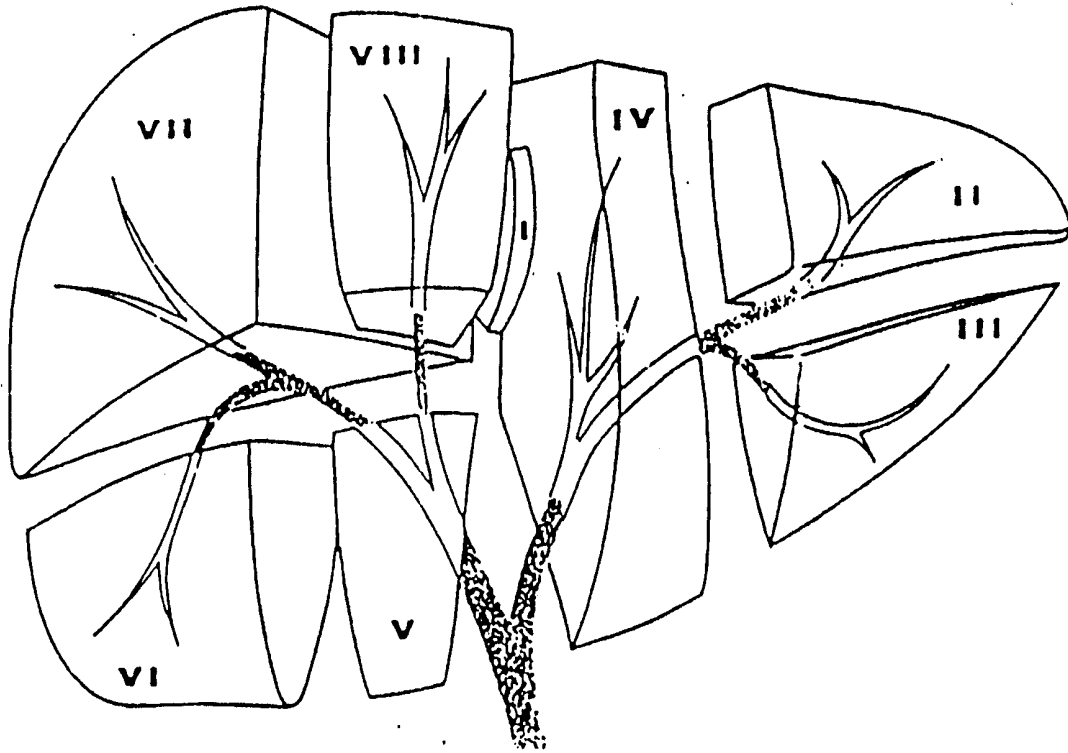
This anatomic classification scheme modified the previously settled one by Couinaud. It uses the planes of the right and left portal branches , the so-called transverse scissura, to divide each segment into superior and inferior sub segments. The Bismuth classification numbers the eight segments based on a clockwise orientation from a frontal projection. (*Bismuth, 1982*)

The following table lists and compares the nomenclature using this more detailed anatomic delineation with traditional anatomy of the liver proposed by. (*Gold smith and Woodbrune, 1957*)

(Gold smith and Woodbrune, 1957)

Gold smith & Woodbrune classification	Couinaud Classification	Bismuth Classification
<u>Caudate lobe</u>	Segment 1	Segment 1
<u>Left lateral segment:</u>		
*superior subsegment	Segment 2	Segment 2
*inferior subsegment	Segment 3	Segment 3
<u>Left medial segment:</u>		
*superior subsegment	Segment 4	Segment 4a
*inferior subsegment		Segment 4b
<u>Right anterior segment</u>		
*inferior subsegment	Segment 5	Segment 5
*superior subsegment	Segment 8	Segment 8
<u>Right posterior segment:</u>		
*inferior subsegment	Segment 6	Segment 6
*superior subsegment	Segment 7	Segment 7

[Table 1] (Quoted from Baron et al, 1992).



(Figer .1): segmental anatomy of the liver according to Couinaud's design

(Quoted from Shamsi et al, 1994)

Gallbladder:

The gallbladder is an elongated pear-shaped organ that is 8 to 10 cm long and 4 to 5 cm wide . When distended it can achieve a volume of 30 to 50 ml. It is attached by its superior aspect to the obliquely situated visceral surface of the liver by loose connective tissue containing blood vessels , lymphatics , and at times some subvesicular bile ducts. The gallbladder lies parallel to and at the inferior margin of the major interlobar fissure of the liver . The inferior ,medial, and lateral aspects of the gallbladder are covered by visceral peritoneum that is continuous with the peritoneum on the inferior surface of the liver.(*Callen ,1979*)

The gallbladder is subdivided into a fundus, body, and neck. The fundus is the blind anteroinferior end of the gallbladder that may extend beyond the inferior margin of the liver to contact the anterior abdominal wall at the tip of the ninth costal cartilage . The inferior aspect of the fundus commonly contacts the right side of the transverse colon. The body is the large intermediate portion of the gallbladder that usually contacts the junction of the first and second parts of the duodenum . The gallbladder neck is the narrowed posterosuperior portion of the gallbladder that approaches the right side of the liver porta and the hepatoduodenal ligament to become continuous with the cystic duct . This is called the infundibulum, or Hartmann's pouch. (*Nahrwold, et al 1991*)

Cystic Duct:

The cystic duct averages 3 cm in length with a range of 0.4 to 6.5 cm. The beginning of the cystic duct is tortuous and forms a cranially directed loop . It contains spirally situated mucosal folds called the valves of Heister. The terminal portion of the cystic duct tends to be smooth walled and pursues a descending course that angles to the right to join the side of the common hepatic duct at an acute angle . The terminal cystic duct may parallel the common hepatic duct for a variable distance before joining and at this point may share a common connective tissue ensheatment with the common hepatic duct . The cystic duct courses within the right border of the upper portion of the hepatoduodenal ligament. (*Moosman, et al 1981*)

Hepatic Ducts:

Most commonly the right and left hepatic ducts join extrahepatically about 0.75 to 1.5 cm caudad to the liver to form the common hepatic duct. Intrahepatically, the longer left hepatic duct develops within the fissure for the ligamentum teres, where it receives medial and lateral segmental branches from its right and left sides. (*Friedman, 1987*)

The shorter right hepatic duct is formed near the liver porta by the junction of its anterior and posterior segmental branches. (*Friedman, 1987*)

The common hepatic duct can be as long as 7.5 cm. As the common hepatic duct descends the hepatoduodenal ligament, it is usually located anterolateral to the portal vein and to the right of the proper hepatic artery. It tends to angle to the left as it descends. (*Gray, et al 1982*)

Common Bile Duct:

The common bile duct varies in length from 5 to 15 cm. By CT the mean diameter of the lumen is 3.6 mm with a range of 3.5 to 10.9 mm. The thickness of the wall of the common bile duct averaged 0.94 mm with a maximal normal thickness of 1.5 mm. (*Schulte et al 1990*)

The common bile duct can be subdivided into four parts: supraduodenal, retroduodenal, infraduodenal or intrapancreatic, and intraduodenal. Like the common hepatic duct the supraduodenal portion of the common bile duct is usually anterolateral to the portal vein within the hepatoduodenal ligament. (*Friedman, 1987*)

Ligaments of the Liver:

The liver is tethered to the undersurface of the diaphragm, the anterior wall of the abdomen, the lesser curvature of the stomach, and the retroperitoneum by seven ligaments, six of which are either parietal or visceral peritoneal folds and of which is a round, fibrous cord. (*Netter 1964*)

These are the coronary, falciform, round (ligamentum teres), right and left triangular (lateral), gastrohepatic, and hepatoduodenal ligaments. An understanding of the liver ligamentous attachments and the caudate lobe

relation anatomy to the lesser sac is important for accurate localization of some lobar demarcations and perihepatic fluid collections. (*Rubenstein, et al 1983*)

1-Coronary ligament:

The coronary ligament connects the posterior liver surface to the diaphragm and consists of anterior and posterior layers, the anterior layer is formed by the reflection of the parietal peritoneum, and the posterior layer is reflected from the caudal margin of the bare area onto the right adrenal gland and right kidney (hepato renal ligament). (*William, et al 1989*)

2-Ligamentum teres:

The ligamentum teres (round ligament) is the fibrous cord resulting from the obliterated left umbilical vein. It ascends from the umbilicus in the free margin of the falciform ligament to the notch in the anterior border of the liver. Here it courses along a fissure on the visceral surface and continuous as the ligamentum venosum, the obliterated ductus venosus, as far back as the IVC. (*Netter, 1964*)

3-Triangular ligament:

The right and left triangular ligaments are so named because of their triangular shape. They are formed by opposition of the upper and lower ends of the coronary ligament and extend from the diaphragm to the liver. (*Netter, 1964*)

The right ligament is attached to the right border at the right extremity of the bare area and passes to the diaphragm. Its anterior layer is continuous with the left layer of the falciform ligament. (*William, et al 1989*)

The left ligament is the larger of the two and attaches to the upper surface of the left lobe, where it lies anterior to the esophageal opening in the diaphragm. (*Netter, 1964*)

4-Gastrohepatic ligament:

It is also known as the lesser omentum, is composed of two folds of visceral peritoneum. It originates on the under surface of the liver, and continuous with the ligamentum venosum and courses caudally to attach to the lesser curvature of the stomach and first portion of the duodenum. Pathologies, such as varices and enlarged lymph nodes are seen in this region. *(Ralls, et al 1987)*

5-Hepatoduodenal ligament:

It surrounds the portal trait (the portal vein, the hepatic artery, and the common bile duct) prior to entering the porta hepatis. It is located in the right free edge of the gastrohepatic ligament forming the anterior boundary of the epiploic foramen (foramen of Winslow), a potential space representing the only communication of the lesser peritoneal sac with the rest of the peritoneal cavity. The IVC and the caudate lobe form the posterior wall of the lesser sac. *(Netter, 1964)*

The size of the caudate process, in part determines the length of the hepatoduodenal ligament and its proximity to the IVC. *(Ralls, et al 1987)*

Blood Supply of the Liver:

Blood supply of the liver delivered through hepatic artery & portal vein.

The hepatic artery:

The common hepatic artery arises as a terminal branch of the celiac trunk and runs a short distance to the right along the superior border of the pancreatic head before giving rise to gastro-duodenal artery. The hepatic artery terminates as right and left branches, which divides into segmental and sub segmental branches, and their distribution is parallel to the bile ducts and the portal vein. It carries the oxygenated blood and accounts approximately for 25% of the hepatic blood flow. *(Taylor, et al 1985)*

The portal vein:

It is upward continuation of the superior mesenteric vein, which changes its name to portal vein after it has received the splenic vein behind the neck of the pancreas. It lies in front of the IVC, passes upward and behind the pancreas and first part of the duodenum then enters between the two layers of the lesser omentum. It runs behind the bile ducts and the hepatic artery to reach the porta hepatic. It divides into right and left branches. It drains the splanchnic circulation and account for 75% of the hepatic blood flow. (Last, 1972)

Venous Drainage of the Liver:

Three main hepatic veins drain into the IVC, high up near the diaphragmatic surface. The venous return differs from the arterial supply that shows a mixing of the right and left halves of the liver. (Last, 1972)

The right hepatic vein:

Separates the right lobe into anterior and posterior segment.

The left hepatic vein:

Separates the left lobe into medial and lateral segments.

The middle hepatic vein:

Separates the right and left lobes. (Mukai et al, 1987)

Lymphatic Drainage of the Liver:

The liver produces a large amount of lymph, about one third to one half of all body lymph. The lymph vessels leave the liver and enter a number of lymph nodes in the porta hepatic, the efferent vessels to the celiac nodes. A small number of vessels pass from the bare area of the liver through the diaphragm to the posterior mediastinal lymph nodes. (Snell, 1986)

Normal hepatic anatomy: anatomic structures useful for identifying the hepatic segments

<i>Structure</i>	<i>Location</i>	<i>Usefulness</i>
RHV	Right intersegmental fissure	Divides cephalic aspect of anterior and posterior segments of right lobe
MHV	Main lobar fissure	Separate right and left lobe
LHV	Left intersegmental fissure	Divides cephalic aspect of medial and lateral segments of left lobe.
RPV(anterior branch)	Intrasegmental in anterior segment of right lobe	Courses centrally in posterior segment of right lobe.
LPV(horizontal segment)	Anterior to caudate lobe	Separates caudate lobe posteriorly from medial segment of left lobe anteriorly.
LPV(ascending segment)	Left intersegmental fissure	Divides medial from lateral segment of left lobe.
GB fossa	Main lobar fissure	Separates right and left lobes.
Fissure for the ligamentum teres	Left intersegmental fissure	Divides caudal aspect of left lobe into medial and lateral segments.
Fissure for the ligamentum venosum	Left anterior margin of the caudate lobe	Separates caudate lobe posteriorly from left lobe anteriorly

[Table 2] RHV indicates right hepatic vein, MHV, middle hepatic vein, LHV, left hepatic vein, RPV, right portal vein, LPV, and left portal vein, GB, gallbladder. Modified from (*Marks et al 1979*)

ULTRASOUND EXAMINATION:-

Types of Ultrasound Display:-

A-mode

In A-mode (amplitude modulation or mode), the most basic form of diagnostic ultrasound, a single beam of ultrasound is analyzed. The distance between the transducer and the structure determines where an echo is seen along the time axis. The time elapsed from the transmission to the return of the signal is converted to distance. An echo (sound wave) is assumed to travel at a constant speed of 1540 m/sec in soft tissue; thus the time it takes for the echo to return to the transducer represents a distance. (*Zagzebski, 1998*)

B-Mode (Brightness Mode)

An A-mode signal can be converted to dots, which vary in brightness depending on the strength of the returning echo. A stronger echo will display a brighter dot than a weaker echo. The depth of the reflector is displayed by the location of the dot. Multiple B-mode images may be displayed together to form a two-dimension B-scan. (*Zagzebski, 1998*)

M-Mode (Motion Mode)

In M-mode, a series of B-mode dots is displayed on a moving time base graphing the motion of mobile structures. M-mode imaging formed the bases of echocardiography prior to real time. M-mode is currently used in conjunction with real-time imaging in adult, pediatric, and fetal echocardiography. (*Zagzebski, 1998*)

B-Scan (Static Scan)

The B-scan –utilize a series of B-mode images to build a two-dimensional view of the tissue. The transducer is attached to an articulated arm, which provides the ultrasound system with information on transducer position and orientation. This type of imaging is not used in modern equipment owing to the numerous disadvantages.

Real-Time, B-scan

Real-time systems provide a cinematic view of the area being evaluated by displaying a rapid series of images sequentially. The following are advantages of real-time scanning

- 1- Scanning plans that best demonstrate the area of interest can be easily found.
- 2- A rapid examination can be performed because there is constant visual feedback on the display screen.
- 3- Extended structures such as vessels can be followed, allowing them to be traced to their origin.
- 4- Movement observation may aid in organ identification
- 5- Infants, children, and uncooperative patients can be examined easily
- 6- Critically ill patients and those with acute conditions can be studied portably
- 7- Pulsed and colour flow Doppler can be performed coincident with the real time examination. (*Sanders et al, 1998*)

Technique of Hepatic Examination:-

Sonography of the liver is ideally performed when the patient has fasted for 8 – 12 hours before the examination, to avoid interference from bowel gas and residue. The examination is performed using 3.5 or 5 MHz sector or curved linear-array transducers. (*Parulekar and Bree, 1998*)

Ultrasonic gel provides an excellent coupling science it can be heavily and used as a cushion between the ribs and transducer face. (*Talmont, 1980*)

In obese patients, it is necessary to use 2.5 MHz transducers for adequate penetration of the right lobe. One can use 5 or 7.5 MHz linear-array transducers to evaluate the surface of the liver. (*Parulekar and Bree, 1998 and Sanders, 1998*)

Scanning View:-

The initial examination is performed with the patient in the supine position, followed by examination in the left posterior oblique position, which is especially useful for evaluation of the deeper posterior portions of the right lobe. Most of the liver is accessible by sub costal scanning. Cranial portions of the liver, especially the sub diaphragmatic portions of the right

lobe, may be difficult to evaluate and better seen by intercostals scanning with sector transducers. Electronic focusing, when available, should be adjusted throughout the examination to optimally evaluate both superficial and deep portions of the liver. (*Parulekar and Bree, 1998 and sanders, 1998*)

The patients were examined in the supine position; the liver was scanned completely in both transverse and longitudinal planes, at 1-cm. increments. The transducer was angled under costal margin, pointing towards the patient's head. In this position, the liver parenchyma was best evaluated. (*Sanders, 1991*)

Longitudinal views should include sections through the midline the lateral left lobe and the inferior vena cava. To scan the midline in a longitudinal view starts in the subxyphoid area. On every longitudinal cut, angle superiorly and inferiorly to see both margins. (*Sanders, 1991 and sanders, 1998*)

Transverse scans starting from the xiphisternum should be carried in the light of the findings on the parasagittal scans. To obtain unimpeded views of liver texture, scan parallel to the right costal margin and angle sharply superior with patients in oblique supine, decubitus or even upright position. The intercostal spaces should also be scanned with varying degrees of inspiration using various intercostal points, in both longitudinal and transverse planes. (*Sanders, 1991 and sanders, 1998*)

Intraoperative US of the Liver

Intraoperative US (IOUS) of the liver is a dynamic and rapidly expanding field, providing vital information to the surgeon at the time of surgery and impacting on clinical management decisions and choices of surgical techniques. (*Kruskal, 1995*)

The technique has found its greatest application in patients with hepatic colorectal metastases undergoing exploratory laparotomy. In these patients, IOUS of the liver is used to identify metastases and has proven to be an important element in surgical decision making and in guiding segmental resection. (*Kane, et al. 1994*)

Technique for Performing Intraoperative liver US:-

It is recommended that IOUS of the liver be performed with transducers designed specifically for this purpose. Small linear array transducers have been developed with higher frequency to improve resolution. These transducers have a wide field of view in the near field with impressive near-field resolution; this is further enhanced by electronic focusing. (Mack, et al. 1991)

We currently use a real-time B-mode electronic scanner system with 5-MHz side-fire T-shaped linear array probe. The probe width is 64 mm with 256 scanning lines. Ethylene oxide gas sterilization is used to sterilize the probe and its supply code, protecting the connecting plug by enclosing it in an impermeable plastic wrap. This obviates the need for a sterile probe sheath covering. The probe is applied directly to the liver surface with acoustic coupling provided by the natural moisture on the liver surface. No gel or other acoustic coupling agents are necessary. (Kane, et al. 1994)

Scanning at a frequency of 5 MHz allows more than adequate penetration of the liver for up to 10 to 12 cm of depth. This is an adequate depth to visualize most livers from the anterior surface, but when incomplete penetration of the entire liver substance occurs, further images are obtained with the probe placed on the posterior surface of the liver as needed. (Scott, et al. 1998)

Application of IOUS of the Liver :-

The most common application of IOUS of the liver is during surgery in patient undergoing segmental resection for colorectal carcinoma metastases. Other application include localization of occult lesions for biopsy, drainage or resection, survey for occult primary or metastatic lesions, definition of lobar and segmental anatomy and vascular supply and drainage, planning and assessment of tumour respectability, evaluation of vessel patency or presence of thrombi, guidance for nonsegmental wedge resection, guidance for cryoablation and other focal tumour ablation techniques, and laparoscopic US. (Scott, et al. 1998)

Laparoscopic US of the Liver

With laparoscopic surgical procedures increasing in frequency, a useful additional application is IOUS performed through the laparoscopy device. Laparoscopic US (LUS) has the advantage of being able to detect small superficial lesions that are frequently missed on preoperative imaging studies. Several transducers have been specifically designed for use during laparoscopy. Laparoscopic Sonography requires that the specially designed US transducer fits through a 10-mm laparoscope port. The transducer, which should be flexible but steerable with precision, should provide as wide a field of view as possible with an optimal frequency of 5 MHz for penetration, or multifrequency of 5-7.5 MHz. *(Roizental M, et al. 1994)*

The probe is inserted via a 10-mm port under direct laparoscopic visualization. The insertion ports must be created away from the liver to allow adequate mobility of the laparoscopic transducer over the liver surface. Indeed, because the falciform ligament prevents passage of the transducer between the medial left and anterior right segments, a second port is usually required on the left side of the abdominal wall to permit adequate visualization of the left lobe. Because a sector scanner is used, overlapping fields must be acquired in the near field to fully evaluate the liver. The transducer has a flexible tip, which must be continuously adjusted and flexed to remain seated on the liver surface being scanned. *(Scott, et al. 1998)*



(Figer .2)

Normal liver parenchyma is homogeneous and moderately echogenic on ultrasound. It is slightly more echogenic than the kidneys and of slightly less or equal echogenicity compared to the pancreas. The spleen is normally of equal echogenicity to the liver. While there are several different anatomic methods of defining liver anatomy, clinically the segmental anatomy of the liver is determined by surgical considerations.

The right lobe of the liver (Figer .2) is divided into anterior and posterior segments by the right hepatic vein (Figer .2, R). The middle hepatic vein (Figer .2, M) runs in the interlobar or major lobar fissure and divides the right and left lobes in the superior portion of the liver. At more caudal levels, the major fissure may be identified as a hyperechoic line due to its fat and collagen content, and by the gallbladder fossa. This fissure is followed as a line between the fossa for the IVC and the gallbladder fossa.

The left lobe of the liver is divided into lateral (Figer .2, LL) and medial (Figer .2, LM), (quadrate) segments by the left hepatic vein (Figer .2, L). The right lobe of the liver is divided into anterior (Figer .2, RA) and posterior (Figer .2, RP) segments by the right hepatic vein (Figer .2, R).

POWER DOPPLER EXAMINATION:-

Power Doppler ultrasound (also known as ultrasound angiography, color power angiography, or color Doppler energy mode, depending on the manufacture) is a new technology that is superior to conventional color Doppler imaging in the detection of blood flow. (*Helenon et al, 1998*)

Power Doppler Sonography is based on the integrated Doppler power spectrum. It is a technique that encodes the amplitude or energy spectrum of the Doppler signal rather than the mean frequency. (*Clautice-Engle et al, 1997*)

The hue and brightness of color signal represent the power in the Doppler signal depend on the amount of red blood cells present, providing an image of a different property of blood flow than that given by color Doppler US .Color Doppler energy mode doesn't display velocity or direction but only the total backscattered energy of the Doppler signal. (*Martinoli et al, 1998*)

To understand power Doppler, it is useful to keep in mind the origin and meaning of the power density spectrum. The spectral Doppler display is a three dimensional graph with time and velocity being the x and y axes, respectively, whereas the gray scale is the z-axis and represents the intensity of the Doppler echo. Taking a single instant in time of the spectral display means that the time axis is eliminated, and only the velocity and echo intensity are left. If these two variables are plotted for this instant in time, the familiar power density spectrum (Diagram .1) Is the result. (*Desser et al, 1998*)

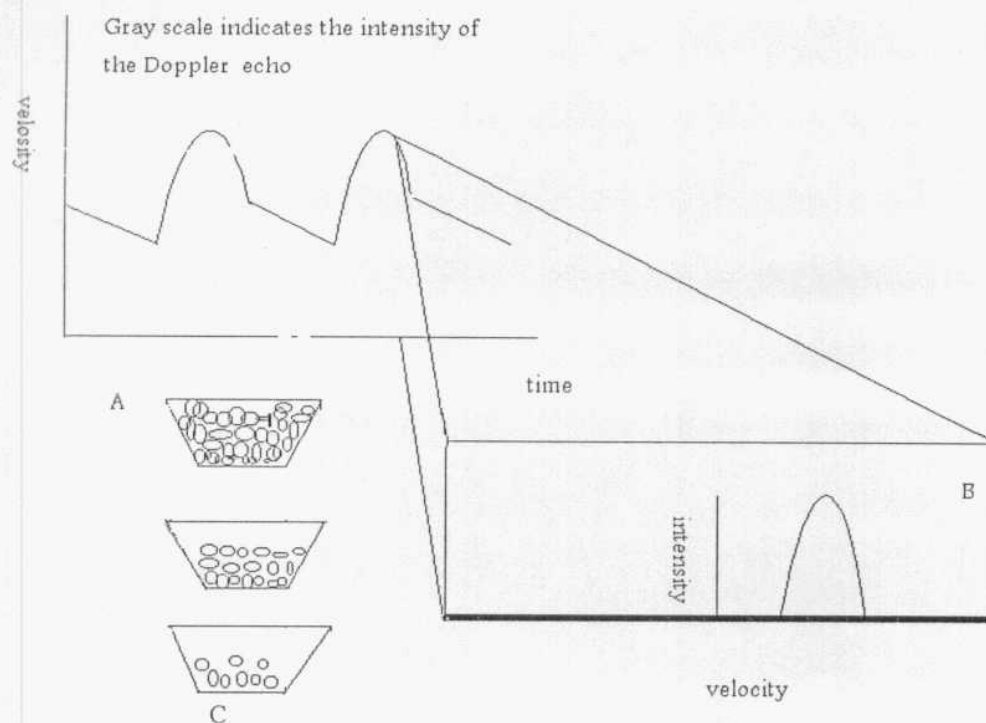


(Diagram .1). A) The power density spectrum is one instant in time in the spectral display. B) Therefore, it is a plot of signal intensity versus frequency or velocity. It is related in a complex way to the number of blood cells moving in a sample volume. (Terry *et al*, 1998).

The color displayed on the image in power Doppler mode is the area under the curve of the power density spectrum, i.e., the sum of the echo intensities at each velocity, and reflects only the total number of scatters in the sample volume, independent of their individual velocities. The relationship can be very complex and can depend in non-linear ways on such variables as shear rates, blood flow velocity, and haematocrit. (Shung, 1993)

This haematocrit dependence tends to decrease the pulsatility in the vessels imaged in fact, pulsatility may totally disappear unless the velocity goes to zero at sometime during the cardiac cycle. (Rubin *et al*, 1994)

The depiction of blood flow with power Doppler is depth dependent, just as it is with color Doppler Sonography. This integral is in some sense analogous to gray-scale imaging, in which the power in the signal corresponds to backscattered amplitude. Hence, just as gray-scale amplitudes fall off with depth, so will the Doppler power. (Rubin *et al* 1994)

Before autocorrelation is performed, the Doppler processing and clutter rejection is identical in PD and CD. Because the clutter rejection is the same as in standard CD, one would expect to see no flow where there is none. A color distribution designed to remove the directional flow information from the power map to change the character of the displayed noise. (*Ronald et al, 1994*)

The processing already resides in many machines, and the information is displayed in real time similar to the standard mean frequency information. (*Rubin et al, 1994*)

Signal-to-noise considerations:

The relationship of random noise to the actual backscattered signal originating from blood cells defines the signal-to-noise ratio and is one of the factors that determine sensitivity. (*Desser et al, 1998*)

Noise has a much different appearance in power Doppler US than in CDUS. Noise has a very low power compared with information-containing signal. Therefore, if the Doppler gain is increased or if the threshold is lowered to the noise floor in the power mode, the resulting image noise assumes a nearly uniform appearance, corresponding to the low- power background .Any information-containing signal, displayed as a signal of higher power, appears as a different color relative to the noise floor. (*Desser et al, 1998*)

PD uses more of the available dynamic range when producing flow images, thus increasing a machine's flow sensitivity.

Angle independence in power Doppler:

Power Doppler is essentially angled independent. This may at first seem paradoxical, as the Doppler shifts are angle dependent. However, the number of scatterers at any given location is angle independent. The number and shear rate, this is fundamentally different from CD, in which the frequency shift is what is being imaged. Once this number of scatterers is determined by the physiologic circumstances, the power looks essentially the same from any direction as long as the Doppler shift is detectable. (*Helenon et al, 1998*)

Therefore, although the shape of the power curve (power spectral density curve) changes with the angle of insonation, the area under the power spectral density curve is angle independent and remains constant. In practice, PD manifests slight angle dependence. This is because flows with a frequency shift very near zero are eliminated or attenuated in signal level by the soft tissue motion (clutter) canceller of the imaging unit; this contribution is usually very small. (*Rubin et al, 1994*)

Non-aliasing in power Doppler:

Finally, PD does not alias. The mean frequency representation of CD varies with the degree of aliasing. (*Rubin et al, 1994*)

When aliasing occurs, the upper portion of the power spectrum will wrap around and appear on the far left side of the spectrum. Mean velocity estimate becomes meaningless, but energy, the area under the power spectrum curve, remains the same. Therefore, although aliasing is present, it does not affect the energy display. (*Desser et al, 1998*)

Convergent color Doppler:

In conventional color Doppler, the mean velocity estimated from the power spectrum is mapped to a color velocity map that displays information in units of cm/sec, whereas in power Doppler, the total backscattered energy is mapped to a color energy map in units of dB. The color bar has two axes: velocity and direction mapped along the vertical axis while energy is mapped along the horizontal axis. This can be complicated because velocity, direction, and energy are contained in a single map. To make sense out of these variables, three conceptually different color maps have been developed. (*Clautice-Engle et al, 1997*)

The threshold map combines velocity, direction and energy. There is a user-selectable threshold below which only energy is displayed, but above which both velocity and direction are displayed. This map allows very low flow to be displayed as energy whereas higher velocity, higher volume flow will be displayed with velocity and direction data.

The directional map combines direction energy and is the simplest map. This map may be useful in setting in which the mean velocity is not very important but flow direction and the presence of flow is of value.

The contour map starts with the display of only energy information for low level Doppler signals but gradually transitions into the display of both energy and mean velocity increases. The map is interesting because it color codes the product of velocity and energy, which is related to volume flow.

Convergent color Doppler is an example of how estimated Doppler display technologies can be combined to show more information than any single technology. The convergent color Doppler display has the freedom from aliasing and angle-to-flow independence of the power Doppler display, and the velocity and direction information of conventional color Doppler. (Desser et al, 1998)

Power Doppler artifacts:

Flash artifact

Power Doppler Sonography is much more susceptible to Flash Artifact from patient motion than is color Doppler Sonography. This annoying artifact can be minimized by the use of motion discrimination algorithms. In addition, temporal persistence levels can be increased, which can contribute to even better sensitivity and, if non-linear persistence is used, may reduce flash artifacts. (Martinoli et al, 1998)

Absence of aliasing artifact

The absence of aliasing artifact in power Doppler imaging may be a liability in clinical settings such as vascular stenosis, for which color flow mapping is performed to identify areas of increased flow velocity or turbulence. Such areas of disordered flow will be readily apparent on color Doppler velocity images, but invisible in power Doppler displays. (Desser et al, 1998)

Hyperechoic artifacts

These may be particularly problematic in power Doppler imaging, where septae within a cyst may appear to have flow because of vibration or slight motion transmitted pulsations. Definitive assessment of the presence or absence of flow requires spectral Doppler sampling of the area in question. (Hamper et al, 1997)

SPIRAL CT EXAMINATION:-

Design limitation of conventional CT

In conventional CT, the X ray tube alone or in combination with a detector array must be rotated around the patient to obtain the necessary projection. This involves the movement of large mechanical and electrical devices as well as repositioning of the tube-detector system between successive slice acquisitions.

Nearly all the designs necessitate a time delay between scans to reverse rotation direction and unwind the high voltage and data acquisition cabling. These limitations lead to the development of slip ring technology.

Introduction to spiral CT

Slip ring technology was development by *Boyd and colleagues* in early 1980 and was introduced into clinical practice in 1989 .The technique is so named because the X-ray can be thought as if tracing a helix or spiral curve on the patient surface. (*Polacin et al, 1992*)

It enables acquisition of true volume of data in a manner that is not possible with conventional CT scanner. In spiral CT the patient is advanced through a continuously rotating gantry that produces data constantly, whereas conventional CT scanners produce discontinuous cross-sectional and axial scans of the abdomen acquired during separate intervals of breath holding. Movement of spiral CT scanning is analogous to that involved in tracing the thread of a screw. The resulting data set therefore differs from that obtained with conventional CT scanners in that the data are acquired as a single without any discontinuity. In addition, spiral CT scanning time is significantly shortened because interscan delays due to intervals between breath holdings are eliminated. The more rapid acquisition of data during breath holding also reduces artifacts resulting from the effect of respiratory motion. (*Paranjpe and Bergin et al, 1994*)

With conventional CT scanning, each rotation of the X-ray tube generates data from which corresponding transaxial images are reconstructed. With helical CT each rotation of the X ray tube can be thought of as generating data specific to angled plane of sections. Transaxial images may

be reconstructed only after a full complement of data specific to each plane of section estimated.

This mathematic estimation is performed by interpolation of the data above or below each desired plane of section. This retrospective estimation of data for transaxial image reconstructions can be beneficial in that, position and spacing of images can be chosen retrospectively and at very small increments resulting in highly overlapping images, for example 100 images may be generated from a single 30 second helical CT exposure. Although not practical for routine interpolation of transaxial images, yet may be used to produce high quality multiplanar and 3-D reformation with smooth margins. (*Brink et al, 1995*)

OPERATOR DEFINED PARAMETERS:-

The performance of helical CT requires more input from the physician and the technologist than does conventional CT.

The choice of the Collimation:

It's largely dependent on the organ of interest;

- Collimation of 2-3 mm is employed for small structures such as nodules and renal arteries
- Collimation of 5 mm is commonly used in the neck & abdomen.
- 8-10 mm Collimation is used routinely in the chest.

Table feed

Is described as the table increment per gantry rotation period. Others prefer to describe this as a pitch ratio.

Pitch ratio

Is the ratio of table increment per 360° gantry rotation divided by the collimation.

$$\text{Pitch ratio} = \frac{\text{Table feed}}{\text{Collimations}}$$

Example: if the table feed is 3 mm and the collimation is 3 mm, so pitch ratio = 1:1, if the table feed is 6 mm and the collimation is 3 mm so pitch ratio = 2:1.

In most scanners table feed is generally set equal to collimation (pitch = 1:1). With modern hardware and software, the table feed may be increased up to twice the collimation (pitch = 2:1). This choice is made to increase the coverage of fixed scan duration.

The scan coverage is determined by multiplying table feed by the helical scan duration, so the higher the pitch value, and the higher the scan coverage and the higher the mAm used. But most commercially available CT scanners have pitch value of 1:1, so no increase in the mAm used.

The operation must also choose the scan timing and the reconstruction interval.

The scan timing

Must be planned both with respect to patient breath hold and with respect to administration of contrast material. Some scanners are capable of performing only one programmed helical scan, other permit the performance of multiple programmed helical scan. Two or three helical separate scan can be performed with a short breathing interval between scans. This is perhaps more advantageous in-patient who cannot hold their breath for a prolonged period and in the study of the lower limb bones and or vasculature. (*Brink et al, 1995*)

Reconstruction interval

Longitudinal resolution depends on the detector collimation, table increment and reconstruction interval. The table increment tend to broaden the section profile in helical CT compared to that in conventional CT conversely, the reconstruction interval in helical CT may be decreased compared with that in conventional CT without increasing the X-ray dose. (*Brink et al, 1995*)

In clinical practice, Urban and colleagues showed a 10% improvement in the detection of small lesions within the liver with helical CT when a 50% overlap was employed rather than contiguous transaxial images. In conventional transaxial images, a small lesion centered between two contiguous sections is poorly visualized because of volume averaging. When the reconstruction interval is chosen to one-half of collimation (50% overlap), the same lesion may fall within the center of an overlapping section. Thus, helical CT permits the substantial improvement in the longitudinal resolution without an increase in the X-ray dose to the patient due to its inherent retrospective reconstruction capability. (*Wang and Vannier et al, 1994*)

Hardware consideration

Critical to the development of helical CT technology was the introduction of slip ring interfaces in the gantry construction. Prior to this technologic landmark, CT scanners incorporated electrical cabling to couple the X-ray tube detector assembly to the reconstruction processor and high voltage power supply externally to the gantry. An oscillating motion of the source - detector assembly was required to permit winding and rewinding of the electrical cables. As such, the source detector assembly required frequent abrupt change in the speed and direction. A process often requiring 5-10 second between scans. (*Polacin et al, 1992*)

With slip ring technology, there are no electrical cables connecting the gantry components to the ground, and the source detector assembly may rotate continuous. In slip ring scanners, there are multiple parallel slip rings with:

- One supplying high voltage to the tube and generator.
- One exchanging digital data between the computer and source detector assembly.
- The third providing low voltage for the control system. (*Brink et al, 1995*)

Because helical CT is most beneficial when an entire organ or region is scanned in a single breath hold, scan duration 20 - 30 second are not uncommon but sometimes continuous scanning of up to 60 second is often desired e.g.; scanning chest and abdomen after single bolus of contrast material. As a result, helical scanning has forced the development of X-ray tubes and generators that are robust enough to deliver a reasonably high tube current for prolonged duration and yet are light weight enough to be mounted

in the slip ring gantry. Most current manufacturers of helical CT scanner have responded and continue to respond to this challenge with significant improvements in tube output with each hardware up grade. (*Brink et al, 1995*)

Software considerations

Once the spiral CT data volume has been acquired axial images are reconstructed by using one of 2 mechanisms, 360° or 180° - linear interpolation (L1) algorithmic. This refers to the mathematical technique used to drive axial scans from spiral data sets obtained. (*Paranjpe et al, 1994*)

360° linear interpolation (L1) using data points separated by a full 360° rotation of the X-ray tube. Transaxial images reconstructed from such data were nearly identical to the conventional scanning. The simplest approach is (L1) between spiral projection data sets from adjacent turns 360° apart. However it diminishes the longitudinal resolution, which can produce volume-averaging artifacts due to increased scan coverage. (*Heiken et al, 1993*)

180° linear interpolation (L1) between data points separated by 180° opposite views thus spiral scan range used for reconstruction of each image is reduced thereby diminishing the problem of partial volume averaging artifacts. (*Heiken et al, 1993*)

Practically, the use of 180° linear interpolation resulted in two obvious improvement to clinical practice:

- First scanning at a pitch greater than 1:1 now seemed possible permitting increase in the scan coverage for a given scan duration.
- Second the increased longitudinal resolution associated with 180° (L1) made possible the production of high-resolution multiplanar and 3-D images without significant longitudinal blurring.

The most notable disadvantages of the 180° (L1) are increased image noise. (*Brink et al, 1995*)

A better estimate of the true value is obtained by higher-order interpolation (HI), which uses more than 2 data points' 180° cubic spline interpolation. (*Polacin et al, 1992*)

Image Noise

Image noise is measured as standard deviation of pixel values in a homogeneous of interest.

With 360° (L1), noise has been shown reduced by 17-18% compared to conventional CT. The decrease in image noise results from relative increase in photon statistics.

With 180° (L1), noise has been found experimentally to be increased by 12-13% due to relative decrease in photon statistics associated with such broad interpolation range.

Empirically, noise was found to be increased by 29% with 180° cubic spine interpolation. (*Brink et al, 1995*)

The combined 180° (L1) with limited power of the X-ray tube result in slightly noised image. This problem is being overcome with the introduction of new X-ray tube with higher heat capacity. (*Heiken et al, 1993*)

Radiation Dose

Because spiral CT employs continuous scanning, the X-ray power is currently limited to less than that used for standard CT scanning. This power limitation is greatest for long scans (24 sec. or longer) and result in increased quantum noise. Given the same X-ray tube power, the radiation dose to the patient for spiral CT scans is equal to that for standard contiguous-section CT if pitch of 1 is used (table speed is matched to the collimation). Radiation dose for spiral CT is decreased when the pitch is greater than 1 compared to the standard contiguous-section CT. Since the X-ray tube power for long duration spiral CT scan is currently less than that used for conventional CT, the radiation dose to the patient is currently less for long duration spiral CT. (*Heiken et al, 1993*)

MULTIPLANAR AND 3-D IMAGING:-

2D Reformation

Once transaxial images has been reconstructed from CT scan data, high quality 2-D reformation may be generated particularly if image data were acquired with a thin collimation settings and transaxial images were generated with high degree of overlap. Most commercially available CT scans offers 2-D reformation in standard sagittal, coronal, parasagittal, paracoronal in addition to oblique multiplanar imaging. Some manufacturers offer the possibility of generating 2-D reformation oriented in a curved plane of section. Curved plane reformations may be useful in depicting non-linear structures such as tortuous artery.

By multiplanar capability, the radiologist may roam through the imaging volume in real time along any direction. Only he has to prescribe the desired plane using a mouse or track-ball roller cursor to recall the 2-D image in any desired plane.

3-D Reformation

To date, maximum intensity projection (MIP) and shaded surface display (SSD) have been the most commonly used 3-D techniques. Both techniques have certain advantages and disadvantages.

MIP for example permits separation of the enhanced lumen for high attenuation structures within the vessel. Thus calcification in the vessel wall can be readily detected.

Conversely, MIP provides poor depiction of vessels that overlap each other. The problem can be circumvented by generating multiple MIPs that rotate around an imaging axis (usually a major anatomic axis). When small degrees of rotation are used (generally 5-10 degrees) overlapping vessels can be unwound in many instances.

In many aspects SSD is complement to MIP. On the SSD, the wall of the vessel can't be differentiated from the contrast-enhanced lumen because an absolute threshold is set and structures of higher attenuation appear black.

Nevertheless, overlapping vessels are better depicted with SSD than with MIP because of the inherent 3-D appearance (due to shading from an arbitrarily positioned imaginary light source) associated with SSD. (*Rubin et al, 1994*)

For 2-D and 3-D image reformation, the first processing step is interpolation of image data longitudinally. Performance of this longitudinal interpolation tends to smooth the longitudinally oriented contours within the image. Mapping selected parts of the matrix into performed grey scale image planes can generate multiplanar reformation.

Applying appropriate 3-D technique to the matrix of interpolated data can generate 3-D images. For best results with MIP and SSD, the 3-D matrix of interpolated image data should be edited to exclude unwanted structures, for example: bone and unnecessary soft tissue are generally excluded from the imaging volume in CT angiography to increase the conspicuity of enhanced blood vessels by lowering black-ground attenuation. This is done to avoid confusing calcified plaques from underlying bone.

MIP

Projecting imaginary rays through the 3-D matrix of interpolated image data and mapping the maximum attenuation value along each ray to the gray scale image generate MIPs. The projected images are obtained in any anatomic plane. (*Brink et al, 1995*)

SSD

SSD images are generated after selection of an arbitrary user-defined threshold. Voxel of the 3-D matrix of interpolated image data with attenuation values greater than the threshold are set to be black.

The threshold matrix of interpolated data is set into 3-D images with depth perception given by shading techniques from an imaginary light source that can be placed at any position. (*Brink et al, 1995*)

ADVANTAGES OF SPIRAL CT:-

Since its recent introduction, spiral CT changed the basic concepts of routine CT scanning. Spiral volumetric CT technique allows continuous data acquisition while the patient is advanced through the CT gantry. Scans may be either prospectively or retrospectively reconstructed using a variety of interpolation algorithms. The results are contiguous set of images obtained without interscan delay obviating potential disintegration (*Naidich et al, 1994*).

In comparison with routine axial imaging, a number of important advantages result from helical scanning. These include: -

1- Reduced-time examinations. With scan acquisition time of 30 sec. or greater. The reduced scanning time is very important in scanning critically injured patients. (*Heiken et al, 1993*)

2- The potential for improved lesion detection by spiral CT is related to two main factors: the elimination of respiratory disintegrations and the ability to reconstruct overlapping images at arbitrary intervals. The benefit of using overlapping image reconstruction was found to be most significant for small lesion. Because spiral CT reconstructions are performed retrospectively. Overlapping images are obtained without additional radiation exposure to the patient. (*Sato et al, 1992*)

3- Improved lesion densitometry is made possible by spiral CT by virtue of its ability to reconstruct images at arbitrarily-chosen position along Z axis, thus the images can be reconstructed through the center of any lesion minimizing the effect of partial volume averaging which is often a problem with single -section acquisition CT. (*Heiken et al, 1993*)

4- Reduced volume of the contrast used. The ability to acquire data in a single breath hold allows more precise delivery of contrast media thus permitting assessment of the lesion vascularity in the peak enhancement phase and also leading to reduction of the volume of contrast necessary for optimal visualization of vascular structures. The ability to perform rapid, high quality CT examination with small doses of contrast material is an important consideration in radiological examinations of elderly patients with either renal or cardiac impairment. The patient receiving large doses of contrast media are at risk of acute tubular necrosis and by use of non-ionic contrast

media, there is increased cost effectiveness by 10-15% but by the use of spiral CT, there is significant decrease in the volume of the contrast and so there is substantial cost saving of 50%. So radiological departments can convert to non-ionic contrast material when using spiral CT with cost saving of 50%. (*Castello et al, 1994*)

5- Repeated scanning due to respiratory-induced disintegration and patient motion artifacts are reduced to minimum by use of spiral CT. (*Brink et al, 1995*)

6- Improved multiplanar and 3-D imaging. The absence of respiratory induced disintegration besides the ability to produce overlapping images without an increase in the radiation dose allows multiplanar reconstruction to be generated in any desired imaging plane without the step like discontinuities that so commonly result from conventional axial imaging. Additionally, volumetric data acquisition allows high quality 3-D imaging using a variety of reconstruction-algorithms. (*Naidich et al, 1994*)

LIMITATIONS OF SPIRAL CT

1- The increased image noise with spiral CT is related to both the interpolation process and the limitation in X-ray tube power necessitated by continuous scanning. The introduction of high heat X-ray tubes will eliminate the latter problem.

2- Reduction in the longitudinal resolution with the CT is due to broadening of the SSP "section sensitivity profile", which result in varying degree of partial volume averaging artifacts. The partial volume averaging effect is decreased when table speed is matched to the collimation. But, it increases as pitch is increased (above 1). However, this effect is minimized by use of 180 (L1) algorithms. (*Polacin et al, 1992*)

3- Spiral CT requires additional time for processing compared with the conventional CT due to large amount of image data generated by spiral CT which requires more frequent archiving and increases the need for large capacity archival devices. However, the use of more efficient storing devices, such as digital audiotapes and optical discs may decrease this problem.

The most time consuming aspect of spiral CT is the post processing time required for the radiologist to review the data and generate multiplanar or 3-D images, if they are required. (*Heiken et al, 1993*)

CT arterial portography (CTAP):

CT with arterial portography (CTAP) is an important method for preoperative detection and localization of liver tumours. The reported sensitivity of this method for lesion detection is among the highest of radiologic techniques, ranging from 81% to 91%. (*Heiken et al, 1989*)

The method involves selective delivery of contrast medium to the portal venous system without distribution or dilution with the central blood volume. Although 80% of hepatic supply is from the portal system, hepatic neoplasm is largely supplied by the hepatic artery. (*Matsui et al, 1991*)

Hepatic neoplasm is detected as hypoattenuating areas, in comparison with the normal contrast medium enhanced parenchyma. Rapid acquisition after injection is mandatory because recirculation of contrast medium to the systemic circulation will result in diminished contrast differences between neoplasm and normal parenchyma. (*Young et al, 1980*)

CTAP can be performed with intra-arterial catheter in the superior mesenteric artery. Since patients were first examined with digital hepatic and mesenteric arteriography, the intra-arterial catheter is left in the superior mesenteric when the angiographic study is completed, then the patient is taken to the CT scan room to complete the procedure, where the catheter is connected to a power injector. A total of 90 to 100 ml of 60% iodinated contrast medium is injected through the catheter at a rate of 0.5 ml/sec. CT scanning is initiated 20 sec after the start of injection. Scans obtained with 8mm collimation. After being scanned during the dynamic phase of intra-arterial contrast enhancement, the patient is rescanned during the equilibrium phase (with 5 minutes after the dynamic phase). Delayed CT scans are obtained 4-6 hours after CTAP. (*Bluemke et al, 1995*)

Spiral CT has led to a new imaging modality termed spiral CT angiography (3DCT), which provides three-dimensional information on intra-abdominal vascular anatomy. (*Rubin et al, 1993*)

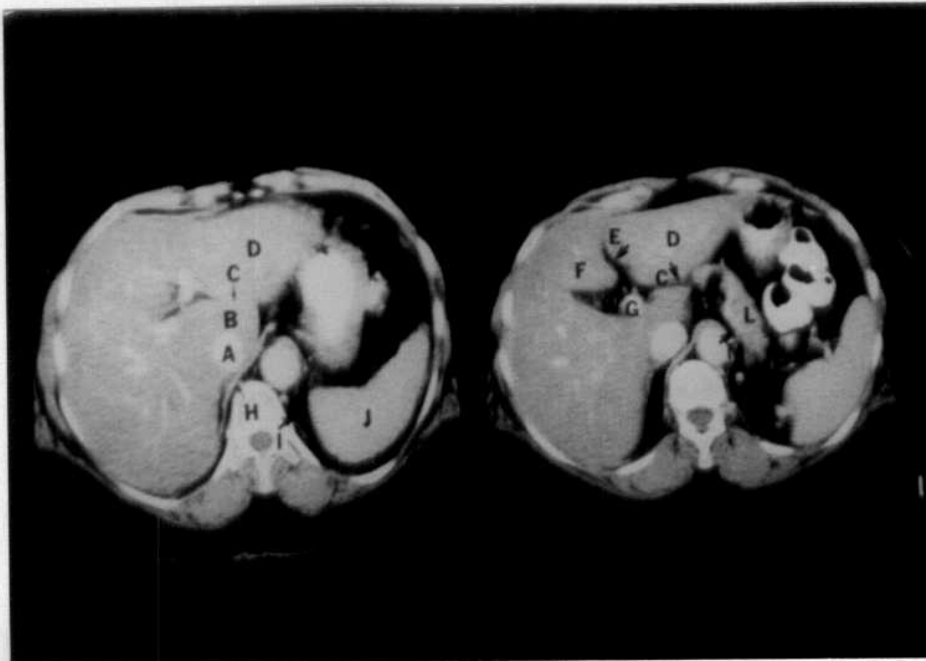
CT during hepatic arteriography (CTIHA):

With CT during hepatic arteriography, lesions will have a hyperattenuating rim compared with the lower attenuation of the surrounding hepatic parenchyma. This reflects the dominant blood supply to hepatic tumour from the hepatic artery. The technique may be performed by placing the tip of a 5F catheter into the proper hepatic artery. If the catheter tip is placed in either the common hepatic artery or the celiac axis, some contrast may also flow in to the portal system via the splenic artery and diminish lesion to liver contrast. CTIHA is simply performed by infusion of 300 ml of 30% iodinated contrast agent via catheter at a rate of 3 to 5 ml/sec. followed by dynamic CT scan with contiguous sections through the entire liver. (*Prando et al, 1979*)

Recently with spiral CT the technique is done by infusion of a contrast medium and scanning obtained during a single breath hold 5 seconds after starting the intra-arterial administration of 20 ml of contrast material at a rate of 1 ml/sec through the catheter in the proper hepatic artery. (*Murkami et al, 1995*)

With lower infusion rates, there may be layering of contrast material along the dependant portion of the artery resulting in differential enhancement of the right and left hepatic lobes. (*Bleumke et al, 1995*)

Recently three-dimensional spiral CT hepatic arteriography is reconstructed from spiral CT obtained during direct hepatic arterial contrast material injection in patients. Usually two techniques used for reconstructed three dimensional spiral CT hepatic arteriography these are maximum-intensity-projection (MIP) and shaded-surface-display (SSD) techniques. (*Masayuki et al, 1996*)

CT OF THE UPPER ABDOMEN

(Figer .3)

The liver occupies most of the right upper quadrant of the abdomen with the right hemidiaphragm as its most superior border. The left lobe of the liver crosses the midline and lies under the left hemidiaphragm related to the heart and left lung. The left lobe is a purely anterior structure while the much larger right lobe extends over most of the right upper quadrant.

On CT evaluation, normal liver parenchyma is of homogeneous density. On unenhanced scans, it is slightly denser or isodense to the spleen and intravascular blood. Intravenous injection of iodinated contrast enhances the liver parenchyma as well as the vessels. The degree of enhancement depends on the size and rate of the bolus injection and the time elapsed between injections and scanning. CT of the upper abdomen is usually performed with oral and intravenous contrast. Various techniques to emphasize differences in attenuation between normal and abnormal structures are employed for detailed examinations. These include scanning pre- and post-contrast, delayed scanning, dynamic scans and direct arterial or portal venous injection.

Nearly all of the intrahepatic vessels identified on CT are veins. The hepatic veins are best depicted on the more superior axial scans. They run in the

intrahepatic fissures and which divides the lobes of the liver (Figer .3, M). The hepatic veins converge at the supero-medial portion of the liver where they enter the IVC (Figer .3, E). In more caudal axial scans, the portal veins are identified branching from the porta hepatis (Figer .3, G, W). The bile ducts and hepatic arteries, which travel with the portal veins, may be identified in normal patients with newer CT scanners.

The ligaments and fissures of the liver are generally easily identified on CT due to their associated fat content, rendering them low-density structures. The falciform ligament originates from the umbilicus, and extends over the superior surface of the liver. It contains the ligamentum Teres or remnant of the umbilical vein, which may be identified as it courses inferiorly toward the porta hepatis (Figer .3, E). This ligament forms the border between the medial and lateral segments of the left lobe. Within the porta hepatis the portal vein and common hepatic duct are variably identified. The gallbladder (Film .3, A) is usually within or may be followed to the main intralobar fissure. Most of the major fissure is not well depicted on CT. A diagonal line drawn between the gallbladder and the IVC approximates the boundary between the right and left lobes of the liver at this level. More cephalad to the porta hepatis but lower than the hepatic veins, the caudate lobe of the liver (Film .3, B) is identified just antero-medial to the IVC. The fissure for the ligamentum venosum (Films .3, C) forms its anterior border and separates it from the lateral segment of the left lobe. The gastro-hepatic ligament extends from the fissure for the ligamentum venosum to the lesser curvature of the stomach.

- A IVC, intrahepatic portion
- B Liver, Caudate lobe
- C Fissure for ligamentum venosum
- D Liver Lateral segment of left lobe
- E Ligamentum teres
- F Liver Medial segment of left lobe
- G Portal vein
- H Crus of right diaphragm
- I Crus of left diaphragm
- L Pancreas, tail
- M Splenic vein
- W Porta hepatis

MRI EXAMINATION:-

Physical aspects

During the past 5 years, multiple techniques have been developed for MR imaging of the liver. Optimization of pulse sequences is a critical issue in MR imaging of the liver, as image quality and diagnostic value greatly depend on imaging protocol. Imaging protocols vary among institutions because of the absence of consensus of the most appropriate sequence. (Soyer et al, 1997)

I. SYSTEM OVERVIEW:-

In principle a magnetic resonance imaging system (M.R.I.) is quite simple, consisting of a large main magnet and smaller auxiliary field coils (gradient coils), radio frequency (RF) antennas (transmitter and receiver coils), associated electronics, and a computer to process the data from the imaging experiment. However, in practice, M.R.I. systems are quite complex, and careful attention must be paid to the design of all components to ensure consistent, high-quality images. (Stetter et al, 1996)

Field strength

Different units using various field strengths are commercially available; most MR scanners have field strengths ranging from 0.5T to 1.5T. (Soyer et al, 1997)

Phased-array multicoils

For many years, MR imaging of the liver has been commonly performed using a whole volume body coil. Phased-array surface multicoils system or (torso-coils) have been developed for body imaging and are made of several surface coils oriented to image a whole volume, and their use results in improved signal to noise ratios. (Soyer et al, 1997)

Surface coils

Using phased array technology have been shown to be superior to conventional body coils for imaging the liver, as their use significantly

improves the lesion detection, the lesion to liver contrast and image definition. (*Campeau et al, 1995*)

II. PULSE SEQUENCES:-

Conventional spin-echo imaging

Spin echo- (SE) pulse sequence was the first technique to be widely used in M.R.I. of the liver. In the last few years, modifications of the SE sequence and many new pulse sequences have been introduced. However SE imaging has not been totally replaced by the new pulse sequence. (*Catasca et al, 1994*)

In the SE sequence, 90° excitation radio frequency (RF) pulses are used to tip the magnetization of the tissue into a plane perpendicular to the main magnetic field. A 180° refocusing RF pulse to produce an echo follows each 90° excitation RF pulse. The time between the two consecutive 90° pulses are called the repetition time (TR). The time between the 90° pulses and collection of the signal is called the echo time (TE) and it is double the time between the 90° and 180° pulses. T1-weighted SE images are obtained using a short TR (approximately 300 msec.) and shortest possible TE (20-30 msec.). T2-weighted SE images are obtained by using a long TR (2500-3000 msec.) and a long TE (at least 80-90 msec.). (*Catasca et al, 1994*)

Soft tissue contrast in a conventional SE sequence is based on differences between tissues in their longitudinal (T1), proton density and transverse relaxation time (T2). T1 and T2 are two time constants that being tipped off the main magnetic field by the RF pulse. T1 determines how fast the magnetization vector in the plane perpendicular to the main magnetic field decreases due to dephasing of the individual spins. T1-weighted image contrast depends primarily on differences in T1 of tissues. On T1-weighted image, tissues with relatively short T1 such as fat have strong signal while tissues with relatively long T1 such as water have low signals. The liver has higher signal intensity than the subcutaneous or intra-abdominal fat. On T2-weighted images, tissue with relatively long T2 such as water, have strong signal intensity while tissues with relatively short T2, such as the liver parenchyma have long signal intensity. On these images the liver has lower signal intensity than the spleen. (*Chenevert et al, 1995*)

In many institutions, T1-weighted SE MR images of the liver are no longer routinely obtained for two reasons, first at high field, liver lesions show relatively poor conspicuity with this type of pulse sequence. Second, T1-weighted SE MR imaging requires a significantly longer examination time than that required with T1-weighted breath hold sequences. (*Soyer et al, 1997*)

Strategies to shorten the acquisition time

1) Asymmetric field of view

With the symmetric field of view (e.g. 50x50 cm) reducing the phase encoding steps (e.g. from 256 to 128) would result in increase of the voxel size with consequent worsening of the spatial resolution. If on the other hand, the field of view has also been decreased in the phase encoding direction to the same proportion as the number of phase encoding steps (i.e. 50 x 50 cm) then spatial resolution will not be affected. This asymmetric or rectangular field of view would allow 50 % shortening of the acquisition time with no change in spatial resolution. However, one of the limitations of the asymmetric field of view is aliasing or wraparound artifacts that occur when a part of the patient lies outside the field of view in the phase-encoding direction. This strategy is best suited to the parts of the body that have one dimension substantially shorter than the perpendicular dimension such as the abdomen (at least in some patients) and whenever wraparound artifacts are not a major problem of the utilized pulse sequence. (*Baileset et al, 1985*)

2) Partial-Fourier imaging

Partial Fourier Se imaging has been practically applied to abdominal imaging in conjunction with short TR and short TE, allowing image acquisition during a single-breath hold. This sequence has been called rapid acquisition spin echo (RASE) and has been used to perform dynamic MRI of upper abdomen after intravenous injection of extracellular gadolinium-containing contrast agents. (*Elster et al, 1993*)

3) Fast-spin-echo (F.S.E.) sequences

Different names have been given to these sequences including fast SE, turbo spin echo, and rapid acquisition with relaxation enhancement. The main

idea in these sequences is hybrid imaging, which means that the TES of the echoes used to produce the final image are not the same. In conventional T2-weighted SE sequence the 90° excitation pulse is followed by a refocusing 180° pulse that produces an echo at a TE. In F.S.E., the initial excitation pulse is followed by a train of 180 refocusing pulses that generate a train of echoes. The number of echoes obtained per excitation is called the echo-train length (ETL) and it ranges from 4 to 128. In contradistinction to the conventional SE sequences, these echoes that have different TES are incorporated into one and the same K-space to produce one image. Because all echoes contribute to the signal, the TE is defined as the TE at which the lowest-order phase-encoding steps are collected. Sequence parameters in (F.S.E.) greatly affect image appearance, for example, a longer TR increases T2-weighting. As the ETL (i.e. the number of 180 refocusing pulses) increases, the lesion-to-liver contrast decreases. Parameters influencing the T2 contrast are effective TE, the ETL and the echo spacing. (*Soyer et al, 1997*)

As a result of improved signal-to-noise ratio, the effective TE can be more easily prolonged in contradistinction to the TE in conventional T2-weighted SE, which cannot be increased beyond a certain limit due to the significant loss in signal-to-noise ratio. Prolongation of the effective TE has two important clinical applications. First, it allows better discrimination between solid hepatic lesions that loose signal at very long effective TE and none-solid hepatic lesions as haemangiomas and cysts, which preserve their strong signal. Second it allows better discrimination and suppression of signal from all types of tissue except the stationary fluid structures such as bile allowing the performance of MR Cholangio-pancreatography (MRCP). (*Mitchell et al, 1996*)

On fast images, fat has a higher signal intensity compared with that observed on conventional SE images, fat brightness increases as the ETL increases and the interecho spaces decreases. Fat signal can be significantly reduced using fat suppression, thereby leading to reduced motion artifacts and slightly increased lesion-to-liver contrast. (*Soyer et al, 1996*)

With fast SE imaging, time of acquisition is significantly reduced compared with the acquisition time needed with a conventional SE sequence (3-4 min. versus 12-16 min.) respectively. (*Low et al, 1993*)

It was shown that T2-weighted fast spin-echo images compare favorably with that T2-weighted SE images in terms of focal hepatic lesion-

to-liver contrast and overall image quality. Although there's no definite consensus regarding the superiority of T2-weighted fast SE imaging over the conventional T2-weighted SE imaging. It is generally accepted that the fast SE imaging can replace conventional SE imaging in routine clinical practice. (*Siewert et al, 1994*)

4) Gradient-Echo-imaging

These sequences generate an echo by gradient reversal rather than 180 refocusing pulse used with the SE sequence. (*Elster et al, 1993*)

These techniques are based on the used of short TR, short TE and variable flip angle. Different combinations of these parameters yield various degrees of contrast so that GRE technique can be used to obtain T1- and T2-weighted MR images. High flip ($>60^\circ$) and short TE maximize T1 contrast, whereas smaller flip angle and long TE minimize T1 contrast. (*Taupitz et al, 1995*)

Although, the GRE technique provides valuable images of the liver, it is associated with pulsation artifacts arising from the aorta that may obscure hepatic lesions located in the left hemi-liver. To diminish the pulsation artifact arising from the aorta, parallel presaturation pulse can be used; however the examination time is increased. (*Elaster et al, 1993*)

Spoiled GRE [fast multiplanar spoiled gradient recalled (FMPSGR) imaging] is a fast sequence based on the use of short TR (80-150 msec.), the minimal TE available (about 2 msec.) and a flip angle between 40° - 80° . This technique allows examination of the liver in about 20 sec. with about 12 sections. (*Low et al, 1993*)

FLASH: Fast-low angle shot = GRASS: gradient recalled acquisition in the steady state: It is a stationary recovery sequence based on interleaved multiple section excitation, a short TR (80-150 msec.), a short TE (4-5 msec.) and a flip angle varying between 60° and 90° . This technique allows examination of the liver in 16 to 30 sec. with 11 to 15 sections. Optimum TR value can be selected according to the number of slices needed to image the whole liver. TR value can also be chosen to reduce breath-hold times. (*Soyer et al, 1993*)

Magnetization - prepared GRE imaging (turbo-flash-snap shot GRASS): is an ultrafast GRE imaging sequence based on single -section

GRE image with a very short TR (about 8- 10 msec.) and a short TE (2-5 msec.) so that a breath-hold sequence can acquire images in less than 1 second. The very short TR requires flip angles of less than 40 degrees, even so, poor tissue contrast results. By introducing a preparatory 180° inversion recovery however, heavily T1-weighted tissue contrast can be produced. This sequence has three beneficial features that are not present in routine breath-hold GRE sequences. The first feature is the absence of pulsability artifact because the ultrashort TR does not allow for periodic intravoxel signal intensity change to occur. Second because this is a single - slice technique vessels have high-signal intensity because of flow related enhancement. Thus, low-signal intensity focal lesions are easily distinguished from high-signal intensity blood vessels, where both are of low signal intensity on breath-hold GRE images. (*Siegelman et al, 1998*)

Turbo-FLASH has been used in dynamic gadolinium-enhanced MRI due to its high temporal resolution and has been used in MRI-guided biopsy because it allows good target definition and because of the ultrashort time in which the needle remains in the patient. (*Siegelman et al, 1998*)

5) *Three-dimensional MR imaging*

In the three-dimensional acquisition of data, no slice selection is performed during the excitation of protons. The excitation pulse is delivered to the whole imaged volume. Spatial localization of the signal is then performed by two-encoding and one frequency encoding in the three perpendicular directions of the imaged volume. This three dimensional acquisition of data allows multiplaner reconstruction of the images in any desired plane. Three-dimensional imaging has been possible in conjunction with many types of pulse sequences such as FLASH and EPI. (*Rofsky et al, 1996*)

6) *Fat suppression*

The frequency of proton precession within the applied magnetic field differs according to their chemical environment (i.e. the chemical structure of the molecule in which they are located). The most relevant example in MRI is the difference in frequency depends on the strength of the magnetic field. This has two important consequences in MRI: first, it is responsible for the chemical shift artifacts at the interface between water and fat second, it

furnishes the basis for two impotent methods of fat suppression: frequency selective fat saturation (FAT SAT) and chemical-shift imaging (C.S.I.). Fat differs also from most of the other tissue in the fact that it has a short T1. This characteristic feature is exploited for the suppression of the fat signal in the short T1 inversion recovery (STIR), sequence. (*Rofsky et al, 1996*)

Fat suppression is needed in MRI of the abdomen for many purposes:

1- To characterize fat: This is particularly important for characterization of hepatic lesion that contain fat, such as Hepatocellular carcinoma, and adenomas and clearing up of pseudolesions produced by focal fatty infiltration and focally spared liver parenchyma in the fatty liver.

2- To suppress motion artifact by suppression of the signal from the moving fatty structures such as the anterior abdominal wall.

3- To reduce chemical shift artifacts: For this purpose however, methods of fat suppression other than chemical shift imaging should be used.

4- To improve dynamic range of the obtained image.

5- To evaluate enhancement by contrast agents in fat-rich areas. (*Martin et al, 1995*)

Nevertheless, fat suppression is not without disadvantages. It may result in loss of valuable diagnostic information if used alone. This is particularly important in hepatic focal lesions that contain fat and in staging of tumour spread where the fat-planes between organs represent a good clue for non-infiltration. Fat suppression may worsen the extrahepatic anatomical details, particularly those of vessels and lymph nodes. Last, interaction of some fat suppression methods with contrast agents may lead to spurious decrease of signal of the enhancing structures. (*Mitchele et al, 1996*)

7) Fat saturation (FAT SAT)

In this method, a FAT SAT pulse is delivered to the imaged volume before the excitation pulse. The result will be that the magnetization of the fat protons will be tipped into the transverse plane with the next 90° excitation pulse this magnetization is retuned to the longitudinal direction and would thus have no influence on the signal. This method can be used in conjunction with T1- and T2-weighted images. One of the disadvantages of this method is the inhomogeneity of the fat suppression. (*Semelka et al, 1992*)

The FAT SAT technique used in conjunction with T2-weighted SE and T2-weighted FSE sequences has improved the detectability of focal hepatic lesions. In the case of FSE fat suppression is more essential because the signal intensity of fat in this sequence is particularly high and usually leads to strong motion artifacts caused by the high signal of the moving anterior abdominal wall. T1-weighted FAT SAT sequences have been used to improve characterization of focal hepatic lesions that contain lesions after intravenous injection of hepato-biliary contrast agents such as Mn-DPDP. (Soyer et al, 1997)

8) Chemical-shift imaging

Chemical shift techniques are currently available in routine. The first is opposed-phase imaging which is based on signal cancellation within each voxel that contains both water and triglycerides. (Felmlee et al, 1987)

The other is selective fat-suppression technique based on selective presaturation of the fat by using a narrow-band excitation pulse that does not affect water protons. At 1.5 T, water protons and fat protons have a difference in resonance frequency (chemical shift) of 200 Hz. It has been suggested that opposed-phase technique might be inferior to in-phase technique for hepatic lesion detection because of diminished lesion-to-liver contrast in patients with fatty liver. (Rofsky et al, 1996)

Although lesion-to-liver contrast may be an important parameter for lesion as depiction, however other parameters (such signal of the lesion itself or artifacts that may obscure focal hepatic lesion) may influence lesion conspicuity

In a case-by-case study performed by Martin et al (1995) combination of in-phase and opposed-phase imaging provides complementary information, thus potentially improving confidence in lesion detection. One advantage of the combination of in-phase and opposed-phase imaging is the ability to detect the presence of fat within the hepatic tumours, aiding lesion characterization. One limitation of using opposed-phase imaging is that tissues that contain predominantly fat have paradoxical decrease in signal intensity after injection of gadolinium chelate. This occurs due to the fact that the contrast agent will increase the signal of water protons and will have little

effect on that fat. Consequently the overall signal of enhancing structures will be spuriously decreased. (Mitchell et al, 1996)

9) Short-time inversion recovery

Short-time inversion recovery sequences rely on the short T₁, relaxation time of fat. To obtain fat suppressed MR images with the STIR technique an appropriate T₁ is applied so that the longitudinal magnetization of the fat protons is nulled. The T₁, value that will null the fat signal is approximately 0.69 times the T₁, of the fat (provided that TR ≥ T₁). (Bydder et al, 1992)

The T₁ value of fat varies according to the field strength of the magnet, e.g. at 1.0 T, the T₁ value at the fat is 200 msec. and the corresponding T₁ is between 135 and 150 msec. At 1.5 T, the T₁ value of the fat is 250 msec. and the corresponding T₁ is between 170 and 175 msec. One must keep in mind that the STIR sequence suppresses signal from any tissue that has T₁ value similar to that of fat. Although signal-to-noise values are relatively low with the STIR sequence, this sequence yields high lesion-to-liver contrast values. (Soyer et al, 1997)

III. MOTION ARTIFACT REDUCTION:-

Motion artifacts may markedly degrade the quality of MR image. These artifacts can be a major limitation in the use of MR for examining the liver. Motion artifact can divide in to two main categories: Those appearing between excitation and data acquisition. To over come the adverse effects of the first category, cardiac gating, respiratory gating or breath-hold imaging, ordered phase-encoding and fat suppression can be used. To reduce artifacts of the second category, presaturation and gradient-moment nulling can be applied. (Soyer et al, 1997)

1) Mechanical techniques

The use of an abdominal belt to subdue respiratory motion may help in reducing motion artifacts. In some cases, mild sedation may be indicated. Breath hold technique also reduces motion artifacts but requires 20 to 30 sec. breath hold capability from the patient. (Wood et, al, 1988)

2) Physiological gating

Another option is the use of respiratory or cardiac-triggered imaging, which allows image acquisition at the same point of respiratory or cardiac cycle, thus greatly decreasing motion artifacts. Because the liver is located close to the diaphragm and the heart, MR images of the liver are simultaneously degraded by both cardiac and respiratory motion. Gating is based on synchronization of the sampling data with periodic physiologic motion, thus image acquisition is performed at a given portion of the cardiac or respiratory cycle. With respiratory gating the data are acquired during one phase of respiratory cycle so that the examination time is greatly increased necessitating the use of fast SE technique in clinical practice. In addition, respiratory gating is only feasible for patient who has regular long and repeatable respiratory cycles. In general, cardiac or respiratory gating is performed to implement SE or FSE imaging and is not needed when using breath-hold imaging. A limitation to the use of cardiac gating is that the TR value depends on the patient's heart rate, which is sometimes not the optimal TR for examining the liver. In addition, the calculated TR value may be extremely long (up to 9000 msec). That increasing the examination time. (Soyer et al, 1997)

3) Reordering and Signal Averaging

Reordered phase encoding is another technique for reducing respiratory artifacts. This technique used an algorithm that retrospectively sorts phase-encoding steps based on the average respiratory cycle. A pneumatic belt placed around the patient's thorax maintains reordering phase encoding. This technique can be routinely used to improve the quality of T1-weighted SE images. (Bailes et al, 1985)

Performance of multiple-signal averages (number of excitation or next) significantly reduced the background noise, there by increasing the signal-to-noise ratio each phase encoding step is performed several times (i.e. the number of signal-average times), and the data obtained are averaged. For a given number (n) of data averaged the net increase of signal-to-noise ratio is the square root of n. Because the examination time correlates with the number of signal averages, this technique is more suited to the use of fast SE imaging rather than be the use of conventional SE imaging. (Soyer et al, 1997)

4) Motion-compensated gradients

Flow compensation technique (gradient-moment nulling) allows elimination of unwanted signal originating from moving spins caused by phase variation. Rephasing is obtained by means of an additional pulse. Flow-compensation technique however results in increased TE and reduced number of images slices per acquisition. (*Soyer et al, 1997*)

Presaturation techniques can be used to eliminate artifacts secondary to motion or flowing blood. (*Felmlee et al, 1987*)

In this technique, additional radio frequency pulses saturate protons located outside the area of interest. These pulses can be applied to tissue either parallel presaturation may be helpful with T2-weighted imaging, because small vessels can be hyperintense, making their differentiation from small hepatic lesions difficult. Presaturation can also be applied to the subcutaneous fat, so that its signal intensity becomes dark. (*Soyer et al, 1997*)

IV. FUTURE TRENDS:-

Echo-planar imaging (EPI)

All the previously discussed pulse sequences have relied on improvement of the software programs that can be applied to the commercially available MR units. Shortening of the acquisition time achieved by these methods is, however, limited by the available gradient hardware of the MRI unit. EPI is a new imaging technique that requires particular gradient hardware to shorten the readout time itself. Shortening of the readout time in EPI is achieved by improving the gradient strength from about 10 mill. Tesla per meter (mT/m) to about 25 mT/m, improving the slew rate (i.e. the rise time of the gradient) from 10-20 mT/m/ms to 30-150 mT/m/ms and performing "under-the-ramp" sampling (i.e. reading out at 0 at the time of rise and full of the gradient and not only at its plateau), while keeping the gradient-induced eddy currents at a minimum. The implementation of these stronger and faster gradient systems, results in marked reduction of acquisition time of MR images. In contrast to conventional SE, technique, echo-planar imaging is a snapshot technique that allows acquisition of a complete data set in one measurement (i.e. single-shot technique) whereas echo-planar imaging can be used to obtain (less than 40

ms); the single-shot technique is limited in resolution due to T2 decay during the readout window. (*Farzaneh et al, 1990*)

Because the data are collected during free-induction decay, data lines acquired beyond the tissue T2 decay time contain little signal intensity. Echo-planar imaging can also be obtained using a multishot acquisition sequence implemented with conventional gradient coil and gradient amplifier. (*Campeau et al, 1995*)

Using a multishot echo-planar technique, the data required for reconstruction of an image are acquired in four to eight shots. Gradient-moment nulling in the phase-encoding direction is necessary in echo-planar imaging to prevent a loss of signal due to blood flow or hepatic motion. (*Soyer et al, 1997*)

The advantages of using the echo-planar technique are reduced imaging time (thus allowing breath hold imaging in almost every patient), reduced motion artifact, and spontaneous fat-suppressed imaging. Echo-planner images may be valuable for differentiating between nonsolid (Haemangioma and cyst) and solid hepatic lesions. Echo-planner imaging may open new applications for MR imaging in the area of perfusion and functional imaging of the liver, but these exciting techniques are still under development. (*Muller et al, 1994*)

Design and implementation of Magnetization Transfer Pulse sequence for clinical use

Magnetization transfer between the protons of macromolecules and proton of water molecules is a recently introduced mechanism for tissue contrast in MR imaging.

The magnetization transfer effect is strong in tissues where an efficient cross relaxation between macromolecular protons and water protons is, and where this interaction is the dominant source of relaxation. Paramagnetic ions shorten relaxation times and decrease the MT effect. These two facts led to the assumption that, in the case of contrast enhanced MRI, the combination of the T1-weighted imaging method and the MT technique may yield increased contrast, compared with standard methods. (*Jukka et al, 1992*)

The transfer of magnetization between a free and a bound pool of spins is described in terms of the respective longitudinal relaxation times and the life times of spins in each pool.

The effect of an off resonance radiofrequency (RF) pulse in producing saturation in the bound pool and a consequent decrease in both the available longitudinal magnetization and the T1 of spins in the free pool is described. The effects of increasing duration of the saturating RF pulse on image pixel signal intensity were used to determine values for the decrease in both T1 and the available magnetization in different tissues. (*Joseph et al, 1992*)

In essence, protons in tissues can be described as existing in two pools. The first or (free) pool consists of mobile proton such as those in water. This pool has a narrow spectral line and a relatively long T2. It provides the bulk of the signal detected with conventional whole body MR systems. The second or (bound) pool consists of protons bound in proteins, other large macromolecules, and membranes. This pool has a very broad spectral line and a very short T2. It is said to be invisible in MR because its signals are not directly detectable with conventional imaging techniques. (*Joseph et al, 1992*)

Magnetization can be transferred from one pool to the other by dipole-dipole interaction between spins or the transfer of nuclei or direct chemical means. Because of the width of the resonance lines of the two pools are so different, it is possible to substantially saturate the bound pool by applying an off resonance radiofrequency (RF) pulse while leaving the free pool virtually unaffected. This process very largely destroys the magnetization in the bound pool, so there is little or no transfer of magnetization from it into the free pool. The T1 of the free pool is then decreased and the available longitudinal magnetization within it is reduced. These changes can be used in the design of pulse sequences to produce substantial changes in tissue contrast. (*Tanttu et al, 1990*)

The two-pool model provides a useful explanation for the changes in tissue contrast produced by off resonance saturating pulse, which are explicable in terms of a reduction in the available magnetization and T1. (*Campeau et al, 1995*)

Proton density weighted or mildly T1-weighted SE sequences may be used to exploit changes in the available longitudinal magnetization and T1. (*Soyer et al, 1997*)

With T1-weighted SE sequences, the reduction in available magnetization tends to reduce the net signal intensity, with the reduction T1 tend to increase it. As a result the net change produced by MT may be small. This reasoning applies in general to lesions with a prolonged T1 and T2 and may be different for those with a short T1. The contrast produced by MT sequences has been described as (T2-link). This occurs particularly with mildly or heavily T2-weighted sequences in which the principle effect of MT is a reduction in the available magnetization in soft tissues. The view that MT images are (T2-link) may be quiet misleading since MT images may also be angiogram like or (T1-link). It is important to realize that the parameters being changed with off resonance RF saturation are the available longitudinal magnetization and T1 and that tissue T2 values are not significantly affected by the saturation condition generally employed to manipulate MT in clinical imaging. Considerably it's worth noting that the effect of MT is to reduce the available magnetization and T1, which is the opposite of that produced by many acute and subacute diseases. There is thus scope for production of iso-intense appearances with MT depending on the sequence and whether the effect in the lesion is greater or less than that in normal tissue. Similarly, reductions in the signal intensity have been observed in normal liver, spleen, and kidney and this may result in an increase in the conspicuity of the lesion. The precise effect depends on the relative degree of MT in the normal and diseased tissue as well as the proton density and T1-weighted of the basic pulse sequence. (*Tanttu et al, 1990*)

Synergistic Enhancement of MRT with Gd-DTPA and Magnetization transfer

Introduction of paramagnetic substances increase the relaxation rates and decrease the level of saturation of the proton pool. Thus both the MT and the relaxation time contrast are sensitive to the concentration of paramagnetic substances. MT does not affect the signal emitted by tissues with a considerable concentration of paramagnetic ions as much as the signal emitted by tissues where macromolecules are the dominant source of relaxation. Application of the off-Resonance technique with paramagnetic contrast agents can be expected to augment the contrast enhancement further. (*Jukka et al, 1992*)

A typical NMR spectrum of biological tissue having no substantial lipid component consists of a narrow peak corresponding to the free hydrogen protons (Hf) and a broad peak corresponding to the protons related to the large macromolecules with restricted mobility (Hr). The peak of Hr is disposed symmetrically around the peak of Hf. The protons of Hr are not directly visible on MR, owing to their short T₂. However, Hr affects the observed relaxation rates of Hf via cross relaxation and chemical exchange. This interaction tends to equalize the level of saturation of Hr and Hf. therefore; a selective saturation of the magnetization of Hr has a saturating effect on Hf via this interaction. The MT technique involving the two interacting spin populations is one application phenomenon, which is called (over Hauser phenomenon). In the MT experiment the magnetization of Hr is saturated with an off-resonance irradiation pulse B₁. The effect of transferred saturation on the magnetization of HF is then observed. The amount of the transferred saturation is tissue dependant because the number of macromolecules in Hr, the cross relaxation rate between Hf and Hr, chemical exchange and other relaxation processes are tissue dependant. The signal emitted by the tissues with a high efficiency of interaction, e.g. due to a low macromolecular concentration. Thus the contrast between tissues with different macromolecular structures can be generated with MT techniques as with the relaxation-weighted technique, at the expense of decreased signal amplitudes. Pathological processes often decrease the macromolecule-to-water ratio of tissues, which results in increased relaxation times T₁, and T₂ and also a decreased MT between the proton pools. Thus, T₂ and MT contrasts are additive in this case. (*Tanttu et al, 1990*)

To study the MT effect the saturation of Hr should be performed without affecting Hf directly. Therefore the frequency offset should be large enough to avoid the direct saturation of Hf.

Relaxation along the effective field may also become important if the frequency offset is small. Magnetization transfer contrast seems to track the T₂ contrast in tissues. There are, however, two major exceptions: fatty tissues and tissues containing paramagnetic ions. Tissues with mobile fat molecules usually have a rather low concentration of macromolecules and therefore the MT effect is small. Paramagnetic substances shorten the relaxation times of both Hf and Hr compared with the cross-relaxation rate. Consequently the MT effect in tissues with a substantial concentration of paramagnetic ions is reduced. (*Tanttu et al, 1990*)

In general, Gd-DTPA would be expected to affect the free pool rather than the bound pool, but the degree to which this occurs may depend, for example on whether or not it crosses the blood-brain barrier. (*Joseph et al, 1992*)

Thus, in a MT-weighted image, the signal intensity of a tissue increases with the uptake of Gd-diethylenetriamine penta-acetic acid (DTPA). The simultaneous shortening of T1 increases the signal in the T1-weighted sequence. These mechanisms are the basis of the synergistic effect of Gd-DTPA and MT in T1-weighted images. Paramagnetic contrast agents reduce the T1 values and as discussed above, the MT effect. Contrast enhancement by paramagnetic substances and by the MT effect is thus additive. (*Tanttu et al, 1992*)

Technical Applications of MT pulse sequence

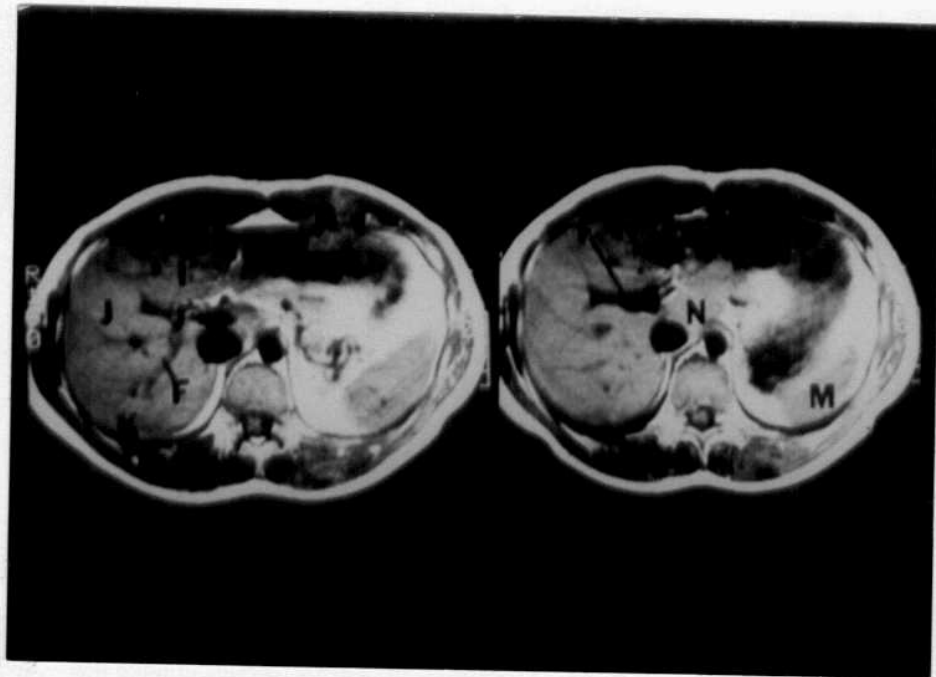
By using relatively small offset frequencies for the saturating irradiation, it is possible to considerably reduce the Rf power required to achieve useful saturation effects and thus remain within established guidelines for SAR even at higher fields. Concerns about power deposition at higher fields may therefore not be a major limitation to the application of this technique. (*Hajnal et al, 1992*)

Irradiating the macromolecular protons in tissue with a low power off-resonance radio frequency field generates magnetization transfer. This results in a decrease in water proton signal intensity where a tight magnetic coupling between water and macromolecules exists. The effect of changes in repetition time, echo-time, and flip angle were also quantitatively evaluated. The intensity of the MR image is decreased in relation to the magnitude of the magnetization exchange rate between the protons in water and those in macromolecules. This rate differs for various tissues, thus generating the tissue contrast associated with MTC. This magnetization transfer exchange process can be quantified in MR images, and has been found to be dependant on the surface chemistry as well as the correlation times of the macromolecules involved. MTC results in quantitatively superior contrast when compared with conventional spin-echo and three dimensional techniques. The lack of signal intensity change in fat and blood with use of irradiated RF pulse is due to their difference in properties. Fat protons do not exchange magnetization with water and are unaffected by the off-resonance irradiation. Blood not only contains a low concentration of macromolecules, but blood

flow prevents an effective saturation of these components by the elastic irradiation. (*Steven et al, 1991*)

Since the absolute interaction of water protons and the macromolecule can be quantities on an MR image, the actual chemistry of the desired tissue in vivo might be assessed non-invasively with this possibility. (*Wolff et al, 1991*)

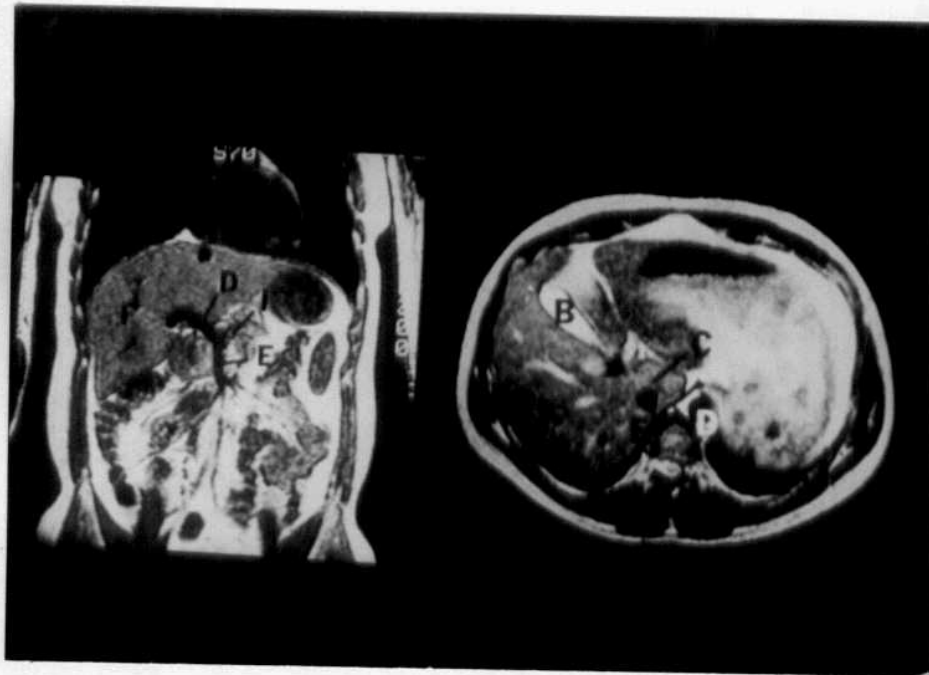
Magnetization transfer images have superior contrast without significantly increasing the time for data acquisition. The full MTC effect can be obtained with a TE of about 400 msec. /and that substantial effects can be generated with shorter Trs. (*Wolff et al, 1989*)

MRI OF THE UPPER ABDOMEN

(Figer. 4)

Magnetic resonance imaging has become a useful adjunct to the available imaging modalities for the abdomen. Its value for evaluation of hepatic neoplasms is well established, as is its ability to depict vascular and biliary anatomy in great detail. MR has become a primary imaging modality for diagnosis of liver tumors. Its value for the routine evaluation of the pancreas and luminal GI tract is not yet clear.

MR images may be obtained in multiple planes. For the upper abdomen, axial and coronal scans are generally the most useful. T1 and T2-weighted sequences are usually required. In selected cases, other imaging sequences are used.



(Figer. 5)

The normal spleen is slightly hypointense compared to normal liver on the T1-weighted (T1W) images. On the T2-weighted (T2W) images, the spleen is hyperintense compared to normal liver. The pancreas is isointense to normal liver on the T1W and T2W images. The normal pancreatic duct is not routinely identified on standard MR imaging. The gallbladder may appear hypointense or hyperintense on the T1W and T2W images. Fluid/fluid levels within the gallbladder are not abnormal. A normal common bile duct may be seen with MRI and usually appears hypointense on the T1W images and hyperintense on the T2W images. The vascular anatomy is well defined with MR.

M Spleen
 N Liver, caudate lobe
 O Pancreas, tail
 P Pancreas, body
 Q Pancreas, head
 R Portal confluence
 S Splenic vein

B Gallbladder
 C Liver - caudate lobe
 D Aorta
 E Inferior vena cava
 F Right portal vein
 G Ligamentum teres
 J Anterior segment right lobe
 K Posterior segment right lobe

PERCUTANEOUS TRANSHEPATIC CHOLANGIOGRAPHY (PTC):-

PTC is an invasive procedure, which is highly successful in determining the cause and site of bile duct obstruction in patients with obstructive jaundice, particularly when the non-invasive diagnostic scans, such as US and CT have shown the presence of dilated biliary tree. The information obtained from PTC can differentiate between Intrahepatic and extrahepatic cholestasis. (*Kumar et al, 1989*)

Technical aspects

The Chiba needle, originally popularized by *Okuda et al, 1974*, is used for diagnostic PTC. This skinny needle has a diameter of 22-23 gauge and is 6-3 inches long. It is made of flexible steel and has a thin inner core. The advent of Chiba needle has added greatly to its safety and success rates so that in expert hands, over 98% of dilated ducts and 80% of non dilated ducts can be punctured. (*Kumar et al, 1989*)

PTC is commonly done via the right lateral intercostal approach where the needle is introduced under aseptic precautions in the mid-axillary line at the 10th intercostal spaces. This approach is advantageous because the liver can be punctured adequately, leakage of bile or blood from the liver are prevented due to the long distance from the punctured bile duct, and the risk of gallbladder puncture is minimal. Less commonly, the anterior approach may be used and provides an easier and shorter route for external biliary drainage. (*Teplick et al, 1984*)

In the right lateral approach, the puncture is done under fluoroscopic control to avoid the costo-phrenic recess of the right pleura. However, this procedure has been also successfully done under US and CT guidance which enabled the needle puncture at the exact sites of duct dilatation. (*Todua et al, 1988*)

PTC has also been done blindly without any guidance in one series; this was successfully done in 24 out of 25 cases of suspected biliary tract obstruction, with few minimal complications. (*Kumar et al, 1989*)

The needle is then introduced and advanced through the liver parenchyma with about 20 degrees cranially, midway between the right dome of the diaphragm and air in the duodenal bulb. (*Todua et al, 1988*)

When the biliary tract is normal or minimally dilated, 6-7 needle punctures may be required to obtain intraductal position for the needle tip. *Harbin et al, (1980)* studied 200 cases that had PTC in a multi-institutional study. It was recommended not to limit the number of needle passes but to persist until the duct system is entered and opacified. (*Pereiras et al, 1982*)

Once the bile duct is entered, 10-15 ml of a contrast medium is slowly injected under fluoroscopic guidance. Whenever possible, equal volume of bile is aspirated before injecting the contrast material to avoid over distention of the biliary tract and to have better opacification. The aspirated bile can be also sent for cytology and microscopic examination and culture for antibiotic sensitivity. Complete filling of the intrahepatic ducts can be assisted by lowering the caudal end of the fluoroscopy table. Conversely, raising the head end of the table (semi-erect position) or turning the patient on his left side may be required when visualization and/or emptying of the extrahepatic ducts is delayed. (*Adam, 1989*)

While the presence of abnormalities in the cholangiograms implies the presence of a gross disease, a normal study does not exclude minimal or moderate disease. (*Harbin et al, 1980*)

Complications of PTC

The most important complications associated with PTC are bile leakage, bile peritonitis, systemic sepsis, cholangitis and bleeding. Less important problems include pain at the puncture site and allergic reaction to the contrast medium. Bile leakage is often minor and asymptomatic in most cases. Low-grade fever and mild tenderness over the right upper abdomen are sometimes found. (*Harbin et al, 1980*)

Systemic sepsis with high fever, rigors, circulatory collapse and leukocytosis indicate contamination of the blood by infected bile during the procedure, i.e. bacteraemia or septicemia. (*Blenkharn et al, 1984*)

The administration of parenteral broad-spectrum antibiotics prior to the procedure has to greatly reduce the incidence of its septic complications. (*Sacks et al, 1992*)

Bleeding is not uncommon after PTC. Its incidence is higher in patients with impaired hepatic functions and prolonged prothrombin time. This bleeding is often intra-abdominal, subhepatic or subdiaphragmatic. Sometimes, it occurs in the thoracic cavity resulting in haemothorax, lung collapse and respiratory distress. However, the use of the skinny Chiba needle has greatly reduced the incidence of this complication. (*Harbin et al, 1980*)

Prophylaxis against bleeding during PTC is achieved by the use of the skinny Chiba needle and correction of coagulation defects prior to the procedure. Prolonged PT is considered contraindications to PTC and its correction may require the parenteral administration of vitamin K (10-12mg/day) for few days. Fresh frozen plasma may be transfused to patients with gross coagulopathy problems. In addition, in patients with bleeding tendency, the number of punctures must be limited. (*Kumar et al, 1989*)

ENDOSCOPIC RETROGRADE CHOLANGIOPANCREATOGRAPHY (ERCP):

ERCP is a combined endoscopic and radiologic procedure that has been developed in 1970.

Instrument:

A side-viewing flexible, fiberoptic duodenoscope is commonly used. It is provided with special channels, the smaller is for flushing with normal saline solution to clean the surface of the lens and the mucosa and, also to inflate the stomach or duodenum with air. The other channel is larger enough to permit the passage and introduction of various diagnostic and therapeutic instruments, such as biopsy forceps, diathermy loop, Dormia stone baskets, cannulation catheters and biliary endoprotheses. (*Tweedle, 1985*)

Technical aspects

The patient has to be fasting for 6 hours before the procedure. Sedation is commonly achieved by intravenous administration of Diazepam. General anesthesia is indicated in pediatric group of patients. The duodenum is rendered atonic by the intravenous administration of 40mg of hyoscine butylbromide (Buscopan) and 0.5mg of glucagon. While the patient is in the left lateral position on the fluoroscopy table, the endoscope is slowly introduced into the oral cavity, pharynx, oesophagous, stomach and lastly, the duodenum. While the duodenoscope is advanced, the mucous membrane is examined for the presence of any pathologic conditions such as gastric or duodenal ulcers or tumors. (Shapiro, 1981)

The major duodenal papilla is identified as a pink elevation in the mucous membrane of the postromedial wall of the second part of the duodenum and is often has a hool-like covering in continuity with a circular mucosal fold. (Silvis & Vennes, 1985)

When the papilla is viewed "en-face", the cannula is introduced into the papillary orifice. The pancreatic duct is first cannulated, followed by the CBD where the contrast medium is injected. Standard water-soluble contrast medium such as Iohexol (Omnipaque) with a concentration of 15-35 % can be used. There is no evidence that any particular contrast is better. Too concentrated contrast medium may obscure small stones in the bile duct. The volume to be injected depends on the degree of dilatation of the pancreatic or bile duct systems. Films are obtained after proper filling of the ducts under fluoroscopic guidance. Raising or lowering the head-part of the fluoroscopy table may help to completely fill the ductal system and show the movement of stones in the dilated ducts. (Shapiro, 1981)

Difficulties during ERCP may be encountered in: (1) entering the duodenum, (2) identifying the duodenal papilla, (3) cannulating the ducts or (4) injecting the contrast material. Pyloric stenosis or duodenal obstruction often precludes the access to the ampulla. Cannulation of the papilla and terminal parts of the ducts, or impaction of a large calculus at papilla. (Silvis and Vennes, 1985)

Indications for ERCP:

ERCP has both diagnostic and therapeutic uses. As mentioned above ERCP not only can differentiate surgical from medical causes of cholestatic jaundice, but also demonstrates the site, level and in most cases, the cause of biliary tract obstruction. Additional diagnostic values include the endoscopic examination of upper gastrointestinal tract and the ability to obtain brush cytology and target biopsy from any suspicious lesion. ERCP is unique among the diagnostic modalities in providing both radiologic and endoscopic examinations in addition to the radiologic examination of both the biliary and pancreatic duct systems. The high diagnostic accuracy of ERCP has greatly reduced the need for exploratory laparotomy. (*Tweedle, 1985*)

ERCP is playing an increasing role in the diagnosis and management of children and neonates with disorders of the biliary tract. While therapeutic ERCP reduces the need for surgery, the pre-operative diagnostic ERCP provides surgeons with a "road map" when surgery is required. ERCP has successfully detected biliary Arteria, congenital biliary dilatation. (*Werlin, 1994-Shirai et al, 1993*)

Contraindications to ERCP

The uncooperative patient is an absolute contraindication to ERCP as it may cause injury to the patient, the duodenoscope or the endoscopist. This can be overcome by additional dose of sedative, or by performing the examination under general anesthesia particularly in children. Close monitoring of patients with cardiac or pulmonary diseases is required. (*Guelrud et al, 1992*)

Complications of ERCP:

It has been agreed that the rate of complication of ERCP is related to the operator experience. In experienced hands, a complication rate of 1-3 % may be anticipated, with a mortality rate of 0.1 % the major complications are pancreatitis and sepsis. Raised serum amylase can be observed after ERCP in 25-75 % of cases. It is generally asymptomatic and returns to its normal levels after few months. Severe acute pancreatitis with abdominal pain, fever and leucocytosis occurs in only 2% of cases. Pancreatitis after ERCP has been attributed to overfilling of the ducts or forceful injection of contrast medium into

the pancreatic ducts. This can be minimized by slowly injecting the contrast medium with constant fluoroscopic monitoring of duct filling. (*Shapiro, 1981*)

Pancreatic sepsis is a lethal complication with an incidence of 0.3 % therefore, if partial duct obstruction or pseudocyst is encountered, high dose antibiotic should be initiated immediately. There is a 0.8 % incidence of biliary sepsis and it almost always occurs in the presence of a partially obstructed bile duct. Thus, prophylactic coverage of antibiotic is advisable when cholangitis is anticipated by the presence of bile duct dilation detected by the other non-invasive imaging procedures such as US or CT. Moreover, the amount of contrast medium must be minimized, just enough to document the disorder. Other complications include cardiopulmonary complications, instrumental injury and drug reaction, which became increasingly reduced with increasing experience. (*Shapiro, 1981*)

RADIOISOTOPE SCANNING OF THE BILIARY TRACT:-

(BILIARY SCINTIGRAPHY)

Radiopharmaceutical agents:

The first agent available for hepatobiliary imaging was rosebengal sodium-labeled I^{131} . In the mid 1970s a new series of Tc^{99m} -labeled radiopharmaceuticals was developed to image the biliary tract. These agents give very high counting rate; have short half life (6 hours) and a relatively low radiation dose to the patient. The first agent of this group was Tc^{99m} labeled N-iminodiacetic acid (IDA), also known as Tc^{99m} HIDA (2, 6 dimethyl IDA). The other agents now being used are the para-isopropyl IDA (PIPIDA or Iprofenin) and diisopropyl IDA (DISIDA or Desofenin). These agent are all taken up by the hepatocytes and immediately excreted unconjugated into the biliary tract. (*Drane, 1991*)

Administration dosage:

The dose required in non-jaundiced patients is 2-5 mCi, given by intra venous injection. With hepatic dysfunction and raised serum bilirubin the amount of radioactivity, particularly HIDA which is taken up by the liver cells,

is reduced. This may indicate an increase in the dose of the agent for jaundiced patients to 5-10 mCi. The newer DISIDA derivative is reported to yield prompt biliary visualisation at very high serum bilirubin levels (as high as 15-30 mg/dl) and appears to be the best overall agent available at present. (*Stadalnik & Matolo, 1981*)

Technical aspects:

The preparation of the patients for this examination consists of fasting for 6 hours, if the gallbladder is aimed as a part of the study, otherwise fasting is not necessary when the technique is essentially employed for tracing the bile flow. This will prevent false positive studies for non-functioning gallbladder caused by the physiologic contraction of the gallbladder. The isotope is intravenously administered while the patient is in the supine position beneath the scintillation gamma camera. The detection of radioactivity is dependant on the interaction of radiation with matter. When it is struck by a photon of X- or gamma rays, it scintillates or gives off energy as a flash of light. The relationship between the energy of the gamma rays and the amount of light produced is critical to the production of good quality scintigraphy images. Images are obtained at 5, 15, 45 and 60 minutes after injection of the agent. Additional images obtained at 2-6 hours and at 24 hours (with a low-energy high-sensitivity collimator) after injection if obstruction is suspected when the extrahepatic system or intestine is not visualized at 1 hour. (*Maurer & Malmud, 1992*)

Normal study:

Within the first few minutes after administration, the radioisotope begins to concentrate in the liver parenchyma. The majority of the radioactivity becomes maximally concentrated in the liver within 15-30 minutes after injection. This is followed by excretion of the radioactivity in the bile ducts and the gallbladder. The gallbladder and the gastrointestinal tract are typically well visualized within one hour. Images are routinely obtained in the anterior view. However, left anterior oblique and right lateral views are often used to avoid the overlap of both biliary and renal activities. (*Vitti & Malmud, 1992*)

Diagnostic value:

The following table shows the clinical indications for Tc^{99m} biliary tract imaging. (Stadalink & Hoffer, 1987)

1. Obstruction of the cystic duct
2. Evaluation of cold defects seen in the liver
3. Study of biliary kinetics
4. Evaluation of post surgical biliary system, bile leakage gallbladder perforation, cholecystocolic fistula or biliary enteric anastomoses
5. Paediatrics:
 - a. Infants Biliary atresia , neonatal hepatitis
 - b. Choledochal cyst
6. predictive value in patients with nonvisualization of gallbladder after oral cholecystography
7. Detection of liver disease; dissociation of reticuloendothelial and hepatocyte function.

[Table 3]: clinical indications for Tc^{99m} biliary scintigraphy
(From: Stadalnik & Hoffer, 1987)

Biliary scintigraphy can be useful in evaluating patients with jaundice. The appearance of radioactivity in the bile ducts and bowel rules out complete biliary tract obstruction. Acute obstruction of the CBD is associated with non-visualization of the biliary tree and the intestine up to 24 injection. Occasionally, Intrahepatic cholestasis (drug-induced) may also produce similar findings. In case of partial obstruction of the biliary tract it may appear as dilated structures proximal to the stenosing lesion. In addition, the gastrointestinal visualization is delayed and the gallbladder may be distended. (Stadalink & Hoffer, 1987)

Egbert *et al*, (1983) reported that the differentiation between extrahepatic biliary obstruction and Hepatocellular disease by Tc^{99m} alone is relatively difficult, particularly in the absence of dilated bile ducts.

Impaired tracer excretion in patient with relatively low serum bilirubin levels (10 mg/dl or less) is most likely associated with biliary tract obstruction.

In patient with higher serum biliary levels and tracer excretion the study tends to be equivocal or non-diagnostic, as this can be due to either an advanced Hepatocellular disease or complete biliary tract obstruction. Thus, accuracy of biliary scintigraphy in the evaluation of jaundiced patients is much better when serum bilirubin level is relatively low. In the absence of Hepatocellular disease, the most reliable characterization of biliary tract obstruction was found to be the stasis of radioactivity in the CBD. (*Molenda & Brykalski, 1992-Kloiber et al, 1988*)

In comparison to ultrasound, Tc^{99m} scan is more useful in the diagnosis of acute or early biliary obstruction, when serum bilirubin is low and no dilated ducts are seen on US examination. (*Shah et al, 1988*)

ANGIOGRAPHY OF THE LIVER AND GALLBLADDER:-

Angiographic technique:-

Patient selection:-

Patient selection for hepatic angiography should be based on the underlying pathology and the likelihood that diagnostic angiography will be beneficial in treatment planning for the patient. In addition, certain patient characteristic most is evaluated prior to performing angiography in a safe and effective manner. (*Scott et al, 1998*)

Prior to diagnostic angiography, many physicians will obtain routine preprocedure laboratory tests such as coagulation studies and serum creatinine. Some autherors advocate only obtaining serum creatinine levels for peripheral diagnostic angiography. (*Roberts, 1994*)

However, patients with hepatobiliary disease may be at higher risk of compromise of hepatic synthetic function and should be considered a separate patient population with regard to preprocedure testing. Decisions about routine laboratory tests are best made on a case-by-case basis. Finally, safe vascular access must be feasible, preferably from a femoral arterial approach. (Cowling, et al, 1996)

General Technical Considerations:-

1- Celiac and SMA Angiography

Angiography of the liver and pancreas is performed by selective injections of the celiac axis and SMA or one or more of their branches. Routine patient preparation and use of a Seldinger technique is typically performed from a common femoral artery approach. Due to the angle of origin of the celiac axis and SMA (usually 90° to 135° in relation to the long axis of the aorta), a right angle or reverse curve catheter such as a Cobra or Simmons is usually the most useful. Catheter size varies from 4 to 7 Fr in diameter, with larger catheter providing greater stability and flow rates, but higher risk of catheter related vascular complications. Although contrast injection rates vary due to the type of pathology being assessed, typical injection rates in the celiac axis would be about 7-8 cc/sec for cut-film angiography and 5-6 cc/sec for digital subtraction angiography (DSA). The contrast volume needed to evaluate the arterial flow is approximately 20-30 cc. Most information can be obtained in standard PA or AP projections. (Scott et al, 1998)

Selective catheterization of the main celiac branches can usually be performed with a standard catheter-wire combination, although use of a hydrophilic guidewire is often helpful. Most currently commercially available coaxial systems use a 5-Fr outer or guiding catheter placed into the main artery. Superselective injections of the pancreatic vessels usually require a coaxial system, with selection of the specific pancreatic branch being performed with the inner 3-Fr catheter. (Cowling, et al, 1996)

2- Visualization of the Portal Venous System

Visualization of the portal venous system is most often performed by using an arterial injection of either the splenic artery or SMA in conjunction with prolonged filming (arterial portography). Injection of either the splenic

artery or the SMA is equally efficacious in allowing filling of the portal system. (McDermott *et al*, 1996)

To further increase visualization of the portal system, injection of vasodilator such as papaverine hydrochloride or priscoline into the SMA just prior to contrast injection. (Soyer *et al*, 1993)

Technically, arterial portography is performed as a splenic or SMA arteriogram with the following caveats: filming must be prolonged to at least 15 sec, and contrast injection volumes must be increased to at least 40 cc for digital subtraction technique and 50-60 cc for cut-film technique. (Scott *et al*, 1998)

Although infrequently used currently, other methods of accessing the portal vein have been described and include direct percutaneous transhepatic puncture of the portal vein, percutaneous puncture of the splenic pulp and contrast injection (splenoportography), catheterization of recanalized portal vein tributaries such as the umbilical vein, and minilaparotomy. The main advantage of such direct catheterization methods is that in addition to diagnostic studies, interventions such as embolotherapy of bleeding portal venous collaterals can be performed. (Durham *et al*, 1995)

3- Free and Wedge Hepatic Venography

Hepatic venography may be used as a diagnostic tool to evaluate central veins for obstruction as well as evaluation of hepatic parenchyma and portal vein during wedge venography. In addition, particularly with the advent of Transjuglar Intrahepatic Portosystemic Shunts (TIPS), free wedge venography may be performed to assess pressure measurements to assist in evaluating the severity of portal hypertension before and after the TIPS procedure. (Scott *et al*, 1993)

Cannulation of the hepatic veins typically occurs from a right internal jugular vein approach due to the relatively straight access obtained through the superior vena cava and right atrium. If necessary, a femoral vein approach may be used, however, the severe angle between the IVC and hepatic veins (90° to 135°) can make catheter exchanges and superselection difficult. The right hepatic vein typically has a separate drainage into the IVC, while the middle and left hepatic veins frequently form a trunk prior to entering the IVC. Differentiating the two hepatic veins can best be performed by noticing the angle used to catheterize the vessels. If the catheter is directed laterally the right

hepatic vein is selected, while if the catheter is directed ventrally the middle hepatic vein is catheterized. (*McDermott et al, 1996*)

Once the catheter has been placed, contrast injection (5-6 cc/sec for 2-3 sec) can be performed to obtain a free hepatic venogram. By advancing the catheter more deeply into the liver and wedging the catheter tip into the liver parenchyma, a wedge hepatic venogram can be obtained. This is performed by a hand injection of contrast material, the volume of injection depending on the underlying liver pathology as well as visualization of the portal vein. Wedge hepatic venography allows visualization of the portal vein by forcing contrast into the hepatic sinusoids and retrograde filling of the portal vein. Utilization of carbon dioxide as a contrast agent has been shown to provide excellent visualization of the portal venous system. (*Ress et al, 1994*)

PATHOLOGY OF HEPATIC FOCAL DISEASE

The liver is functionally complex organ involved in manufacture of proteins, metabolism of carbohydrates and excretion and detoxification of metabolites. It is also one of the most frequently injured organ in the body and target of a wide range of inflammatory, neoplastic and circulatory disturbances, all of which have an impact on hepatic function. (*Bluemke et al, 1995*)

The classification of hepatic focal diseases is mentioned in the following table (*Stephens et al, 1977*)

1-Congenital:

- Unifocal cyst.
- Polycystic liver disease.

2-Traumatic injury.

3-Bacterial and parasitic liver infections, which include:

- A-Pyogenic hepatic abscess.
- B-Amoebic hepatic abscess.
- C-Echinococcosis (Hydatidosis).
- D-Fungal abscess (candidiasis).

4-Sarcoidosis.

5-Hepatic tumours: Which are classified into:-

A-Benign hepatic tumours.

B-Malignant hepatic tumours.

A. Benign hepatic tumours include:

A.Hepatocellular tumours, which are:

- 1-Hepatocellular adenoma.
- 2-Focal nodular hyperplasia.
- 3-Nodular transformation.

B.Bile duct tumours, which are:

- 1-Bile duct Hamartoma.
- 2-Biliary Cystadenoma.

C.Vascular tumours, which are:

- 1-Cavernous Haemangioma.
- 2-Infantile Haemangioendothelioma.
- 3-Peliosis hepatis.

D.Mesenchymal Hamartoma.

B. Malignant hepatic tumours include:

1-Primary hepatic tumours:

- a.Hepatocellular carcinoma.
- b.Intrahepatic cholangiocarcinoma.
- c.Combined hepatocellular-cholangiocarcinoma.
- d.Hepatoblastoma.
- e.Angiosarcoma.
- f.Epithelioid haemangioendothelioma.

2-secondary hepatic tumours: metastatic hepatic tumours developed mainly from carcinoma of the lung, breast, colon, or pancreas. Lymphoma and leukaemia also metastasis to the liver. (*Stephens et al, 1977*)

<i>1-Congenital:</i>	1-Unifocal cyst. 2-Polycystic liver disease
<i>2-Traumatic injury.</i>	1-Subcapsular haematoma. 2-Intrahepatic haematoma. 3-Bile pseudocyst. 4-Pseudoaneurysm.
<i>3-Bacterial and parasitic liver infections</i>	A-Pyogenic hepatic abscess. B-Amoebic hepatic abscess. C-Echinococcosis (Hydatidosis). D-Fungal abscess (candidiasis).
<i>4-Sarcoidosis.</i>	
<i>5-Hepatic tumours:</i>	
<i>A-Benign hepatic tumours</i>	
a.Hepatocellular	1-Hepatocellular adenoma. 2-Focal nodular hyperplasia. 3-Nodular transformation.
b.Bile duct	1-Bile duct Hamartoma. 2-Biliary Cystadenoma.
c.Vascular	1-Cavernous Haemangioma. 2-Infantile haemangioendothelioma. 3-Peliosis hepatis.
d.Mesenchymal Hamartoma.	
<i>B. Malignant hepatic tumours</i>	
<i>1-Primary hepatic tumours:</i>	a.Hepatocellular carcinoma. b.Intrahepatic cholangiocarcinoma. c.Combined hepatocellular-cholangiocarcinoma d.Hepatoblastoma. e.Angiosarcoma. f.Epithelioid haemangioendothelioma
<i>2-secondary hepatic tumours:</i>	Metastasis from carcinoma of the lung, breast, colon or pancreas.

[Table 4] Focal hepatic lesions
After (*Stephens et al, 1977*).

1-congenital cysts:

Hepatic cysts are common and often multiple. They usually are asymptomatic unless they are very large. Multiple liver cysts are found in over 50% of patient with polycystic kidney disease, complication of cysts in this disease are rare but tumour, infection, and biliary obstruction have been described with it. (*Levine et al, 1985*)

Hepatic cysts vary in size from a few millimeters to several centimeters in diameter and appear as sharply delineated, round or oval lesions. There is no internal separation and the cyst wall is very thin layer of fibrous tissue (less than 1mm thickness). It is surrounded by normal hepatic parenchyma, although the simple hepatic cyst thought to be of congenital, developmental origin, usually it is discovered in adults. (*Litwin et al, 1987*)

Hepatic cysts can occur singly, in small numbers, or as numerable multifocal cysts in polycystic disease. Congenital hepatic fibrosis and polycystic disease are part of the spectrum of fibropolycystic disease of the liver. Typically, the cysts of congenital hepatic fibrosis are only visible with magnification. However, numerous large and small cysts, which are pathologically identical to simple, or bile duct cysts are present with fibrosis in polycystic liver disease. In polycystic liver and /or kidney disease, the liver is not normal and frequently contains hamartomas and increased fibrous tissue. Hepatic involvement occurred in 30% to 40% of patients with polycystic kidney disease. Most patients with congenital hepatic fibrosis present in childhood with complications of portal hypertension such as bleeding varices. (*Kairaluoma et al, 1989*)

2-Traumatic cyst:

Traumatic injuries to the liver can occur as a result of blunt or penetrating abdominal trauma and as a complication of surgery, percutaneous cholangiography, biopsy, portography or biliary drainage procedures. Injuries include intrahepatic and subcapsular haematoma laceration, hepatic necrosis, bile pseudocyst pseudoaneurysm, arteriovenous and arterioportal fistula and intraperitoneal bleeding. The most common hepatic injuries are lacerations, subcapsular and intrahepatic haematomas resulting from blunt abdominal trauma, percutaneous transhepatic cholangiography, or liver biopsy. (*Federle et al, 1981*)

Hepatic artery pseudoaneurysm and arteriovenous or arterioportal fistulae are all potential sequelae of hepatic vascular injury. Of hepatic vascular injury. Traumatic hepatic injuries are less frequent than those of kidneys and spleen, but they have a high mortality rate. (Foley *et al*, 1980)

Whereas most intrahepatic haematomas and contusions resolve spontaneously within weeks to several months. Post-traumatic cysts or pseudoaneurysm may develop in some cases. Bilomas or bile pseudocysts usually are subcapsular or perihepatic in location. They are caused by iatrogenic, spontaneous or traumatic perforation of the biliary system, they usually present as large homogenous, thin walled fluid collections. (Federle *et al*, 1981)

3-Echinococcosis (Hydatid cyst):

Echinococcosis is the most common cause of hepatic cysts worldwide, with a particularly high incidence in the Middle East, Greece, Australia and some parts of South America. It is caused by cestodes (tapeworms) of the genus echinococcosis. Echinococcosis granulose (the agent of cystic Hydatid disease) is the most common curative type. Infection by *E. multilocularis* (alveolar Hydatid disease) is less frequent, this disorder may mimic a solid neoplasm and it is found in central Europe, Russia, Alaska, Japan and USA. In both forms, the liver is the most frequent involved organ.

The dog is the definitive host for echinococcus granulose, 70% of echinococcal cysts are found in the liver, where they most commonly appear as single lesions of the right lobe. The cysts are unilocular and fluid filled, the germinal layer gives rise to broad capsules attached by a short stalk. Scolices (future head of adult worm) develop within broad capsules; they contain a double row of hooklets. Detached broad capsules are called daughter cysts, calcification of the cyst outer wall, occur in up to 20% and can be detected radiographically. Although the identification of daughter cysts is virtually pathognomonic of echinococcal granulosis infestation, other multiloculated cysts may simulate echinococcosis. (Schnyder *et al*, 1979)

Clinically, it varies depending on the site, the stage of development, and whether the cyst is alive or dead. The uncomplicated (unruptured) hydatid cyst may be silent and found incidentally at autopsy. It should be suspected if a rounded, smooth swelling continuous with the liver is found in a patient who is not obviously ill. (Schnyder *et al*, 1979)

4-Fungal abscess:

Fungal abscess is mainly caused by candida albicans. Hepatic abscesses resulting from fungal infection are uncommon and usually occurs in-patient who have compromised immunologic systems. Although large single or multiple abscesses due to fungal infections do occur, a pattern of multiple micro abscesses have been more frequently observed in patient with acute myelogenous and lymphocytic leukaemia. These are often clinically suspected owing to elevation of the liver function tests in-patient who is immunosuppressed. Fungal disease in the liver is also associated with pregnancy and total parenteral nutrition. (*Bluemke et al, 1995*)

5-Sarcoidosis of the liver:

Sarcoidosis is a multisystem granulomatous disorders of unknown cause. Pulmonary manifestation are common and occur as non caseating, non-necrotising granulomas are found in 40% of patient with sarcoidosis but they are also common in other diseases particularly primary biliary cirrhosis. (*Walter et al, 1996*)

In gross appearance, the sarcoid tissue is pearly grey in colour and forms discrete or confluent masses in the liver, which all may be clinically palpable. (*Warshauer et al, 1995*)

An important diagnostic test is the Kveim test, in which an extract of sarcoid tissue (usually obtained from patient's spleen) produces a much-delayed inflammatory reaction when injected intradermally into a patient with sarcoidosis. The test is virtually pathognomonic when positive (it is occasionally negative in long standing disease) but it is important to use a reliable source of sarcoid tissue. The test is read by selctioning a biopsy of the lesion 4-6 weeks after injection. A positive result is indicated by the presence of non caseating (sarcoid) granulomas in the dermis. (*Walter and Israel, 1996*)

In 5% to 15% of cases sarcoidosis manifests as multiple, low attenuation nodules. This appearance can be easily mistaken for metastatic disease or infection; however, differentiation can be established by CT through the association between the nodules, hepatosplenomegally and abdominal adenopathy. The most common site of lymph node involvement was found to be

the porta hepatis, followed by the paraortic region, celiac, superior mesenteric artery, retrocruial and mesenteric areas. (*Warshauer et al, 1995*)

The reason of some patients with marked organ enlargement without nodules but others with normal or only mildly enlarged viscera with marked nodularity is unclear. (*Bach et al, 1991*)

6- pyogenic liver abscess:

The most common cause of pyogenic liver abscess is biliary obstruction, which leads to ascending cholangitis (cholangitic abscess). Other causes include bacterial seeding of portal venous blood (pyelophlebitic abscess, occurring with intra-abdominal sepsis) and bacterial seeding of hepatic arterial blood (accompanying generalized bacterimia or distant localized infection). (*Brown et al, 1986*)

In about 20% of cases, the bacterial source is unknown; half the cases involve more than one type of microbe, often including anaerobes. *Escherichia coli* are the most common causative organism. Pathologically, abscess may be single or multiple and usually appears in the posterior segment of right lobe of the liver. It consists of creamy, yellow, foul smelling pus containing necrotic liver tissue. (*Scott et al, 1993*)

Patient having a pyogenic liver abscess usually presents with fever and abdominal pain, occasionally hepatomegally and rarely jaundice. Approximately 20% to 30% of pyogenic abscesses contain gas, where as amoebic abscess does not contain gas unless secondary infected, abscess usually has a well-defined outer margin, thick capsule and irregular inner margin. A chronic solitary liver abscess may persist for as long as two years before death on diagnosis. (*Mc Donald et al, 1984*)

They frequently have a well defined outer margin may have a thin capsule or irregular inner margins. The cavities may appear homogeneous, or they may contain material of different densities. Aggregates of solid matter often gravitate to the dependant part of a cavity, where as gas tends to rise giving an air-fluid level. The location of these substances however, may be affected by the viscosity and specific gravity of the fluid or by the presence of internal adhesions. (*Bluemke et al, 1995*)

7- amoebic liver abscess:

Entamoeba histolytica exists in a free-living vegetative form and as cysts, which survive outside the body and are highly infectious. Amoeba reaches the liver through portal blood. Hepatic abscess is the most common extraintestinal complication of amoebiasis. Amoebic abscess usually appears in the periphery of the liver near the border of adjacent viable hepatic tissue. The amoebic abscess usually varies in size, the most frequently site is the right lobe, often supero-anteriorly just below the diaphragm. Initially, the abscess has no defined wall. It is most frequent in middle-aged males between 30-50 years; they are affected 3 to 10 times more than females. (Greany et al, 1985)

The onset is usually gradual but rarely may be sudden with rigors and sweating. Fever is variously intermitted, remittent or even absent unless an abscess becomes secondary infected. (Greany et al, 1985)

Differentiation between pyogenic abscess and amoebic abscess is sometimes impossible, even after guided aspiration of the contents, since most of amoebic liver abscesses present after secondary infection. Biopsy from the wall of the abscess to visualize the parasite is the only method to differentiate between them. (Terrier et al, 1983)

In many cases the diagnosis is already known or strongly suspected and the role of imaging procedure is to confirm the presence of abscess and to determine the location, extent, and number of lesions. CT and ultrasound, because of their ability to define the size of these abscesses, are excellent methods to monitor the response to medical therapy. (Baret et al, 1980)

8-hepatic tumours:

A-Benign Hepatic Tumours:

a- Hepatocellular Adenoma (HA):

About 95% of patient with Hepatocellular adenoma are female (mostly between 30 to 50 years). In up to 90% of cases, the tumour presumably stems from oral contraceptive use. It also arises in men on hormonal therapy (androgens also may induce it). (Freeny et al, 1981)

Haemorrhage and growth of the liver cell adenomas may occur despite of the stoppage of oral contraceptive pills and therefore surgical resection remains the therapy of choice for symptomatic liver cell adenomas. (*Mariani et al, 1989*)

Hepatocellular adenoma usually appears as a solitary subcapsular, well circumscribed mass in a noncirrhotic liver, its diameter ranges from 5 to 15 cm. occasionally, and extensive haemorrhagic necrosis causes the tumour to resemble a haematoma. The tumour is a well-encapsulated, true hepatic neoplasm and it is composed entirely of hepatocytes, the hepatocytes and capsule may be vacuolated by fat globules, fibrous septations. Bile ducts and Kupffer cells are not found. Clinically, liver with adenomas is usually asymptomatic until growth of the tumour produces an abdominal mass or massive haemorrhage in the tumour occurs which may lead to shock and even death. (*Mariani et al, 1989*)

b- Focal Nodular Hyperplasia (FNH):

This tumour affects woman aged between 30 to 50 years. Only 5% to 15% of patient is a male. An abdominal mass is the most common presenting sign; however, the tumour is an incidental finding in 50% to 80% of cases. Focal nodular hyperplasia typically occurs as a solitary, well circumscribed, subcapsular nodular mass with a diameter of less than 5 cm on diameter, fibrous septa that divide the lesion into nodules, merge centrally or eccentrically to form a scar. It is mainly composed of Kupffer cells, hepatocytes and bile ducts. (*Scott et al, 1993*)

Haemorrhage, necrosis and malignant degeneration are very rare and the vast majority of patient remains entirely asymptomatic. As a result of the benign nature of focal nodular hyperplasia, no therapy is recommended unless torsion, infarction and / or lesion size forces for surgical resection. FNH lesions may be single or multiple and usually are discrete. (*Bluemke et al, 1995*)

Several articles have considered calcification as one of the major radiologic clues to diagnose fibrolamellar HCC, however calcification in FNH may occur, the exact mechanism of calcification in FNH is unclear, however, Filipe Caseiro considered this focal lesion to be a vascular malformation, thus thrombotic phenomena may occur owing to turbulent flow and subsequent platelets injury which may predispose to fibrosis and subsequent calcification. (*Caseiro et al, 1996*)

Hepatic scintigraphy with sulphur colloid may be especially helpful. In about 50% of patient there is uptake of sulphur colloid particles within the lesion to the same degree or to greater degree than within normal surrounding liver. (*Bluemke et al, 1995*)

c- Cavernous Haemangioma:

It is one of the most common benign hepatic tumours, it is found in about 5% of routine autopsies. It most likely represents a hamartomatous malformation rather than a true neoplasm. Most of these tumours do not cause symptoms and are found incidentally, but giant lesions may cause abdominal pain or bleeding. Cavernous Haemangioma typically is solitary and soft with a diameter of less than 2 to 4 cm (one with a diameter greater than 4 to 10 cm is termed a giant cavernous Haemangioma). More than 70% of cavernous Haemangioma occur in women and although all ages are affected, it is rarely diagnosed before adulthood. (*Bluemke et al, 1995*)

Differentiation of cavernous Haemangioma from hepatic metastases can be made after contrast enhanced CT according to the following findings:

1-Type of enhancement: globular, linear, diffuse and homogenous or diffuse and heterogeneous (globular enhancement was considered to be present when enhancing nodules less than 1 cm in diameter was seen within the lesions).

2-Continuity of enhancement continuous or noncontinuous: (uninterrupted collections of contrast material within at least 50% of a lesion, either peripherally or centrally, were considered continuous. Multiple, separate collections of contrast material were considered noncontinuous).

3-degree of enhancement: hypo, iso or hyperdense relative to the aorta.

4-distribution of enhancement: peripheral, central or mixed. (*Silverman et al, 1995*)

d- Nodular Regenerative Hyperplasia (Nodular Transformation)

This condition typically affects persons between the ages of 40 and 70 years. Often confused with cirrhosis, it represents a form of noncirrhotic portal hypertension. Conditions associated with nodular transformation include connective tissue disease (especially rheumatoid arthritis and the variants of scleroderma), myeloproliferative and lymphoproliferative disorders. (*Scott et al, 1993*)

Some patients have a history of cytotoxic or immunosuppressive drug use; the liver shows nodules measuring from 1 to 4 cm in diameter, which may almost completely replace the hepatic parenchyma. The nodules may be mistaken for cirrhosis or a metastatic tumour. Tumour rupture, hepatic failure and bleeding oesophageal varices are important causes of tumour related fatality. (*Virginia et al, 1993*)

e- Bile Duct Hamartoma (Von Meyenburgh's complex) and Bile Duct Adenoma:

Hamartomas are much commonly found than adenomas. These tumours appear as small, firm grayish-white subcapsular masses usually less than 1 cm in diameter. Hamartomas may be multiple but adenomas usually occur as solitary lesions. Multiple Hamartomas may grossly simulate metastatic carcinoma, abscesses or multiple granulomas. It may be associated with polycystic liver disease and increase fibrous tissue. (*Power et al, 1994*)

f- Biliary Cystadenoma:

It is a rare benign tumour arising from the common bile duct as well as the body and tail of pancreas in elderly women. It is usually divided into two types: microcystic Cystadenoma and mucinous Cystadenoma. Microcystic Cystadenoma is a multilocular tumour that reaches up to 10 cm in diameter, it is an incidental finding, but when present when in the head of pancreas it may be associated with gastrointestinal bleeding. (*Virginia et al, 1993*)

Mucinous Cystadenoma occurs chiefly in women from the fifth to seventh decades, small foci of carcinoma in situ or even invasive carcinoma may be found in a largely benign appearing mucinous Cystadenoma, it has a great potentiality to be a malignant neoplasm. This tumour is most multilocular, large and filled with sticky mucus. (*Virginia et al 1993*)

g- Infantile Haemangioendothelioma (IHE):

This is the most common mesenchymal liver tumour among children. Nearly 90% of patients are less than 6 months old at the time of diagnosis. In about half the cases, the tumour is found incidentally. The tumour may be solitary or multicentric with a nodule diameter ranging from 0.2 to 15 cm. (*Scott et al 1993*)

IHE accounts for 12% of all childhood hepatic tumours with females being affected more often than males. Hepatomegally and congestive heart failure may occur in up to 25% of cases. Thrombocytopenia due to trapping of platelets by the tumour, and occasional rupture with haemoperitoneum may also be seen. (*Powers et al, 1994*)

Cutaneous haemangiomas may be associated with the multinodular form of IHE (occurring in up to 40% of patients) and may involve other organs. Although IHE may grow to a large size with resulting haemodynamic compromise, spontaneous involution will occur with time if the child survives. (*Powers et al, 1994*)

h- Peliosis Hepatis:

Initially linked with such wasting disease as tuberculosis and cancer, recently it has associated with steroids and contraceptive use. Usually, it is discovered accidentally, however in some patients it leads to sever hepatic dysfunction, hepatic rupture and even death. It appears as a multiple reddish-purple, blood filled spaces measuring 0.2 to 5 cm in diameter, giving the liver honeycombed appearance. (*John et al 1993*)

Recently, it has been recognized as vasoproliferative disorder of the liver, which is associated with infection caused by *Rochalimaea* species affecting patients with human immunodeficiency virus. (*Bluemke et al, 1995*)

i- Mesenchymal Hamartoma:

This congenital malformation is the second most common benign liver tumour of childhood after IHE. The tumour measures about 15 cm or more in diameter, usually show both solid and cystic areas. It is a well-defined tumour that may be encapsulated or pedunculated. Mesenchymal Hamartoma is uncommon and accounts for only 8% of all childhood liver masses. The majority of cases are found by age three years with a slight male predominance. Although usually slow, progressive, painless abdominal enlargement is seen, occasionally rapid enlargement may result from rapid fluid accumulation in the cysts. Mass effect from the bulky tumour may cause respiratory distress and lower extremity oedema. No tendency to malignant transformation has been reported. (*John et al, 1993*)

B-Malignant Hepatic Tumours:-

I-Primary hepatic malignancy:-

1-Hepatocellular carcinoma

Incidence:

The highest incidence rate is in sub-Saharan tropical Africa and South-East Asia (China and Japan), with a rate of over 100 per 100,000. the highest incidence in the world is in Mozambique where it constitutes two-thirds of male cancers and one third of female cancers. The median age is 30 years in high incidence areas and 56 years in the west. Male predominance is 8:1 in high incidence areas and 3:1 in low incidence areas. (*El Bolkainy, 1998*)

Etiology:-

- 1) *Hepatotropic virus:* namely hepatitis B virus (HBV) and hepatitis C virus (HCV). In Africa and China HBV is endemic, but in USA and Japan HCV predominates.
- 2) *Hepatocarcinogens:* such as Alfa-toxins (a product of the fungus *Aspergillus flavus* contaminating grains), anabolic steroids, contraceptive pills and estrogens.
- 3) *Chronic liver disease:* such as cirrhosis (viral or alcohol induced), genetic hemochromatosis and hereditary tyrosinemia.

Pathogenesis:-

Both chronic liver disease and malignancy are more frequent complications of HCV than HBV. Thus, the development of HCC after 15 years is 27% in HBV and 75% in HCV infections. The role of the virus is properly indirect by producing liver necrosis, with subsequent regeneration and cirrhosis. Liver cells dysplasia, particularly the large cell type, is considered a precancerous lesion. The yearly incidence rate of malignancy in patients with cirrhosis is 3% both in Africa and the West. Recently, direct role of the virus is considered possible. Thus, the virus genome after integration into DNA may encode a regularity element (X-protein) that transactivates cellular protooncogenes. Another possible role of viral oncoprotein is to inactivate protein product. (*El Bolkainy, 1998*)

Repeated cycles of cell death and regeneration are important in the pathogenesis of HBV-HCV associated liver cancers. The accumulation of mutations during continuous cycles of cell division may eventually transform some hepatocytes. (*Greissler et al, 1997*)

In virtually all cases of HBV-associated liver cancer, viral DNA is integrated into host cell genome, and the tumours are clonal with respect to their insertions. Despite of our incomplete understanding of HCC carcinogenesis, one fact is clear: universal vaccination of children against HBV in endemic areas may dramatically decrease the incidence of HCC. (*Collins et al, 1999*)

Pathology:-

Grossly, HCC appears yellowish or greenish in color. Collaborative multinational study of HCC determined three major patterns of tumour growth, namely: expanding, spreading and multifocal. Unclassified cases constitute 23% of cases because of large advanced growth. Expanding tumours affect non-cirrhotic livers and grow by expansion compressing surrounding tissues. Sclerosing tumours (fibrolamellar) are a subtype of the expanding variant. (*Okuda, 1984*)

Six histological variants are recognized in HCC, namely: trabecular, solid, acinar, fibrolamellar, clear cell, and pleomorphic. Normally, the liver cell plate lying in between two sinuses is only one cell thick. In HCC the liver plate is stratified, Kupffer cells are absent and the trabeculae dissociate from each other with widening of the sinuses. In the solid type the sinuses are compressed. In the acinar type the cells are arranged around a central lumen, which may be, contain bile. Fibrolamellar carcinoma arises in non-cirrhotic liver and is characterized by groups of polygonal cells with eosinophilic cytoplasm surrounded by a markedly fibrotic stroma. (*Crawford, Cartran, et al, 1994*)

The cells of HCC are characterized by cytoplasmic eosinophilia, hyaline cytoplasm inclusions, prominence of nucleoli and nuclear inclusions of cytoplasmic origin. Needle aspiration cytology may be done to distinguish between HCC and metastases. Features favoring HCC include:

- Polygonal nuclei with centrally placed nucleoli,
- Cells separated by sinusoidal stroma,
- Nuclear pseudo inclusions,

-Eosinophilic cytoplasmic globules and bile secretions. (Crawford, Cartran, et al, 1994)

Staging:-

The TNM classification and group staging criteria for primary liver carcinomas are shown in the following table:

TNM classification & staging of HCC

<i>I</i>	<i>T1</i>	<i>N0</i>	<i>M0</i>
<i>II</i>	<i>T2</i>	<i>N0</i>	<i>M0</i>
<i>IIIA</i>	<i>T3</i>	<i>N0</i>	<i>M0</i>
<i>IIIB</i>	<i>T1</i>	<i>N1</i>	<i>M0</i>
	<i>T2</i>	<i>N1</i>	<i>M0</i>
	<i>T3</i>	<i>N1</i>	<i>M0</i>
<i>IV</i>	<i>T4</i>	<i>Any N</i>	<i>M0</i>
<i>V</i>	<i>Any T</i>	<i>Any N</i>	<i>M1</i>

[Table 5] (Quoted from Husband et al, 1996).

The stage of the tumour is upgraded by the presence of lymph nodes (N) or distant metastasis (M). the extend of tumour within the liver (T) can also affect the stage of tumour, depending on:

- 1) Number of tumour nodules present.
- 2) Size of tumour.
- 3) Presence of vascular invasion.
- 4) absence of vascular invasion.

T1: Solitary tumour ≤ 2 cm in greatest dimension, without vascular invasion.

T2: Solitary tumour ≤ 2 cm in greatest dimension, with vascular invasion, or multiple tumours in one lobe only ≤ 2 cm in greatest dimension, without vascular invasion. Or solitary > 2 cm in greatest dimension, without vascular invasion.

T3: Solitary tumour > 2 cm in greatest dimension, with vascular invasion, or multiple tumours in one lobe only ≤ 2 cm in greatest dimension, with vascular invasion, or multiple tumours only > 2 cm in greatest dimension, with or without vascular invasion.

T4: Multiple tumours involving more than one lobe, or involvement of major branch of portal or hepatic veins, or direct invasion of adjacent organs other than the gall bladder, or with perforation of visceral peritoneum.

N0: No regional lymph node metastasis.

N1: Regional lymph node metastasis.

M0: No distant metastasis.

M1: Distant metastasis.

(Husband, Reznik et al, 1996)

Differentiating large regenerative nodules and dysplastic nodules of cirrhosis from HCC can be difficult with any imaging modality. *(Dodd III, Miller et al, 1992)*

Altered portal venous haemodynamics, coupled with the increased hepatic arterial blood flow to the cirrhotic liver, makes tumour detection with contrast enhanced CT more difficult in cirrhotic patients. (*Takayosuk, Mariyama et al, 1990*)

HCC is a vascular tumour, and it has been shown that such vascular tumours can rapidly become isodense with the liver on contrast-enhanced CT. So biphasic contrast enhanced CT is more beneficial. (*Baron, Olive et al, 1996*)

Types of HCC:

-**The extending type:** in which the boundary between the tumour and the parenchyma is discrete as the tumour expands, compresses, and distorts the surrounding parenchyma.

-**The spreading type:** in which there is a poorly defined tumour margin and is further subdivided into cirrhotometric and infiltrative types. (*Okuda et al, 1984*)

2-Fibrolamellar Hepatocellular carcinoma:

Fibrolamellar hepatoma is a distinctive clinical and pathological type of Hepatocellular carcinoma that occurs in younger patients (mean age 20 years) who have no underlying parenchymal disease. Although it's a malignant lesion, the prognosis is better than for typical Hepatocellular carcinoma, with 25% of patients having respectable lesions. Central calcifications are present in one third of lesions. The appearance is nonspecific but may be suggested in the proper age group. (*Bluemke et al, 1995*)

3-Cholangiocarcinoma:

Cholangiocarcinoma is the second most common primary hepatic tumour and is a malignancy arising from the bile ducts, fifty percent of tumours arises at the common duct bifurcation or in the distal bile duct. The so-called Kalkskin tumour is an infiltrating cholangiocarcinoma arising at the Y-shaped junction of the left and right hepatic ducts. These tumours produce bilobar biliary duct obstruction and are unrespectable. There may be little evidence of an associated hepatic mass because a thin sheet of tumour invades the bile duct. Peripheral cholangiocarcinoma may occasionally be respectable when it does not involve the inferior vena cava or caudate lobe. (*Bluemke et al, 1995*)

Vascular invasion and portal nodes should be searched for carefully as these findings preclude resection of the tumour. Solitary peripheral masses appear similar to hepatoma or hepatic metastases. It may also produce changes as capsular retraction adjacent to the tumour. (*Soyer et al, 1994*)

4-Angiosarcoma:

A rare neoplasm that is 30 times less common than HCC, angiosarcoma occurs most commonly in men in the seventh decade of life. It is associated with previous exposure to radiation, thorotrast or toxins such as polyvinyl chloride (PVC), arsenics, and steroids. It also has been associated with haemochromatosis. Patients may present with weakness, weight loss, abdominal pain, ascites and hepatomegally. Rupture with haemoperitoneum may rarely occur. (*Powers et al, 1994*)

When related to thorotrast exposure, the reticular pattern of thorotrast deposition may be well seen in the liver, with significantly increased density of the spleen and lymph nodes. Usually circumferential displacement of thorotrast in the periphery of a nodule is a characteristic finding of angiosarcoma. (*Silverman et al, 1995*)

5-Hepatoblastoma:

Hepatoblastoma usually is found in the first 3 years of life, it has a peak incidence between 18 and 24 months of age. However, it may be present at birth or may develop in adolescents and young adults. It is more frequent in males than females. The child with hepatoblastoma may present with abdominal swelling often with anorexia or weight loss. The serum alpha-fetoprotein level is usually significantly elevated. (*Powers et al, 1994*)

6-Epithelioid Haemangioendothelioma (EHE)

Epithelioid Haemangioendothelioma (EHE) is a very rare malignant neoplasm of the liver of vascular origin. EHE develops in adults and should not be confused with infantile Haemangioendothelioma, which occurs in young children. These tumours are often multiple consisting of neoplastic cell that infiltrate the sinusoids, hepatic veins, and portal vein branches. Although usually an incidental finding, EHE may occasionally cause jaundice, hepatic failure, and rupture with haemoperitoneum. It is more common in women than men. The

prognosis of EHE is more favorable than that of angiosarcoma with extrahepatic metastases occurring in only one third of reported cases. Metastatic lesions may also be found in the lungs and soft tissues. (*Powers et al, 1994*)

7-Lymphoma:

Primary lymphoma of the liver is rare, but secondary involvement of the liver is common in both Hodgkin's and non-Hodgkin's types. Lymphomatous lesions of the liver may be focal, but often they are diffusely distributed within the liver. In both Hodgkin's and non-Hodgkin's types the portal area is typically initially involved because this is the region where lymphatic tissue of the liver is present. The liver may or may not be enlarged, and patient may present with the right upper quadrant pain or a tender mass of the upper abdomen. (*Miller et al, 1992*)

II-Secondary hepatic malignancy:

Metastatic disease is approximately 20 times more than primary hepatic malignancies. The most common primary sites with hepatic metastases are colon, breast, lung and pancreas. Metastatic disease usually manifests as focal hepatic masses, but infiltrative involvement also may be found, particularly with lymphoma and breast cancer. (*Bluemke et al, 1995*)

Metastatic tumours of the liver receive most of their blood supply from the hepatic artery. As with Hepatocellular carcinoma, metastatic tumours can be divided into two categories based on their enhancement compared with the normal liver. Hypervascular lesions enhance rapidly and are hyperattenuating compared with the liver. Hypervascular tumours include metastasis from breast, islet cells, and renal cell neoplasms as well as sarcoma and melanoma. Hypovascular tumours are relatively hypoattenuating compared with the liver. Most gastrointestinal neoplasms are hypovascular. (*Patten et al, 1993*)

ACUTE INFAMMATORY DISORDERS OF THE GALLBLADDER

1- Acute Calculous Cholecystitis:

Acute calculous cholecystitis is inflammation and infection within the gallbladder due to cystic duct obstruction by a gallstone. This may result in mechanical, chemical, or infectious insult, as the obstructed gallbladder becomes abnormally distended.

2- Acute Acalculous Cholecystitis:

Acute cholecystitis without stones is most frequently seen in the very old, the very young, and in specific clinical setting. The common underlying cause appears to be a chemical or vascular insult to the gallbladder. Acute acalculous cholecystitis is reported to be represent 2-15 % of all cases of acute cholecystitis. Predisposing conditions include major trauma, multisystem organ failure, major surgery, burns, parenteral nutrition, narcotics, shock, mechanical ventilation, vasculitis, and diabetes. (*Babb, 1992*)

Infectious enteritis with biliary tract spread has also been implicated as a cause (Campylobacter or Salmonella in immunocompetent patients or cytomegalovirus and cryptosporidium in the immunocompromised). Acute acalculous cholecystitis in HIV-infected patients may occur from opportunistic infection by Cytomegalovirus, Cryptosporidium, and/or microsporidia. (*French et al, 1995*)

In contrast to inpatients, virtually all outpatients with acalculous cholecystitis have symptoms, and 75 % have severe arteriosclerosis. Rapid diagnosis and intervention are critical to improving outcome. However, even with prompt intervention, the perioperative mortality associated with cholecystectomy in the setting of acalculous cholecystitis is 6-7 %, which is higher than for cholecystectomy in the setting of calculous cholecystitis. (*Shapiro et al, 1994*)

Complicated Acute Cholecystitis:-

1-Gnagrenous Cholecystitis

Gangrenous cholecystitis is a form of complicated acute cholecystitis characterized by severe mural necrosis and microabscess formation. The inflammation may or may not be associated with Clostridia superinfection, if it is associated with Clostridia or other gas-forming organisms, it can evolve into emphysematous cholecystitis. Diabetes and hypertension are commonly associated concomitant disease. (Croley et al, 1992)

2-Emphysematous Cholecystitis

Emphysematous cholecystitis is severe acute cholecystitis complicated by infection, which leads to the formation of gas in the gallbladder lumen or wall. The infection is usually due to gas producing bacteria such as Clostridia or E. Coli, or less commonly anaerobic streptococci and staphylococci. Although no single bacteria predominate, Clostridia welchii is isolated in one third of patient. Emphysematous cholecystitis is usually produced by gangrenous cholecystitis, but it can be associated with gangrenous calculous cholecystitis and acalculous cholecystitis. The presence of gas indicates necrosis, and may be related to ischemia due to cystic artery occlusion with superimposed infection. (Mentzer et al, 1975)

Emphysematous cholecystitis has a higher associated mortality than uncomplicated cholecystitis, with five times the risk of perforation. It typically occurs in elderly patients, one quarter of whom are diabetics. Men are affected at least twice as commonly in women. Emphysematous cholecystitis has also been described following (ERCP). Early recognition is vital, and emergent cholecystectomy is indicated once the diagnosis is established, especially in diabetics. However, if surgery is contraindicated percutaneous drainage may be beneficial, at least as a temporizing measure. (Vazsquez et al, 1985)

Early in the course of the disease, gas is most often in the gallbladder wall, and the identification of this finding is diagnostic. However, the gas may also extend into the gallbladder lumen, and occasionally the bile ducts. This latter finding occurs either because of persistent cholecystopathic ducts, or because of incomplete occlusion of the cystic duct. Rarely, gas can even dissect into the pericholecystic fat, falciform ligament, stomach, or colon. Gas may be seen in the bile ducts even in the presence of high-grade cystic duct obstruction;

however, there is usually no gas in the common bile duct. This is the opposite of cholecystoenteric fistula, where gas is usually in the common bile duct, occasionally in the gallbladder lumen, and never in the wall of the gallbladder. With only gallbladder lumen gas, a fistula must be extended before a confident diagnosis of emphysematous cholecystitis can be made. Free intraperitoneal gas in this setting suggests perforation of a gangrenous gallbladder. (*Vazsquez et al, 1985*)

3-Gallbladder Empyema

An infected inflamed gallbladder may evolve into an empyema if antibiotics are given, or if cholecystectomy is not promptly performed. Gallbladder empyema represents a distended gallbladder filled with pus. Static bile is an excellent culture medium for organisms, and while only one fourth to one third of patients have positive cultures early in the course of acute cholecystitis, 80 % will have infected bile 1 week after the onset of disease if surgery is not performed. *E. coli* and *Klebsiella* species are the most common bacteria cultured from bile in gallbladder empyema. (*Slot et al, 1995*)

4-Gallbladder Perforation

perforation is reported to occur in anywhere from 2-15 % of cases of acute cholecystitis. However, it is commonly walled off or confined locally by inflamed pericholecystic tissues and omentum. Less commonly, communication with the peritoneal cavity occurs, followed by bile and/or purulent peritonitis. The patient will often feel better immediately after the gallbladder perforates but once the peritoneum is exposed to bile, painful bile peritonitis ensues, often with rigors. (*Slot et al, 1995*)

CHRONIC INFLAMMATORY CONDITIONS OF THE GALLBLADDER

1-Chronic cholecystitis

A gallbladder subjected to repeated bouts of acute calculous cholecystitis is at risk for developing chronic cholecystitis. Most cases of chronic cholecystitis have cholelithiasis. Overall, chronic cholecystitis is actually several times more common pathologically in cholecystectomy patients than acute cholecystitis, and both often present simultaneously. Furthermore many of the

cases that are pathologically diagnosed as chronic cholecystitis have been given the imaging diagnosis of acute cholecystitis because the finding on cross-sectional imaging studies may be identical. However, the gallbladder may also be shrunken, full of stone, and fibrotic. (*Rappaport et al, 1994*)

2-Chronic Acalculous Cholecystitis

It represents less than 5% of all cases of chronic cholecystitis. The clinical, pathological, and radiological criteria for diagnosis are controversial and vague, and actually represent a spectrum of disease, rather than a "yes-or-no" categorization. This is due, at least in part, to variable definitions of normal gallbladder aging and the uncertain significance of fibrotic changes and inflammatory cellular infiltrates in the setting of mild symptoms. It may be due to biliary stasis, infection, bile duct abnormalities, recent stone passage, or chronic disease such as diabetes, connective tissue, and collagen vascular disease. (*Zeman et al, 1994*)

3-Hydrops of the Gallbladder

Hydrops is distention of the gallbladder with bile and mucus, usually due to mechanical cystic duct obstruction. This is most commonly due to a cystic duct stone, although occasionally it can be caused by simple edema of the cystic duct and gallbladder neck from passage of a stone. On plain films, the large gallbladder may cause mass effect or impression upon adjacent gas-filled bowel. (*Salvador, et al. 1995*)

4-Porcelain Gallbladder

Porcelain gallbladder describes the gross appearance of the brittle, blue, calcified gallbladder resulting from chronic inflammation of the gallbladder wall. The well known association with gallbladder carcinoma, in these otherwise asymptomatic patients, makes this finding potentially life saving. Gallbladder carcinoma is reported to complicate porcelain gallbladder in 11-62% of cases, though at least on the high end, these estimates may overstate the risk of malignancy. The reason for the association with carcinoma is uncertain, but it may be due to a carcinogen forming in stagnant bile, or to inflammation-induced, cyclical regeneration of the epithelium. (*Salvador, et al. 1995*)

5-Cholesterolosis

Cholesterolosis has been called “strawberry gallbladder” because of the pathological appearance of the hyperemic mucosa with yellow branching linear deposits of xanthomatous macrophages in the lamina propria. Histologic analysis reveals abnormal deposits of triglycerides. Cholesterol esters and cholesterol precursors in the gallbladder wall. Cholesterolosis commonly occurs diffusely throughout the gallbladder. The discrete cholesterol polyps seen in the less common polypoid form of this condition differ from adenomas by the absence of glandular with uniformly coarse and granular mucosa. The discrete cholesterol polyps seen in the less common polypoid form of this condition differ from adenomas by the absence of glandular element. Cholesterol polyps is not premalignant, while some adenomas may harbor carcinoma in situ. Adenomas are less common than cholesterolosis. (*Tilvis, et al. 1982*)

Cholesterolosis may be related to abnormal bile or increased cholesterol absorption by the gallbladder wall. There is no association with systemic atherosclerosis, coronary artery disease, diabetes, obesity, serum lipid levels, cholesterol gallstones, or supersaturation of cholesterol in bile. Gallstones occur in 10- 15% of gallbladders with cholesterolosis. The surgical literature reports even higher numbers, but the population is skewed in series of patients treated surgically. (*Scott, et al. 1998*)

Cholesterolosis usually causes only minor surface irregularities and is therefore not easily detected by imaging. Oral cholecystography shows the more extensive or polypoid irregularities. Cholesterol polyps are seen as irregular filling defects on oral cholecystogram. (*Scott, et al. 1998*)

6-Adenomyomatosis

Hyperplastic changes in the gallbladder mucosa. muscular wall thickening. and multiple inner diverticulae in the wall characterize adenomyomatosis (also called adenomyosis). The diverticulae are herniations of the mucosa through weak areas in the muscularis propria. They may contain bile, stones, or concretions. The muscularis thickening may appear to block the opening of a diverticulum, mimicking a cyst. The etiology remains unknown, but may be related to increased pressure, defective contraction, compartmentalization, or neural or muscular proliferation. (*Zeman, et al. 1994*)

Several types of hyperplastic changes are differentiated by pattern of involvement, and include generalized and segmental, the latter of which is divided (or fundal adenomyomatosis) may present as a defect or a localized diverticular outpouching, often near the fundus. In the annular type, muscular thickening encircles the gallbladder and focally narrows it like a napkin ring, effectively dividing it into adenomyomatosis may be impossible to differentiate from a septum. In the small percentage of patients with associated stones, the adenomyomatosis may limit the movement of stones to the dependent portion of the gallbladder, complicating their discovery. (Scott, et al. 1998)

Gallbladder Carcinoma:-

Gallbladder carcinoma will be discussed in a separate chapter. Gallbladder carcinoma is associated with chronic cholecystitis, porcelain gallbladder, and chronic gallbladder inflammation. In fact, primary gallbladder carcinoma often cannot be distinguished from chronic cholecystitis by imaging methods. If gallbladder carcinoma perforates, it may mimic calculous or acalculous cholecystitis on cross-sectional imaging. (Scott, et al. 1998)

Because of the clinical and imaging overlap between inflammatory and neoplastic biliary entities, malignancy often cannot be excluded without serial studies demonstrating absence of change over time. A reliable screening method of detecting early gallbladder carcinoma is not available, thus presentation more commonly follows the development of symptoms, which unfortunately often implies unresectability. (Scott, et al. 1998)

ACUTE INFLAMMATORY DISORDERS OF THE BILIARY TRACT

Bile Duct Obstruction: Clinical Considerations

Surgical jaundice, biliary dilation, and obstruction are terms with different implications. Acute biliary obstruction usually leads to dilation followed by elevation in alkaline phosphatase and bilirubin. The biliary tree rapidly dilates following high-grade obstruction. This dilation may be seen within several hours of obstruction, and occurs before the onset of jaundice. If the distal common bile duct is blocked, dilation of the extrahepatic duct is often greater than the intrahepatic ducts, and may precede the intrahepatic duct dilation, as predicted by the law of Laplace. (Zeman, et al. 1994)

Peak serum bilirubin levels correspond to the degree of biliary narrowing or blockage, but not to degree of duct dilation seen on imaging studies. Partial, early, and thus more commonly result in imaging and clinical uncertainty. Elevated alkaline phosphatase may be an indication of segmental or focal obstruction of the biliary tree. These patients usually have more than the 40% residual hepatic function and duct patency required to clear the body's daily pigment load; which is why the serum bilirubin may normal. The key finding in segmental obstruction is focal intrahepatic duct dilation in a segmental distribution on a cross-sectional study. The common etiologies, which may result in this finding, include cholangiocarcinoma, liver lesions with mass effect and intrahepatic stones, and less commonly, sclerosing cholangitis and oriental cholangiohepatitis. (Scott, et al. 1998)

Ascending Cholangitis

Ascending (or obstructive) cholangitis results from stasis above an obstruction. The cholangiographic spectrum of disease is broad, as intrahepatic or extrahepatic biliary may be involved. Pus and bilious sludge may cause filling defects on cholangiography or echogenic debris within the biliary tract on US. Cholangitic abscesses are characteristic, forming extraluminal outpouchings from the ducts (more commonly intrahepatic), of different sizes and shapes. (Vinegrad, et al. 1980)

The ductal changes range from mild dilation to bizarre angulation and loss of the usual fine ductal branching. The imaging appearance may be identical to that of sclerosing cholangitis, metastases, or cirrhosis. However, sclerosing cholangitis causes outpouching that are bigger, more irregular, less uniform and more symmetric than in ascending cholangitis. Metastatic disease and cirrhosis in more characteristic draping, pruning, and encasement of the biliary tree. (Scott, et al. 1998)

Mirizzi syndrome

A cystic duct or gallbladder neck may become impacted near the insertion into the common hepatic duct, causing compression of the common hepatic duct or common bile duct, with local inflammation and subsequent obstruction of the common hepatic duct. When this occurs, it is called Mirizzi syndrome. The stone may even erode into the duct, creating a cholecystocholedochal fistula, which some refer to as Mirizzi type II. A milder version of Mirizzi syndrome may occur when an inflamed gallbladder compresses may cause an inflammatory stricture of the common bile duct or common hepatic duct. Once

the duct is strictured, recurrent cholangitis and chronic biliary cirrhosis can result. (Berta, et al. 1995)

Mirizzi's description of this uncommon entity has acquired new significance in the era of laparoscopy. Although it is possible to treat Mirizzi syndrome laparoscopically, it is generally considered a contraindication to laparoscopic cholecystomy. Low cystic duct insertion into the hepatic duct not only predisposes to Mirizzi syndrome, but also increases the likelihood of inadvertent if it is mistake for the cystic duct. This is an understandable mistake at open and laparoscopic cholecystectomy, given the single duct extending from an inflamed gallbladder. In cases of Mirizzi syndrome, the cystic duct may not be identifiable lies within the inflammatory cavity, which forms around the common duct. (Moser, et al. 1993)

Gallstone Ileus And Biliary-Enteric Fistula

A gallstone may erode into gastrointestinal tract and then cause bowel obstruction. This usually occurs in the setting chronic gallbladder and or biliary inflammation. The bowel obstruction. Which result if the stone is large enough so as not to pass through the large and small intestine has been misnamed gallstone "ileus"? The classic plain film findings of this entity include bowel obstruction, gas in the biliary tract, and a radiodense gallstone in the gastrointestinal tract, although the latter two are not identified in all cases. It important to distinguish gas in the biliary tree, which tends to be globular and centrally located, from portal venous gas, which is more linear, finally arborizing, and peripheral. (Simeone, et al. 1989)

Small stones generally pass unimpeded through the bowel. Large gallstone (> 2cm), however, can cause obstruction anywhere, most commonly at the level of the ileocecal valve, duodenum, ligament of Treitz or the sigmoid colon in areas of diverticular spasm. (Scott, et al. 1998)

Gallstone ileus may be difficult to diagnose clinically, and is more common in elderly patients. The reported frequency is greatly overstated in some literature, which claims 20 – 24 % of obstruction in patients over 65 to 70 is caused by this entity. The diagnosis can be made 25 – 50 % of the time alone. However, unrelated simultaneous gallstones and obstruction are far more common than gallstone ileus in our experience. (Scott, et al. 1998)

CHRONIC INFLAMMATORY DISORDERS OF THE BILIARY TRACT

Sclerosing Cholangitis

Primary sclerosing cholangitis (PSC) is a chronic cholestatic disease of unknown etiology. The hallmarks of which, or acutely angulated bile. Extrahepatic and intrahepatic involvement is usually present. However, one fifth of patients may have extrahepatic involvement with minimal or intrahepatic change. A similar number of patients may have intrahepatic and proximal extrahepatic disease only. Idiopathic sclerosing cholangitis affects males twice as often as females, and typically presents in the third to fifth decade of life. The spectrum of disease ranges from subtle caliber changes to an attenuated "pruned tree" appearance. Stones from stasis proximal to (above) a stricture, as well as pseudodiverticulae (multiple small ductal outpouchings) are characteristic of this disease. (*Stockbrugger, et al. 1988*)

The high association between sclerosing cholangitis and inflammatory bowel disease is well documented. In one large series of patients with sclerosing cholangitis, 54% had coexistent inflammatory bowel disease, most of which was ulcerative colitis (6% had Crohn disease). Others have reported that up to 70 % of patients with PSC will have inflammatory bowel disease. However, the severity and rate of progression of PSC appear unrelated to the extent of associated inflammatory bowel disease. Likewise, colectomy does not tend to improve the course of the sclerosing cholangitis. In a series of patients with PSC and inflammatory bowel disease, 84% had pancolitis. In that same series, the biliary changes were more severe in the patients who required extensive medications, suggesting that there may be a weak relationship between severity of bowel disease and biliary disease. However, the same study showed no relationship between bile duct changes at diagnosis and clinical course. (*Scott, et al. 1998*)

Less common associations include collagen deposition diseases such as Reidel's thyroiditis, orbital pseudotumors, and retroperitoneal fibrosis. The terms "primary" and "secondary" sclerosing cholangitis are ambiguous and should be qualified, as inflammatory bowel disease-associated cholangitis may be included in either group by different authorities. We prefer to classify all idiopathic sclerosing cholangitis as primary sclerosing cholangitis. (*Scott, et al. 1998*)

Asian Cholangiohepatitis

Asian cholangiohepatitis (also known as recurrent pyogenic cholangiohepatitis or Oriental cholangiohepatitis) is the most common biliary disorder in parts of China, Japan and the Far East. The etiology has not been completely established. However, Chronic portal venous bacteremia appears to play an important role. In addition, many patients have concurrent biliary infestation with *Clonorchis sinensis*, *Fasciola hepatica*, or *Ascaris lumbricoides*. (*Khuroo, et al. 1993*)

When caused by parasitic infestation. The small liver flukes migrate to the liver from the duodenum. *Clonorchis* is acquired by eating uncooked freshwater fish. Eggs in stool may be a prerequisite and clue to biliary involvement. In one series, gallbladder contractility was depressed in two thirds of patients with *Fasciola*, infection may also related to the frequency and severity of fluke-associated hepatobiliary diseases. Biliary ascariasis results from adult worms migrating through the ampulla of Vater, causing blockage, cholangitis, or even cholecystitis or frank cholangitic abscesses. This may appear on US as a nonshadowing, echogenic worm in the duct (with shadowing if it calcifies or leads to stones). (*khuroo, et al. 1993*)

Pigment stones are characteristic of Asian cholangio-hepatitis. This may be related to chronic coliform bacterial colonization of bile, which causes portal vein bacteremia and triggers the presence of B-glucuronidase in the bile. This enzyme deconjugates bilirubin. Stimulating the formation of pigment stones. Liver flukes may lead to biliary obstruction directly. Or may act as a nidus for stone, pus, and biliary mud formation. Secondary and chronic sequelae include strictures and biliary cirrhosis. (*Khuroo, et al. 1993*)

BILE DUCT STONE DISEASES

Choledocholithiasis is one of the most common causes of biliary diseases. A variety of imaging testes may be used to diagnose bile duct stones directly by visualization of the calculus, and indirectly by demonstration of biliary dilation. Noninvasive testes include ultrasound (US), computed tomography (CT), and magnetic resonance imaging (MRI). When combined with 2D and 3d postprocessing techniques, CT and MRI permit depiction of the biliary tree on longitudinally oriented images, which mimic direct cholangiograms, so-called "CT and MR cholangiography." Biliary scintigraphy may diagnose choledocholithiasis indirectly by demonstration of biliary obstruction. However,

definition of the obstructing stone is not permitted with this technique. (Scott, et al. 1998)

Choledochocysts and Caroli Disease

Cystic abnormalities of the bile ducts are unusual entities that may predispose to stone formation due to chronic stasis and infection. Choledochocysts are thought to develop due to anomalous connection of the common bile duct, and pancreatic duct with either an anomalous duct joining the two or an abnormal angle of incidence between the two ducts permitting reflux of pancreatic secretions into the bile duct. Type I choledochocysts are characterized by fusiform dilation of the extrahepatic duct. Type II cysts involve a diverticular out pouching of the extrahepatic duct. Type III cysts are true choledochoceles, which manifest as dilation of the distal intramural portion of the common bile duct within the duodenal wall and with protrusion into the duodenum? In addition to stasis, which may lead to stone formation? patients with choledochocysts have an increased incidence of bile duct tumors, including cholangiocarcinoma. (Kurtz, et al. 1996)

Caroli disease, also known as communicating cavernous ectasia of the biliary tract, is a rare congenital abnormality of the biliary tree characterized by a saccular dilation of the intrahepatic bile ducts with sparing of the extrahepatic ducts. Typically, multiple complications of biliary stasis, including ductal stones and obstruction, cholangitis and liver abscesses, may occur. Caroli disease is also associated with cystic disease of the kidney, especially tubular ectasia (medullary sponge kidney). At cross-section imaging, one sees multiple intrahepatic cysts, which may be difficult to differentiate from polycystic liver disease; however, most of the cysts in Caroli disease are arranged in a branching pattern. Secondary signs of portal hypertension (which results from associated hepatic fibrosis) or cystic renal disease may suggest the diagnosis. Cholangiography or hepato-biliary scintigraphy may be needed to document communication between the cysts and the bile ducts. The "central dot sign" is a very specific sign of Caroli disease in which portal radicals are partially or completely surrounded by abnormally dilated and ectatic bile ducts. (Kurtz, et al. 1996)

Benign and Malignant Tumors of the Biliary Tree

EPIDEMIOLOGY:-

primary malignancy of the bile ducts is an uncommon tumor with an autopsy incidence of 0.01 to 0.5%. There tends to be a slightly higher incidence in men than in women. Bile duct cancer is a disease of older age groups with a peak incidence in the sixth and seventh decades. Bile duct cancers are distributed throughout the biliary tree and originate most frequently in the larger bile ducts. Relative rates in large series are as follows: 8 to 13% intrahepatic ducts; 10 to 26% at the confluence of the hepatic ducts; 15 to 30%, proximal common duct; and 30 to 36%. distal common duct. There is no geography variation in the incidence of extrahepatic bile duct carcinomas, whereas the incidence of intrahepatic cholangiocarcinomas varies with geography. In several areas where liver fluke infestation is endemic, the incidence of intrahepatic cholangiocarcinomas is relatively high. it seems that intrahepatic cholangiocarcinomas are nearly 10 times more common in Japan and Asian countries than in the United States or the United Kingdom. (*Dachman, et al. 1996*)

ETIOLOGY AND PATHOGENESIS:-

Intrahepatic cholangiocarcinomas

Intrahepatic cholangiocarcinomas has been associated with liver fluke (*Clonorchis sinensis*) in Southeast Asia. *Clonorchis sinensis* is a parasite of cats, dogs, and human. Humans are infected by eating raw freshwater fish. The usual habitat of the fluke is the intrahepatic bile ducts, although occasionally the gallbladder and the common ducts are involved. Several investigators found the relationship between primary liver cancer and liver fluke infestation. In addition, experimental studies have shown that severe *Clonorchis sinensis* infestation produces adenomatous hyperplasia and bile duct carcinoma. Other etiological factors include intrahepatic lithiasis. it is generally accepted that intrahepatic lithiasis occurs more frequently in patients with intrahepatic cholangiocarcinoma compared to the general population, though the causal relationship between intrahepatic lithiasis and cholangiocarcinoma remains only speculative. Ulcerative colitis and primary sclerosing cholangitis have been related to hilar cholangiocarcinoma. Developmental anomalies of the biliary tract, including Caroli's disease, congenital hepatic fibrosis, choledochal cysts, Biliary hamartomas (also known as von Meyenburg's complexes), and solitary

and multiple liver cysts. are all known to be complicated by the development of intrahepatic cholangiocarcinoma? Hyperplasia of the biliary epithelia with variable atypia and proliferative changes in the cystically dilated bile ducts may give rise to malignant transformation. Cholangitis associated with bile stasis in the dilated ducts may be a contributing factor. Cholangiocarcinoma is the most common malignant hepatic tumor in patients who have a history of exposure to Thorotrast. (Rosen, et al. 1990)

Extrahepatic Cholangiocarcinoma

Patients with ulcerative colitis and primary sclerosing cholangitis often develop carcinoma of the extrahepatic ducts. Patients with ulcerative colitis have approx. 30 times greater risk of developing Cholangiocarcinoma than does the general population. However, the mechanism by which these two diseases induce carcinomas of the bile ducts is unknown. Choledochal cysts are also predisposed to extrahepatic Cholangiocarcinoma. The incidence of carcinoma in choledochal cysts has been estimated to be 20 times greater than that in the general population. In patients with ulcerative colitis and choledochal cyst. bile duct cancers can occur two or three decades earlier than expected. In the Asia. liver fluke (*Clonorchis sinensis*) infestations have been associated with carcinoma of the extrahepatic bile ducts as well as intrahepatic bile ducts. Gallstones. Which are strongly associated with gallbladder carcinomas? are not significantly associated with common bile duct carcinomas. (Mir-Madlessi, et al. 1987)

BENIGN NEOPLASM OF

THE BILE DUCT

Adenoma, Papilloma and Papillomatosis

Adenomas are classified as tubular, papillary. and tubulopapillary type. Histological. They are indistinguishable from intestinal adenomas. Sometimes, they contain a population of endocrine cells. In addition, they often show severe dysplasia and carcinoma in situ Incidence of adenoma is reported as 0.04-0.12% in autopsy series, however. symptomatic lesion is rare. In 13-33%, cholelithiasis is accompanied. in ampullary adenoma, pancreatitis is infrequently accompanied. (Albores, et al. 1992)

Papillomatosis is defined in clinicopathological term as multifocal papillary lesions prone to local recurrence that may be extensive and involves the extrahepatic bile ducts, the gallbladder. and in some instances, the intra-

hepatic bile ducts. Because cytological atypia is often present, it is difficult or impossible to differentiate the lesion from the papillary carcinoma. This lesion can be interpreted as a low-grade papillary carcinoma rather than papillomatosis with a potential for malignant transformation. Sometimes, they secrete large amount of mucinous material and may obstruct bile ducts. Obstructing mucus may be either proximal or distal to the neoplasm, leading to confusion regarding the location of the tumor. (*Albores, et al. 1992*)

Biliary Cystadenoma

Biliary cystadenomas are rare, but distinctive benign tumors arise in the liver, and less frequently from the bile ducts. Their histologic features are similar to mucinous cystic tumor of the pancreas or ovary. They are more common in women over 30 years of age. Presenting symptoms typically include an abdominal mass, pain, and nonspecific complaints, such as dyspepsia, anorexia, nausea, and jaundice, occasionally occur. A spectrum from unilocular to multilocular cystic mass with variable size is reported. (*Albores, et al. 1992*)

Carcinoid Tumor

Carcinoid tumors arise from neuroendocrine cells. Carcinoid of biliary tree is extremely rare, probably due to the paucity of neuroendocrine cells in this location. In a review of 12 reported patients, the average age of the presentation is 48 years and the presenting symptom was jaundice or abdominal pain. Serum 5-hydroxy-indole-acetic acid is increased in about half of the patients. Radiological features of biliary carcinoid are variable. (*Scott, et al. 1998*)

Paraganglioma

Paraganglioma is usually an incidental finding on cholecystectomy specimen. Because of its small size, it may be easily overlooked on gross examination as well as radiological examinations. However, paraganglioma of the extrahepatic bile duct may give rise to biliary obstruction. (*Albores, et al. 1992*)

Granular Cell Tumor

Granular cell tumor of the extrahepatic bile ducts is nonmetastasizing, multicentric tumor usually found in the skin, oral cavity, or subcutaneous tissue. It is a rare tumor most commonly reported in young Black women. Less than 50 cases have been reported until 1992. This tumor is thought to be of Schwann

cell origin, is usually not capsulated, and is less than 30 mm in diameter. (Foulner, et al. 1994)

Because these tumors occurred at or near the confluence of the cystic, hepatic and common bile ducts, their symptoms may be confused with those of cholelithiasis, choledocholithiasis or other form of biliary obstruction. Cholangiograms generally show concentric narrowing, which mimics cholangiocarcinoma or segmental sclerosing cholangitis. (Foulner, et al. 1994)

Biliary Hamartoma

Biliary Hamartomas are benign liver malformations consisting of focal disorderly collections of bile ducts, lined with single layer of low columnar, cuboidal or flattened epithelium, surrounded by abundant fibrous stroma. The bile ducts within the lesion are of varying caliber, ranging from narrow to ectatic. Biliary hamartomas usually appears as subcapsular or parenchymal whitish nodules less than 0.5 cm in diameter. However, when detected by imaging methods. They are larger (0.5 to 3 cm). Autopsy series reveal their presence in 0.96 to 2.8%. They are usually multiple in number. (Gallego, et al. 1995)

Amputation Neuroma

Amputation neuroma is reported after surgery, typically after cholecystectomy. It is not a neoplasm, but rather a reactive hyperplasia. They do not usually reach substantial size to cause symptoms. It appears as a firm bulbous mass or a dense irregular mass of tissue embedding the blind end of a bile duct. Histologically, it is identical with amputation or traumatic neuroma found elsewhere. (Gallego, et al. 1995)

MALIGNANT NEOPLASM OF THE BILE DUCT

Peripheral Cholangiocarcinoma

Cholangiocarcinoma may arise from either intrahepatic or extrahepatic duct. An intrahepatic cholangiocarcinoma may be classified as: (a) a peripheral cholangiocarcinoma, which originates in an interlobular duct; (b) a major – duct cholangiocarcinoma, which arises in the right or left hepatic of the common hepatic duct; or (c) a hilar develops at the cholangiocarcinoma, which develops at the bifurcation of the common hepatic duct. Some hilar carcinomas extend along the ducts. However, which makes it differentiate them from major-duct

carcinomas. Therefore, cholangiocarcinomas of the liver are usually classified into two types; peripheral and hilar. Primary intrahepatic and peripheral cholangiocarcinomas are relatively uncommon compared to hilar carcinomas. (Choi, et al. 1995)

In patients with peripheral cholangiocarcinomas, abdominal pain is the chief complaint in the majority of cases, whereas jaundice is the chief complaint in patients with hilar cholangiocarcinoma. Initial symptoms are usually nonspecific, including abdominal pain and discomfort, easy fatigue, and indigestion. Jaundice occurs infrequently. Serum bilirubin values are usually within the normal range, and serum alkaline phosphatase levels are sometimes elevated. The simultaneous presence of chronic liver disease and peripheral cholangiocarcinomas occurs infrequently, although the tumor occasionally occurs in cirrhotic liver. Peripheral cholangiocarcinomas are usually large because they are rarely symptomatic early in their course. (Choi, et al. 1995)

Combined Hepatocellular And Cholangiocarcinomas

Primary carcinoma of the liver can usually be classified histologically as either hepatocellular carcinoma or intrahepatic cholangiocarcinoma. Occasionally, carcinomas in the liver show histologic evidence of hepatocellular and biliary epithelial differentiation. These combined hepatocellular and cholangiocarcinomas are sometimes encountered in resected livers. Parenchymal liver cells and biliary epithelial cells are developed from a common liver primodium. At a relatively early stage of embryogenesis, the hepatic cord differentiates into the parenchymal liver cells, from which the intrahepatic biliary epithelial cells are derived. Although they have the same cellular origin, the two cell types have completely different phenotypes, such as cellular morphology and the structural components, and they constitute the different tissues. This rare liver cancer is designated as the combined hepatocellular cholangiocarcinoma, where the area of cholangiocarcinoma differentiation is observed continuously with the typical hepatocellular carcinoma region. By definition, this cancer must contain unequivocal elements of hepatocellular carcinoma and cholangiocarcinoma. (Choi, et al. 1995)

Hepatocellular carcinoma with areas of ductal or glandular changes is fairly common and is often confused with the combined type. This has led to the mistaken impression that mixtures of hepatocellular carcinoma and cholangiocarcinoma are common; however, "pseudoglandular" growth patterns in hepatocellular carcinoma should not be referred to as "combined. True

mixtures of hepatocellular carcinoma and cholangiocarcinoma are quite rare, comprising 2.4-5% of primary liver cancer. The sex ratio of combined type has been 3-5:1 with male predominance, and 73.7-100% of these tumors have arisen in a cirrhotic liver. (Goodman, et al. 1985)

Hilar Cholangiocarcinoma

Hilar Cholangiocarcinoma arises from the main hepatic duct or near its bifurcation. Although this is an uncommon tumor, current use of Sonography and CT in patients with obstructive jaundice makes it possible to detect this tumor. Sonography is the most common initial examination in the patients with obstructive jaundice, and sonographic findings in hilar cholangiocarcinoma have been reviewed. CT is also a good modality in the evaluation of hilar cholangiocarcinoma, and the CT appearance of this tumor has been the subject of recent reports. (Garber, et al. 1993)

Extrahepatic Bile Duct Carcinoma

cholangiocarcinoma originate most frequently in the larger bile ducts. In a collected series of 1229 extrahepatic bile duct cancers. the locations of the tumors were: right and left hepatic ducts. 6% ; hepatic duct bifurcation, 30%: common hepatic duct, 20% ; common bile duct, 39% ; cystic duct, 5%. Growth patterns are either infiltrating or scirrhous. nodular, or papillary. The former is the most common and characteristically presents as a focal biliary stricture, often without evidence of mass, at times producing longer strictures or even infiltrating a large part of the biliary tree. mimicking sclerosing cholangitis. (Choi, et al. 1995)

The most common presenting sign is jaundice frequently accompanied by weight loss, pruritus. and anorexia. Additional complaints include abdominal pain. acholic stools, weakness, and diarrhea. (Choi, et al. 1995)

Biliary Cystadenocarcinoma

Biliary Cystadenocarcinoma are rare biliary ductal neoplasms that arise in the liver or, less frequently. the extrahepatic biliary tree. They resemble mucinous cystic neoplasms of the pancreas. (Hodgson, et al. 1991)

More than 80% of cystadenomas occur in women. More than 80% are seen in patients older than 30 year Patients with intrahepatic Cystadenoma and Cystadenocarcinoma usually present with abdominal mass, Pain and, less

frequently. nonspecific complaints such as dyspepsia, anorexia, nausea, and vomiting. The majority of the tumors are large. frequently exceeding 10 cm in largest diameter, with a reported range of 3.5 to 25 cm. Almost all biliary cystadenomas are multiloculated. Only two unilocular ones have been reported. however, unilocular biliary cystadenomas are not rare. Multiple masses are rare. An isolated multilocular cystic mass is characteristic. (*Hodgson, et al. 1991*)

Mucin-Hypersecreting Biliary Neoplasm

The term mucin-hypersecreting carcinoma has been applied to malignant biliary neoplasms that excrete excessive mucin in the biliary tree, dilate the ducts, and show a distinct radiological appearance as a result. Papillary cholangiocarcinomas and Cystadenocarcinomas are in this category. In these cases, the mucin rather than the tumor itself plays an important role in the clinical course and radiological appearance. (*Lim, et al. 1995*)

Clinical symptoms are recurrent abdominal pain and jaundice because excess mucin in the extrahepatic bile ducts appears to impede the passage of bile, creating obstructive jaundice. (*Lim, et al. 1995*)

Cholangiocarcinoma in a Choledochal Cyst

Choledochal cyst (cystic dilation of the extra- or intrahepatic bile duct or both) is a rare malformation most frequently seen in oriental females. Malignant changes have been described in rare instances. usually in the type I cyst. (*Todani, et al. 1985*)

The prognosis of the malignancy is poor because of extensive local or regional spread of the tumor. The clinical features of choledochal cyst are variable (abdominal pain. jaundice. fever, palpable mass, and back pain). while the main feature of malignancy in cases of choledochal cyst is abdominal pain combined with back pain and weight loss. Choledochal cysts are said to be caused by reflux of pancreatic enzymes into the common bile duct due to malunion of the pancreaticobiliary duct. Todani et al. speculated that the degenerated mucosa of the choledochal cyst is at risk for carcinoma because of chronic irritation, ulceration, and subsequent regenerating of the cyst epithelium. The frequency of these biliary malignant changes increases with age and is reported to be 14 to 50%. These rates are remarkably high compared with the rate of biliary carcinoma in the general population (0.003 to 0.004%). (*Scott, et al. 1998*)

Intraluminal Bile Duct Hepatocellular Carcinoma

Jaundice is found in 19-44% of patients with hepatocellular carcinoma at presentation, but this is usually due to underlying cirrhosis or parenchymal damage. Causes of obstructive jaundice in hepatocellular carcinoma include tumor compression of the intrahepatic ducts, necrotic tumor fragments in the duct lumen, hemobilia, and tumor infiltration. Occasionally, tumor debris within the common bile duct can float causing intermittent biliary obstruction. Invasion of the biliary tree is generally thought to be rare; in one analysis of 322 cases only 4 patients were noted to have intraductal tumor. (Lau, et al. 1990)

The study of *Kojiro et al.* on 238 autopsy and 21 surgical cases of hepatocellular carcinoma documented a 90% incidence of intraductal tumor. It is important to recognize this group of patients, in some relief of the obstruction gives good palliation and occasionally curative surgery is possible if the disease is localized. At the present time, detection of this group is not so difficult because of remarkable advances in various diagnostic imaging techniques. Intrabile duct tumor growth is not merely one of the terminal signs in advanced hepatocellular carcinoma. This type of growth is mainly caused by a direct invasion of the infiltrative tumor located near the major bile duct, regardless of tumor size. Intraluminal bile duct hepatocellular carcinoma without a mass lesion in the liver. (Scott, et al. 1998)

Embryonal Rhabdomyosarcoma

(Sarcoma Botryoides) of the biliary tree

Rhabdomyosarcoma of the biliary tree are rare, however, sarcoma botryoides is probably the most common cause of obstructive jaundice in children past infancy. After choledochal cyst. Other reported tumors arising from the extrahepatic bile duct in children have been a massive pedunculated papilloma. A lipoma, a congenital teratoma. And endodermal sinus tumor associated with benign teratoma. (Kim, et al. 1993)

Age range is 16 months to 7 years. Children present with malaise, fever, and jaundice that is often initially attributed to viral hepatitis. The average survival after onset of symptoms is 5.3 months, with a range of less than 1 month to over 16 months. Although late metastases occur, death is usually from local invasion of contiguous structures. Wide surgical resection, radiation, and chemotherapy yield significant prolongation of life and palliation but not cure. (Kim, et al. 1993)

Lymphoma of the Bile Duct

Patients with lymphoma may develop jaundice for a variety of reasons; diffuse lymphomatous liver involvement, cholestasis due to lymph node enlargement in the porta hepatis, and hepatocellular disease related to the toxic effects of chemotherapy are the most common causes. Rarely, lymphoma may directly infiltrate the wall of the biliary tree, producing biliary obstruction. There are three clinical situations in which lymphomatous infiltration of the biliary system may occur: (a) as a solitary site of extranodal lymphoma; (b) as one of many sites in a systemic lymphoma; and (c) as a site of recurrence after therapy directed to systemic lymphoma. (Choi, et al. 1992)

Case No. 1
Hepatocellular Carcinoma.



(Figer. 6)



(Figer.7)

The plain scan demonstrates a large hypodense, sharply margined mass in the right lobe of the liver (figer. 6; arrow). During portovenous contrast medium distribution, peripheral enhancement and capsular structures appear accenting the capsular structures (figer 7; arrow). Regressive changes appear as hypodense areas in the late film.

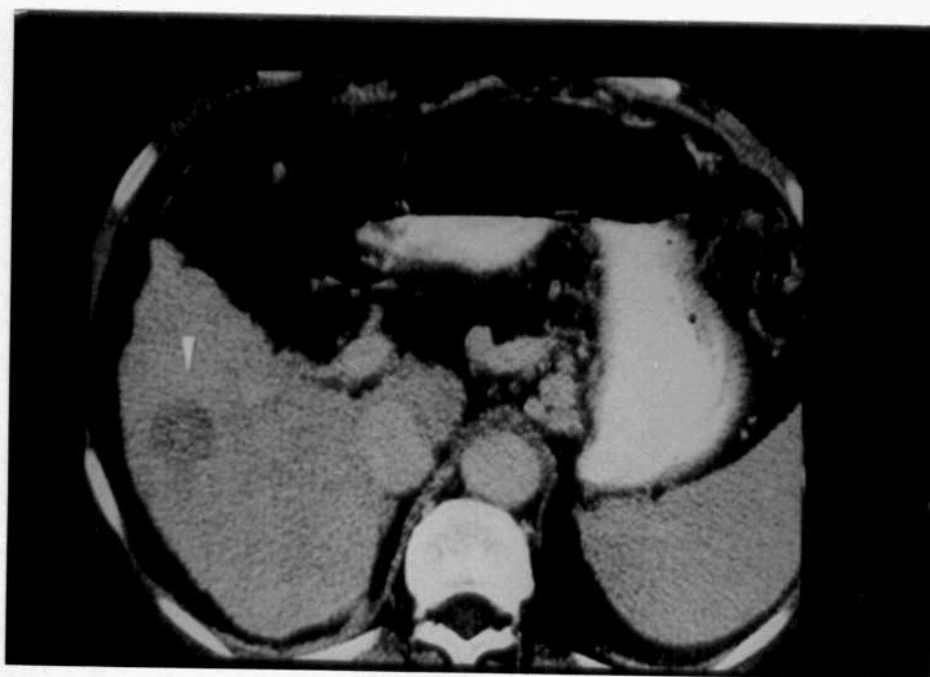
Case No. 2

Hepatocellular carcinoma.

(Figer.8)

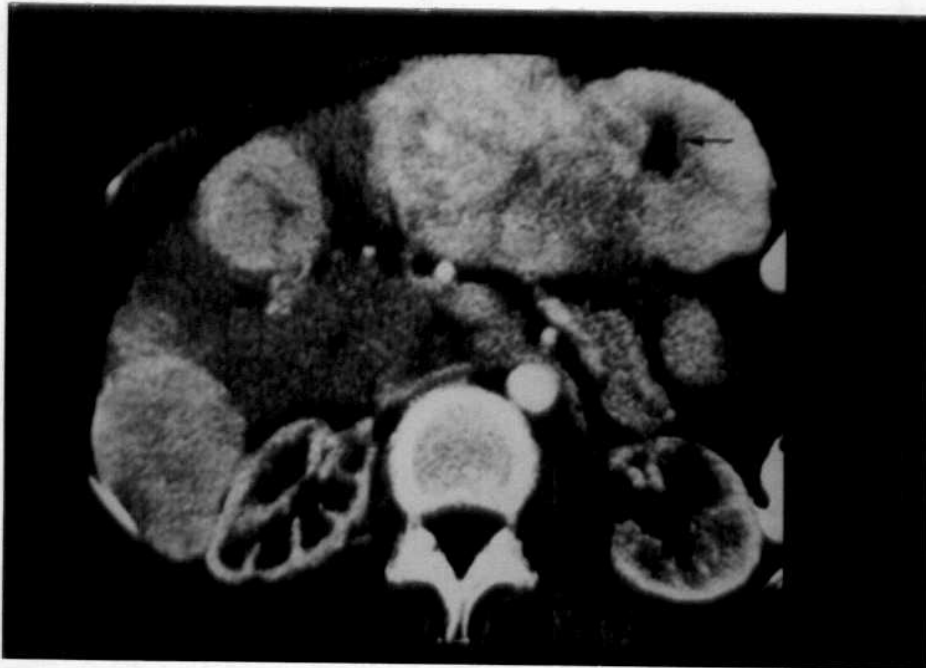
actual

A large mass occupies the entire right lobe of the liver, which appears distended. During the early portovenous contrast medium phase, irregular blood vessel structures (wedge) were detected within the tumorous hypodense structure, indicating the development of an arteriovenous shunt. The portal venous thrombosis is apparent in the sharply margined hypodense structures (arrow). Perihepatic ascites is detected (double arrow).



(Figer. 9)

Hepatocellular carcinoma with cirrhosis of the liver. A hypodense structure measuring 3 cm is detected in hepatic tissue exhibiting nodular transformation.

*Case No. 3**Hepatic Metastases.*

(Figer. 10)

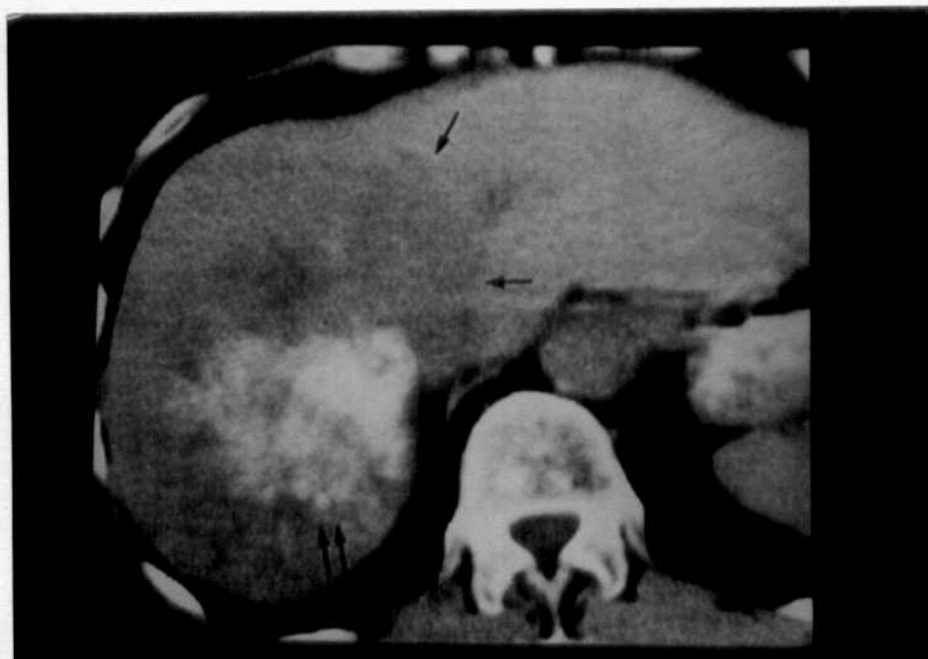
Hepatic metastases from a Carcinoid. In the early arterial contrast medium phase, a sharply margined hypervascularized mass is visible in both lobes of the liver. Only slight, centrally located regressive changes (arrow) can be detected as focal areas of hypodensity.

Case No. 4
Hepatic Metastases.



(Figer. 11)

Regressive changes due to metastases. Necrosis can cause a homogeneous reduction in attenuation value, resulting in a cystic appearance. In this case (bronchial carcinoma), viable tumor tissue exhibits peripheral enhancement (arrow).



(Figer. 12)

Calcified hepatic metastases from a colonic carcinoma. The broad hypodense structure (arrow) contains amorphous calcification indicative of necrobiotic metaplastic processes (double arrow).

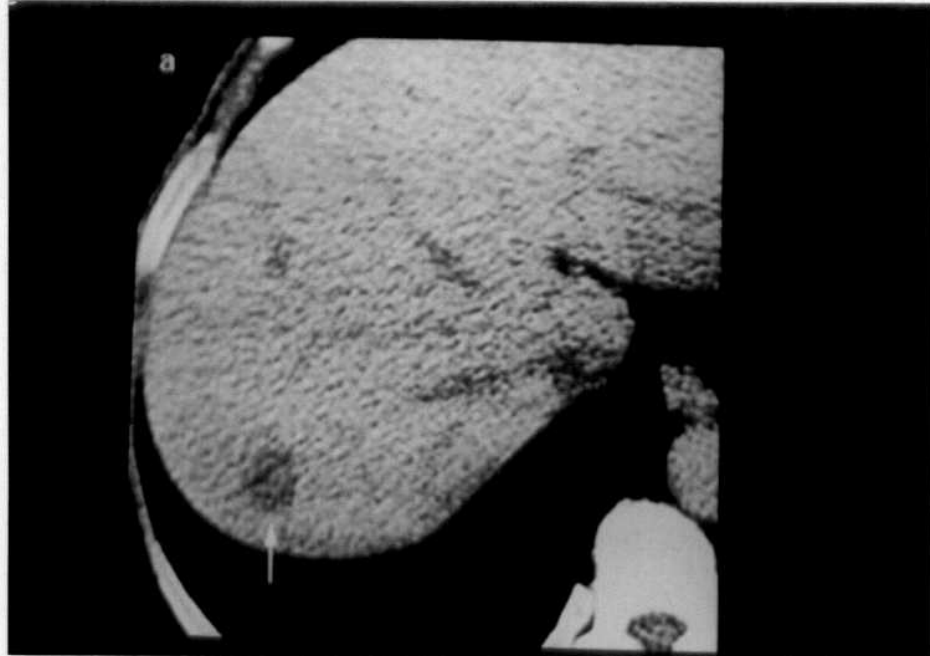
*Case No. 5**Hepatic Metastases.*

(Figer. 13)

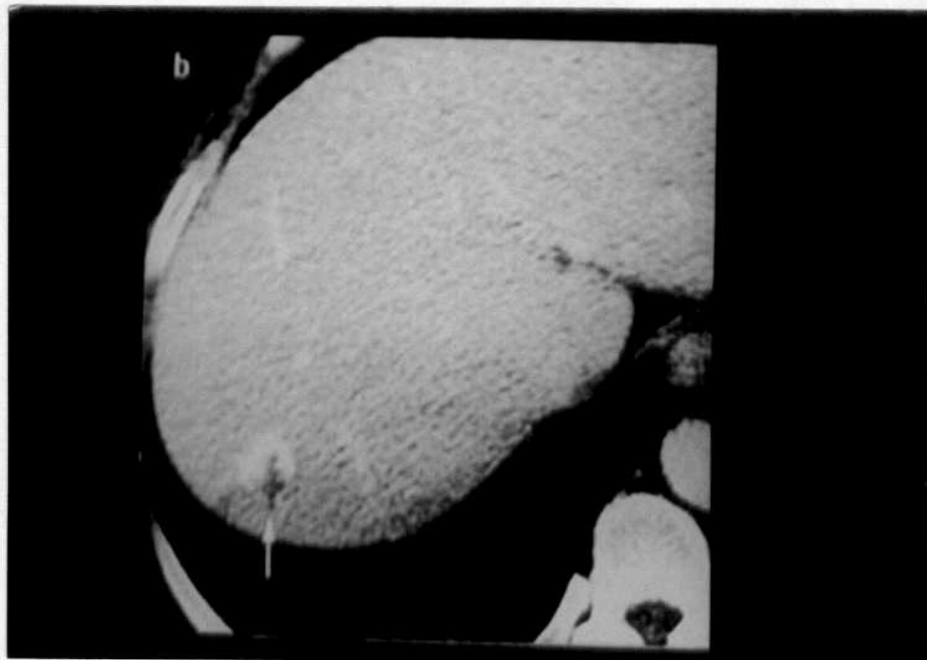


(Figer. 14)

Metastases from a gastrinoma. The sharply marginated homogeneous hypodense structure in the right dorsal lobe of the liver exhibits a homogeneous hyperdense structure indicative of hypervascularization during the early arterial phase

*Case No. 6**Hepatic Haemangioma.*

(Figer. 15)



(Figer. 16)

Plain scans revealed a sharply demarcated hypodense area of 1.2 cm (figer 15; arrow). It becomes strongly enhanced after contrast medium administration, and a small filling defect is revealed (figer 16; arrow). In the late film, the defect is filled with contrast medium and forms a homogeneous hyperdense structure.

*Case No. 7**Adenomyomatosis of the Gallbladder.*

(Figer. 17)



(Figer. 18)

The preliminary abdomen film for the OCG shows segmentation compartmentalization of the gallbladder and a somewhat irregular contour. The compression spot film (Figer .17) of the OCG shows tiny outpouchings filled with contrast material in the fundus and near the neck (arrow). A fatty meal was administered, and films of the contracted gallbladder show the outpouchings to better advantage (Figer .18). There is pronounced segmentation, and the diverticula are shown to be more diffuse. These diverticula are Rokitansky-Aschoff sinuses, characteristically seen in adenomyomatosis of the gallbladder.

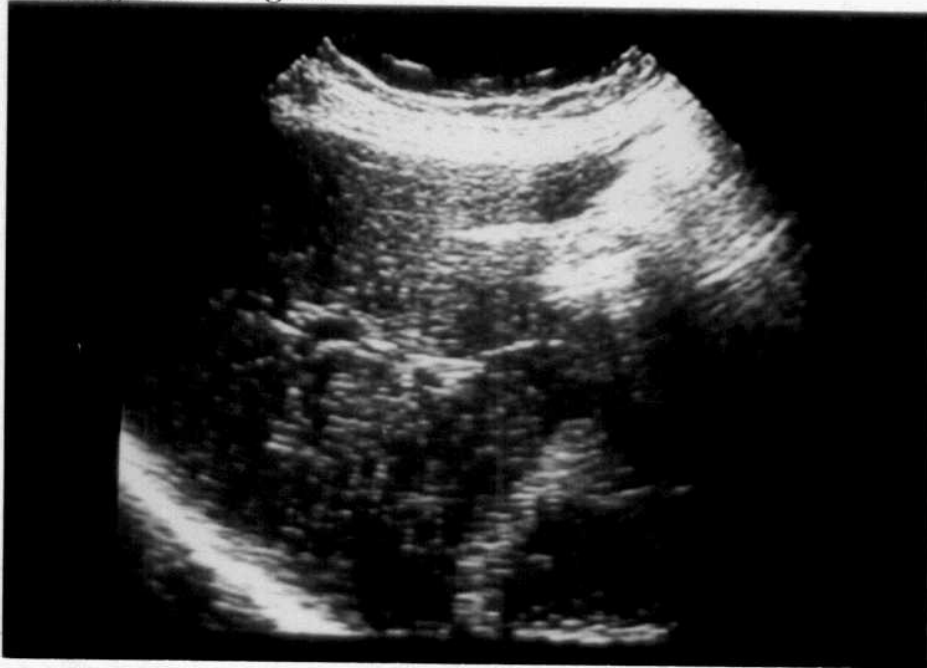


(Figer. 19)



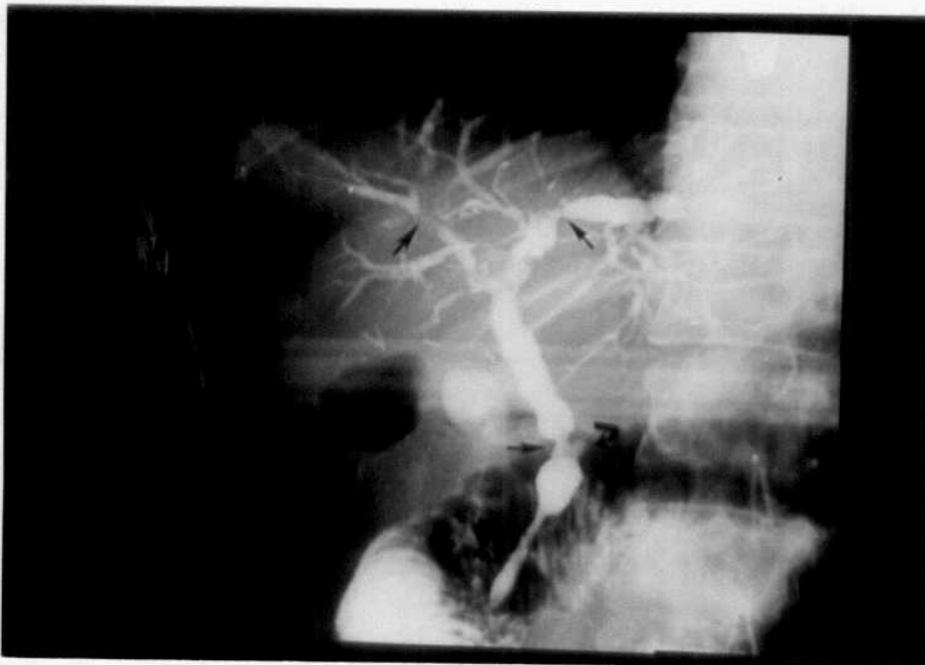
(Figer. 20)

CT (Figer .19) and US (Figer. 20) from a different patient demonstrate marked thickening of the gallbladder wall with small, fluid-filled outpouchings representing the Rokitansky-Aschoff sinuses. The gallbladder wall enhances on CT, the lumen is small and surrounded by tiny fluid-filled cysts. The markedly thickened gallbladder wall is noted on US with tiny echogenic foci paralleling the luminal surface (arrows), representing the intramural diverticula filled with sludge and small calculi. Adenomyomatosis was proven at surgery. (Case courtesy of Arnold Friedman, M.D., Temple University.)

*Case No. 8**Primary sclerosing Cholangitis.*

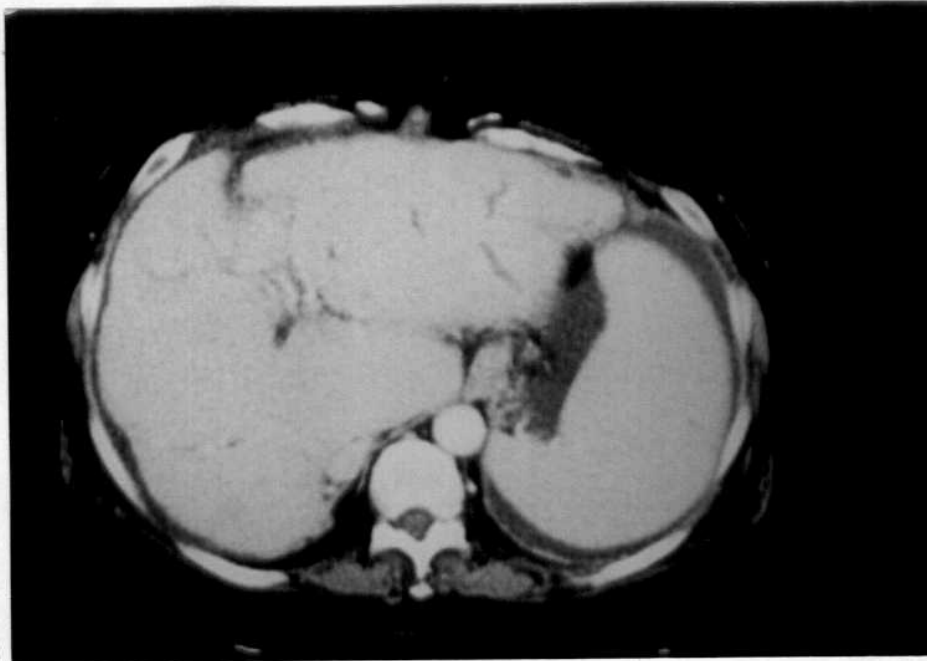
(Figer. 21)

Because of the elevated LFT's, an ultrasound was performed first (Figer .21). Mild intrahepatic biliary ductal dilatation was seen. The extrahepatic duct was normal caliber.



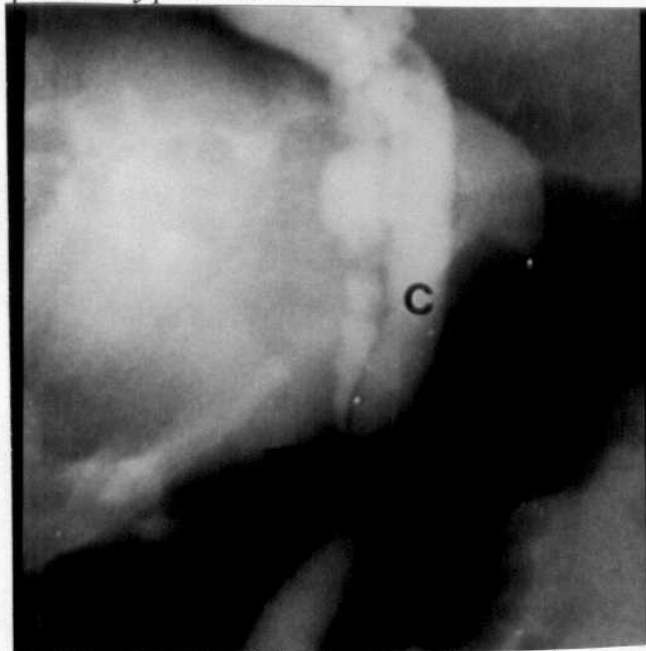
(Figer. 22)

The ERCP (Figer .22), reveals intermittent strictures (arrows) of the extra- and intrahepatic ducts. There is also irregularity of the margins of the extrahepatic duct and pseudodiverticula formation (curved arrow). The intrahepatic ducts show variation in caliber with intermittent dilatation of the left ductal system. The findings are consistent with sclerosing cholangitis.



(Figer. 23)

A CT scan 7 months later (Figer. 23) reveals patchy, discontinuous areas of intrahepatic ductal dilatation, more marked in the left lobe and in the posterior right lobe. The extrahepatic duct is not dilated; no portahepatis mass is seen. The patient has now developed biliary cirrhosis. The CT shows the characteristic changes of cirrhosis with a shrunken nodular liver and enlargement of the left lobe and caudate lobe. There is also splenomegaly from portal hypertension.

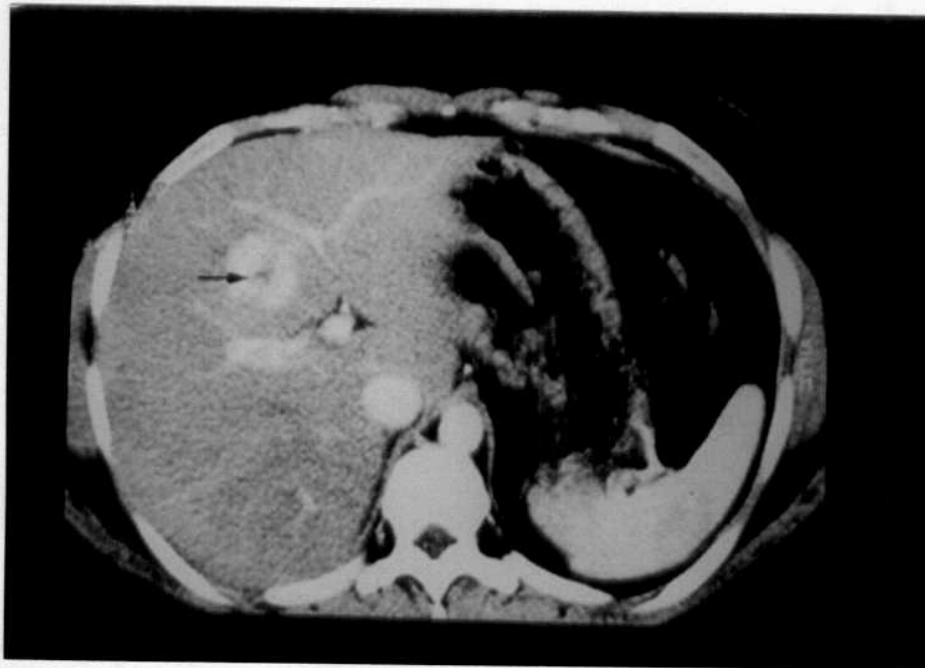


(Figer. 24)

In Figer. (24), there is "beading" of the intra and extrahepatic ducts with short segment strictures. The patient has a low medial insertion of a normal cystic duct (C) and there is a high grade stricture of the CHD (arrow) as it joins with the cystic duct. The CBD is normal.

Case No. 9

Focal Nodular Hyperplasia.



(Figer. 25)



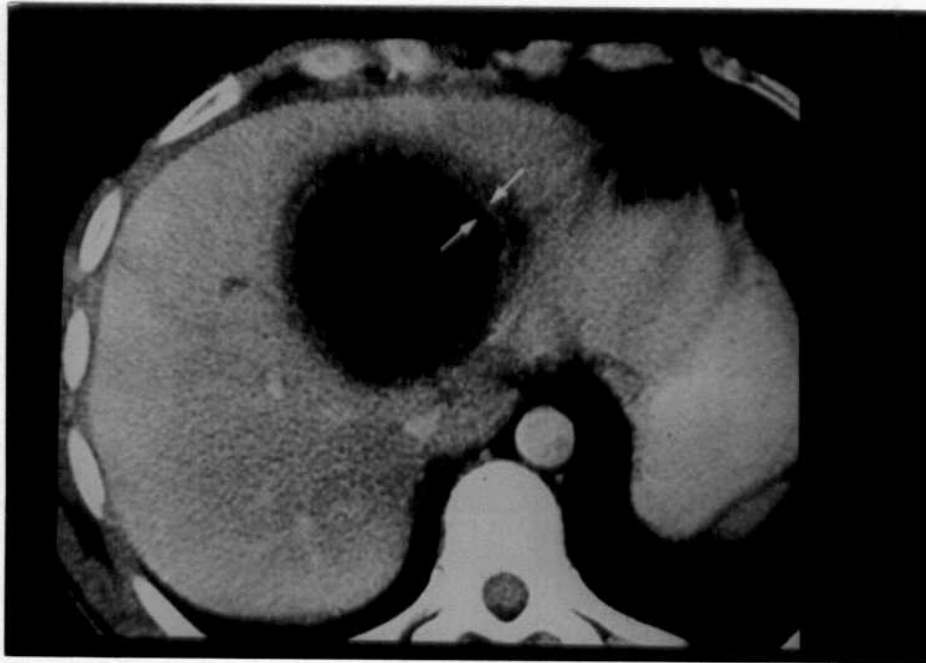
(Figer. 26)

Discretely hypodense, sharply defined regions were revealed on plain scans. After bolus injection of contrast medium, they demonstrate sharp, brief contrast enhancement (arrow). One of the two lesions exhibits a typical central scar (figer. 25, arrow).

*Case No. 10**Multiple Liver Abscesses.*

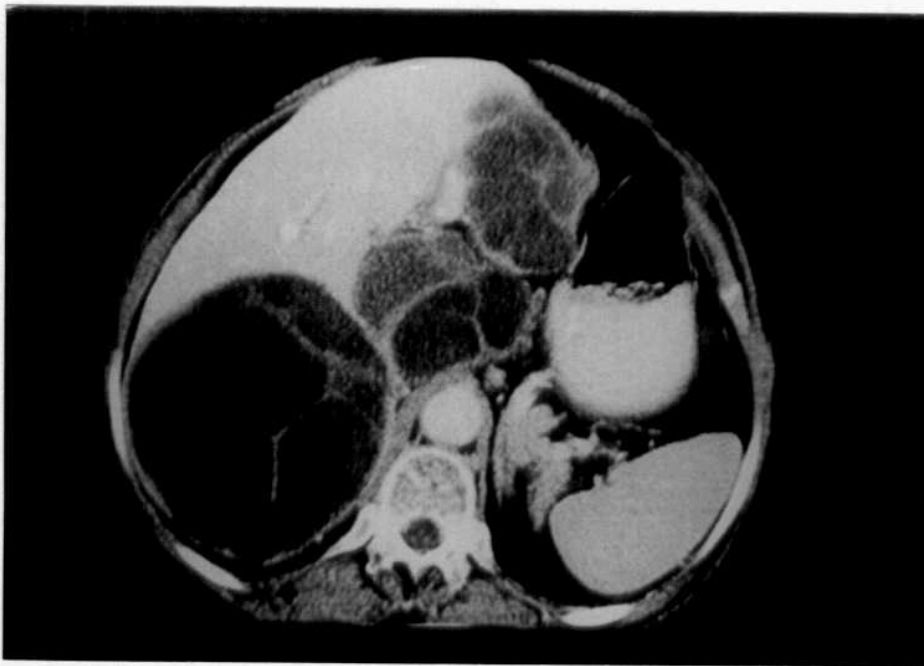
(Figer. 27)

The hypodense structures are sharply demarcated against the hepatic parenchyma. Hyperdense septal structures corresponding to the abscess membranes are also detectable inside the formations. The granulation tissue is less prominent against the liver.

*Case No. 11**Pyogenic Liver Abscess.*

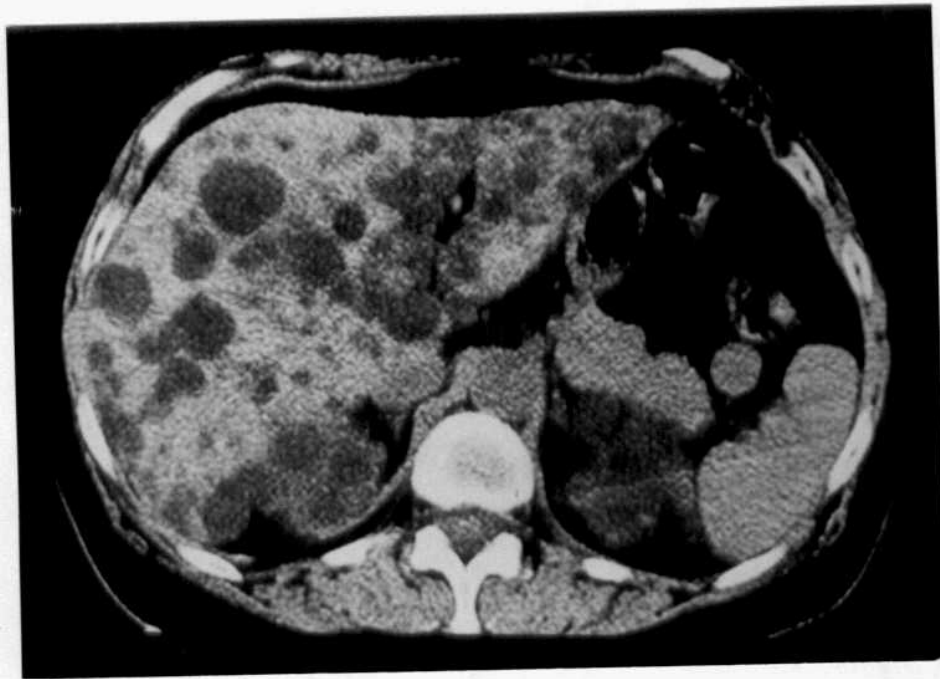
(Figer. 28)

The hypodense structure is contrasted by a sharply delineated peripheral enhancement (abscess membrane; arrow). The structure is demarcated against the liver tissue by a broad hypodense border corresponding to the granulation tissue. The density values of the contents of the abscess are approx. 25 HU.

*Case No. 12**Echinococcosis granulosa.*

(Figer. 29)

Several cystic structures are detected in the liver. A capsule is sharply demarcated from liver tissue. Typical cordlike septa can be seen.

*Case No. 13**Cystic liver.*

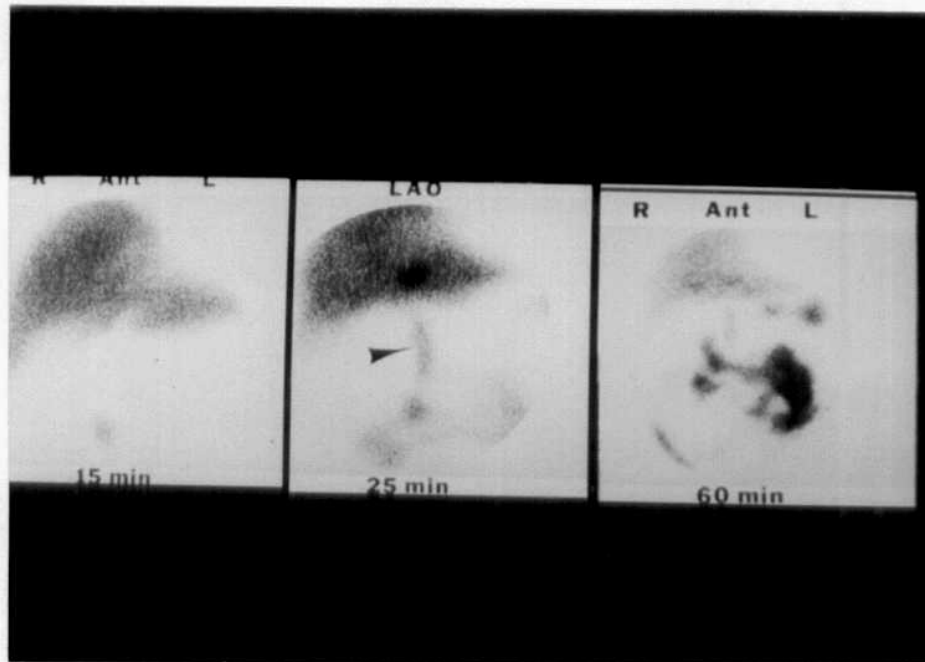
(Figer. 30)

Numerous sharply marginated hypodense structures of water density of various sizes are distributed throughout the liver. The simultaneous appearance of renal cysts is indicative of a hamartosis.

*Case No. 14**Acute Cholecystitis*

(Figer. 31)

The RUQ sonogram (Figer. 31) demonstrates a thickened gallbladder wall (arrow). There is gallbladder sludge with several small shadowing opacities representing gallstones contained within the sludge. No biliary ductal dilatation is seen. The patient had focal tenderness when the transducer was applied over the gallbladder (sonographic Murphy's sign).



(Figer. 32)

A ^{99m}Tc -DISIDA hepatobiliary scan (Figer.32) was positive, showing no visualization of the gallbladder on scans done up to 60 min. This is indicative of cystic duct obstruction as seen in acute cholecystitis. The CD is well-seen (Figer. 32, arrow) and later scans show radionuclide outlining bowel. At surgery, acute cholecystitis was found. The gallbladder wall was thick with patchy areas of necrosis. There were multiple small stones.



(Figer. 33)

A CT scan from a different patient with acute cholecystitis (Figer. 33) reveals a dilated gallbladder containing high density bile and multiple calcified stones. The gallbladder wall is slightly thickened and there are inflammatory changes in the adjacent fat.

*Case No. 15**Emphysematous Cholecystitis.**(Figer. 34)*

Supine and coned-down RUQ abdominal films demonstrate air within the gallbladder wall and throughout the gallbladder. A decubitus film shows an air-fluid level within the gallbladder lumen and air in the gallbladder wall.

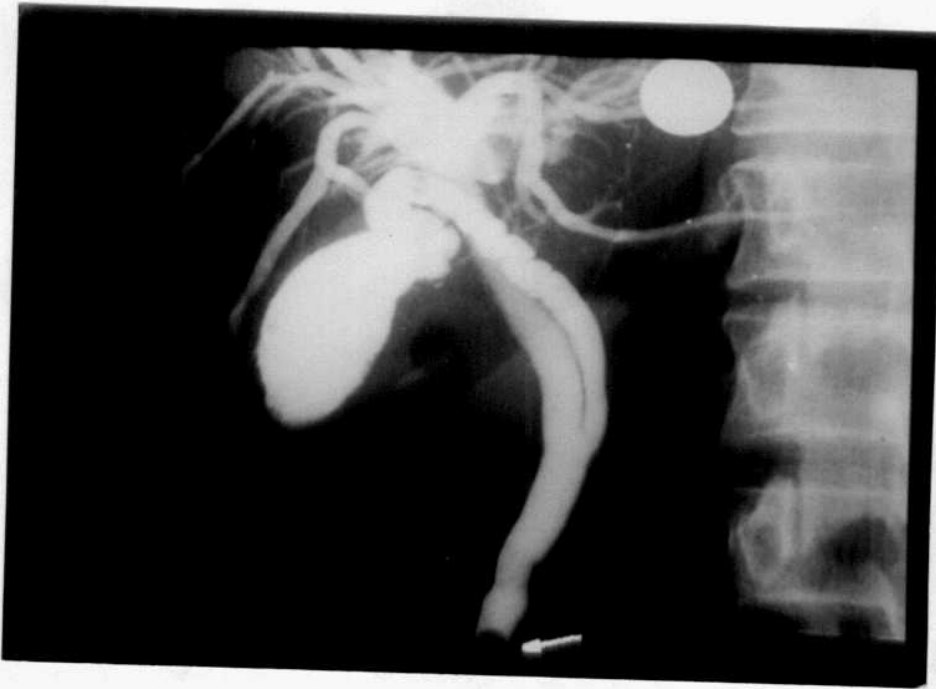
*(Figer. 35)*

A CT scan (Figer.35) from another patient with the same diagnosis demonstrates gas within the gallbladder lumen (arrows).

*Case No. 16**Choledocholithiasis*

(Figer. 36)

Transverse, sagittal and oblique images through the RUQ (Figer. 36) demonstrate a dilated common duct to the level of the head of the pancreas. In the dilated CBD is a shadowing echogenic focus representing an intraductal calculus. This was shown on real-time scanning to move with change in patient. Also noted are multiple stones in the gallbladder casting a distal acoustic shadow. Choledocholithiasis and cholelithiasis were confirmed at surgery.



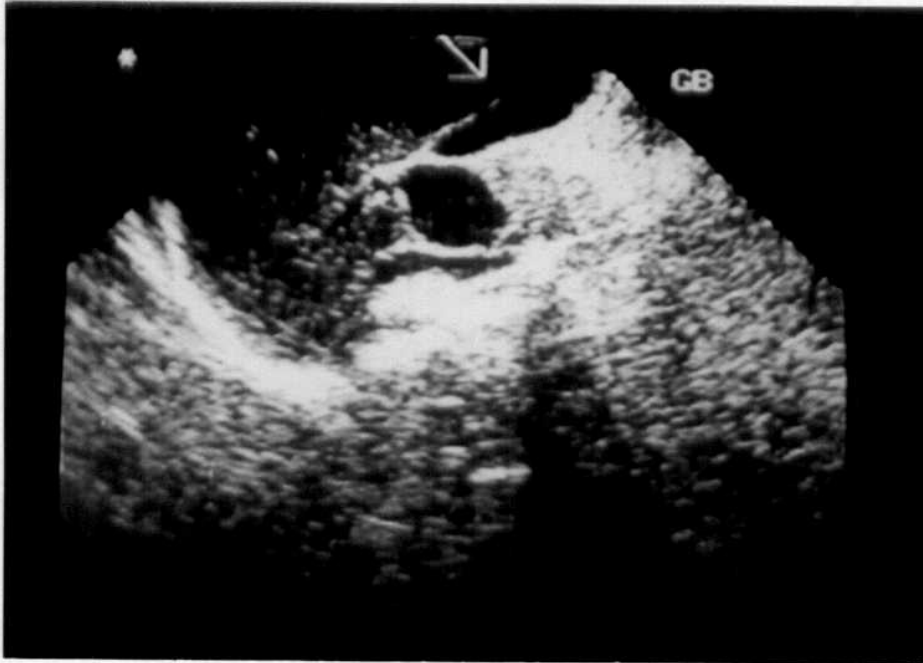
(Figer. 37)



(Figer. 38)

On PTC (Figer. 37) a meniscoid filling defect (arrow), characteristic of the cholangiographic appearance of a distal common duct stone is seen. Common duct stones may also be identified by ERCP (Figer. 38). Note the round, radiolucent filling defect in the dilated contrast filled CBD (arrow). Following sphincterotomy, the stone is successfully extracted using a wire basket for retrieval. Common duct stones may also be identified on T-Tube cholangiography and operative cholangiography. The appearance is the same as on PTC or ERCP.

Case No. 17
Choledochal Cyst.



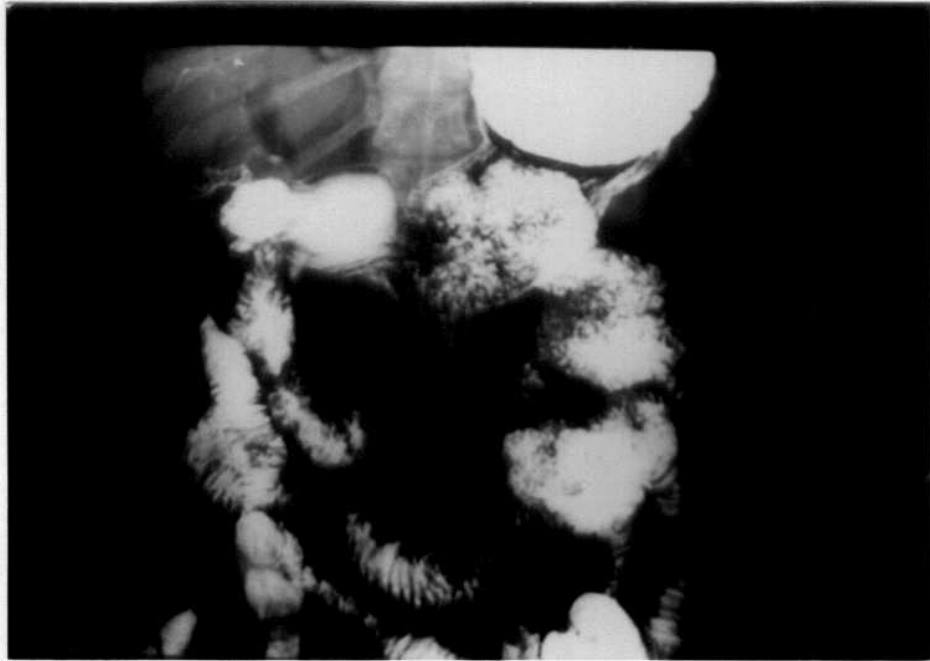
(Figer. 39)

The sonogram (Figer. 39) shows a normal gallbladder with no stones and no dilated ducts. There is a large echo-free mass medial to the gallbladder.

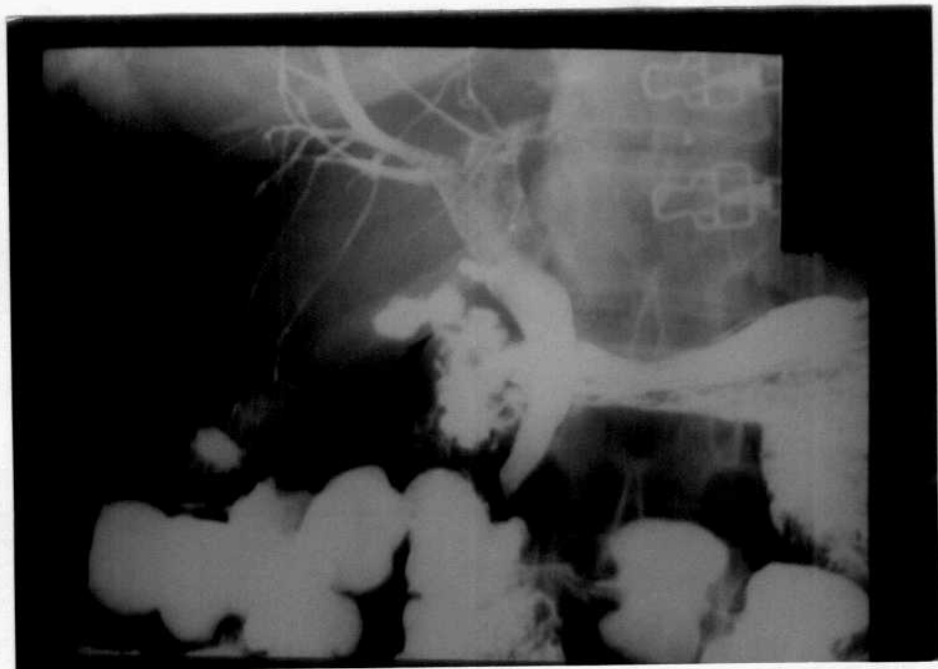


(Figer. 40)

A hepatobiliary scan (Figer. 40) was performed next. Excretion of the radionuclide into the bile ducts fills a large cystic structure inseparable from the extrahepatic bile ducts. This could be confused with an overlapping gallbladder. However, on 4.5-hr. delayed scans, the gallbladder fills and is clearly separate from the cystic structure, which is in continuity with the common bile duct. This confirms the diagnosis of choledochal cyst.

*Case No.18**Biliary-Enteric fistula.*

(Figer. 41)



(Figer. 42)

The plain abdominal film shows air in the bile ducts. The UGI series (Figer .41) shows filling of the biliary ductal system via a fistula from the postbulbar duodenum to the neck of the small, shrunken gallbladder (Figer. 42, arrow). No gallstone is seen.

Case No.19
Gallbladder Carcinoma.



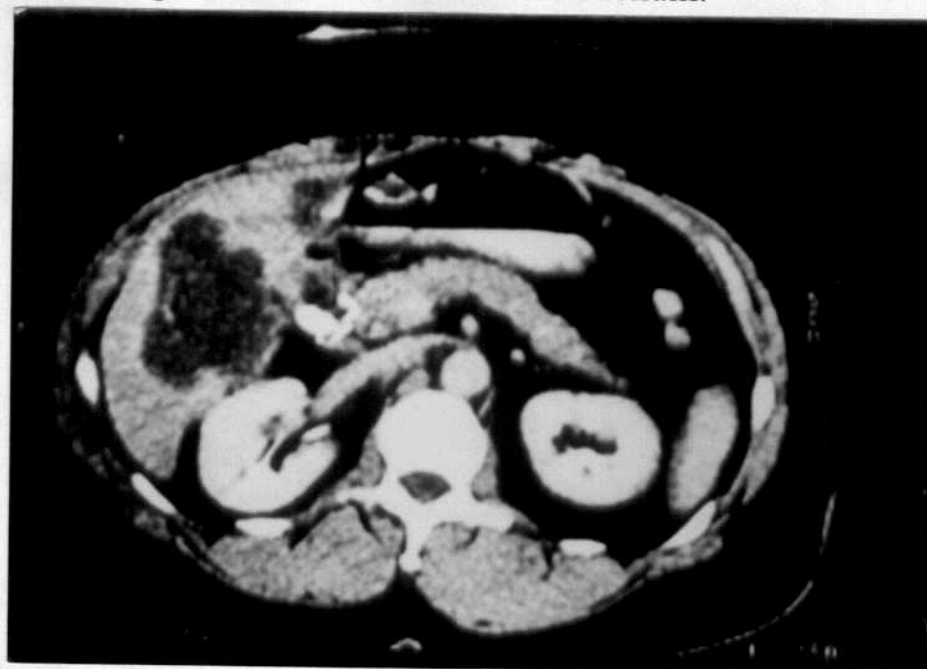
(Figer. 43)

A PTC was done to better define the extent of ductal involvement (Figer .43). The films show high grade obstruction of the CHD near the hilus with medial displacement of the duct by adjacent tumor mass. The intrahepatic ducts are markedly dilated. The findings of a mass partially filling the gallbladder lumen and extending into the liver with ductal obstruction at level of the portahepatis and the presence of a gallstone are characteristic of gallbladder carcinoma. This diagnosis was surgically confirmed.



(Figer. 44)

The CT (Figer. 44) demonstrates dilated intrahepatic ducts, no dilated extrahepatic ducts, and a mass partially replacing the GB lumen and extending into the liver posteromedially. Lower cuts show a round hypodensity in the GB (arrow) representing a large non-calcified gallstone. Note the mass effect against the contrast-filled duodenum.



(Figer. 45)

Two additional cases of gallbladder carcinoma demonstrating characteristic findings on imaging studies are included. A CT scan (Figer. 45) from a patient with tumor replacing the gallbladder lumen (HU #31) and locally invading the liver is shown. Note the irregular margins, a large mass in the gallbladder fossa and the presence of calcified gallstones (arrow).

Disorders of the biliary and pancreatic ductal system are routinely imaged using ultrasound and CT. Interventional procedures, such as percutaneous transhepatic cholangiography (PTC) and endoscopic retrograde cholangiopancreatography (ERCP), provide projection images of the biliopancreatic ductal system. These frontline techniques are mainly used for therapeutic purposes. Occasionally they are needed to clarify a diagnosis, but they are associated with complications, such as sepsis, pancreatitis, gastric or duodenal perforation, and hemorrhage.

Sonography and CT are the most commonly used noninvasive techniques for imaging the pancreas and hepatobiliary system. Both modalities accurately depict parenchymal abnormalities and can detect bile and pancreatic duct dilatation. Neither provides adequate information on the finely detailed anatomy of bile and pancreatic ducts, however. Endoscopic retrograde cholangiopancreatography (ERCP) is predominantly used for this application, but it is invasive, expensive, and time-consuming.

Power Doppler ultrasound (also known as ultrasound angiography, color power angiography, or color Doppler energy mode, depending on the manufacture) is a new technology that is superior to conventional color Doppler imaging in the detection of blood flow. Power Doppler Sonography is based on the integrated Doppler power spectrum. It is a technique that encodes the amplitude or energy spectrum of the Doppler signal rather than the mean frequency.

Reports show an increasing use of MR cholangiopancreatography (MRCP), which provides images approaching the sensitivity and specificity of those obtained with ERCP. MR is highly effective when one specific organ can be targeted for evaluation. It is more cumbersome, however, when screening for diffuse or unspecified abdominal problems, and CT and ultrasound continue to be the primary modalities for this task.

In Sonography the initial examination is performed with the patient in the supine position, followed by examination in the left posterior oblique position, which is especially useful for evaluation of the deeper posterior portions of the right lobe. Most of the liver is accessible by sub costal scanning. Cranial portions of the liver, especially the sub diaphragmatic portions of the right lobe, may be difficult to evaluate and better seen by intercostals scanning with sector transducers. Electronic focusing, when

available, should be adjusted throughout the examination to optimally evaluate both superficial and deep portions of the liver

CT images of the biliary tract are usually obtained with spiral data acquisition from the top of the gallbladder fossa through the bottom of the pancreatic uncinate, using 5-mm-thick sections and a pitch of 1. Images from the spiral data set are then reconstructed in 2-mm increments. A low mA technique will minimize radiation exposure and limit tube heating. Data acquisition is performed during a single breath-hold, with an average scan time of 20 seconds. Patients unable to perform a prolonged breath-hold should undergo imaging with two overlapping breath-hold data acquisitions.

Magnetic resonance cholangiopancreatography (MRCP) is an innovative noninvasive diagnostic technique that visualizes the anatomy and pathology of the pancreatobiliary ducts. This application of MR, which provides both cross-sectional images of ductal structures and projectional images of pancreatobiliary ducts, is based on a heavily T2-weighted sequence. As a result, MRCP images show stationary fluid, including bile and pancreatic juice, with high signal intensity, and solid organs with low signal intensity.

MRCP may be performed with a variety of heavily T2-weighted sequences that depict the fluid-filled biliary tract as high-signal-intensity structures. Thin-slab, multislice scanning with a half-Fourier rapid acquisition relaxation-enhanced sequence is the most common technique. Imaging is usually performed in the coronal oblique plane at angles that have optimal delineation of the bile ducts. Axial images confirm or exclude the presence of intraductal filling defects.

MRCP is a noninvasive procedure. Compared with endoscopic retrograde cholangiopancreatography (ERCP), its advantages include no injection of contrast material, no ionizing radiation, no pain, and no complications. MRCP can be performed in patients with acute pancreatitis and acute obstructive suppurative cholangitis, both of which are contraindications for ERCP. MRCP provides information about pancreatobiliary ducts in patients with biliary enteric anastomoses, Billroth II gastrojejunostomy, stenosis of the upper gastrointestinal tract, and poor general condition, in whom ERCP is difficult to perform.

1. *A.Arslan, J. T. Geitung, E. Viktil, M. Abdelnoor and M. Osnes.* Acta Radiologica 41 (2000) 621-626.
2. *Abbitt PL (1995):* Ultrasound: A pattern approach, New York, MC Graw-Hill, 1995.
3. *Adam A:* Percutaneous techniques in the liver and biliary system Recent advances. Br Hosp Med 1989; 42:102-110.
4. *Albores-Saavedra J, Henson DE, Sobin LH,* The WHO histological classification of tumours of the gallbladder and extrahepatic bile ducts: A commentary on the second ed. Cancer 1992; 70:410-414.
5. *Babb RR.* Acute acalculous cholecystitis: A review. J Clin Gastroenterol 1992; 15:238-241.
6. *Bach D, Vellet A, Glazer GM:* retroperitoneal Sarcoidosis. ASR;156:520. 1991.
7. *Bailes DR., Gilderdale DJ., Bydder GM., et al:* Respiratory ordering of phase-encoding (ROPE): A method for reducing respiratory motion artifacts in MR imaging. J Comput Assist Tomogr 9:835, 1985.
8. *Baret AL, Wackenheim A, Jeanmart L:* Abdominal CT. AJR; 133:1037-1042, 1980.
9. *Baron RL, Freeny PC, Moss AA (1992):* The liver. In Moss AA, Gamau G, Genant Hk (eds.): Computed Tomography of the whole body 2nd edn, WB Saunders, Philadelphia. PP: 735-822, 1992.
10. *Baron RL, Olive JH III, Dodd GD III et al (1996):* HCC evaluation with biphasic enhanced helical CT. Radiology 199:505-511, 1996.
11. *Berta R, Pansini GC, Zamboni P, et al.* laparoscopic treatment of Mirizzi syndrome. Minerva Chi 1995; 50:547-552.
12. *Bismuth H (1982):* surgical anatomy of the liver. World journal of surgery; 6-13, 1982.

13. *Bismuth H (1988):* Surgical anatomy & anatomical surgery of the liver, In: Bismuth H (eds.): surgery of the liver & biliary tract. Edinburg, Churchill Livingstone. Vol. (3), pp: 3-9, 1988.
14. *Blenkharn JJ; McPherson GA and Blumgart LH:* Septic complication of percutaneous biliary drainage. Am J Surg 1984; 147:318-321.
15. *Bluemke AD., soyer PA., Bliss DF., Fishman EK., Calboun PS.,* spiral CT during arterial portography technique and application. Radiographics; 15:623,639, 1995.
16. *Bluemke AD., Soyer PA., Fishman EK.,* Helical CT of the liver R.C.N.A., 33(5):863-887, 1995.
17. *Bluemke DA, Soyer P, Bitss, Fishman ER, (1995):* Helical CT of the liver. Radiol Clin North Am; 33:863-887, 1995.
18. *Brink M., Daveros D:* Helical CT; principals and a practical approach New York, McGraw and Hill: 1-26, 1995.
19. *Brown BM, Filly RA, Callen PW (1982):* Ultrasonography anatomy of the caudate lobe. Ultrasound Med. 1982; 1:189-192.
20. *Brown RJ, Memsie LD, Pusey EJ:* hepatic abscesses in liver transplantation. Clin. Nucl Med; 11:233-238, 1986.
21. *Bydder GM & Young IR:* MR imaging: Clinical use of the inversion recovery sequence. J Comput Assist Tomogr 9:659, 1985.
22. *Callen PW, Filly RA:* Ultrasonographic localization of the gallbladder, Radiology 133:687-691, 1979.
23. *Campeau NG., Johnson CD., Felmlee JP., et al:* MR imaging of the abdomen with a phased-array multicoil: Prospective clinical evaluation. Radiology 195:769, 1995.
24. *Caseiro FA, Zins M, Mahfouz AE, Didier M,* Calcification in focal nodular hyperplasia. Radiology; 198:889-892, 1996.

25. *Castello P.*, thoracic helical CT, Radiographics, 193-918, 1994.
26. *Catasca JV., Mirowitz SA:* T2-weighted MR imaging of the abdomen: Fast spin echo vs conventional spin echo sequences. AJR AM J Rontogenol 162:61, 1994.
27. *Choi BI, Han Jk, Shin Ym, et al.* peripheral cholangiocarcinoma: Comparison of MRI with CT. Abdom Imaging 1995;20:357-360.
28. *Choi BI.* Sonographic and CT findings of the bile duct cancer. In Herlinger H, Megibow A (eds.): Advances in gastrointestinal radiology. Philadelphia: mosby ;1992. pp161-180.
29. *Cico GR, Neumater CE, Derchi LE, et al (1983):* The patent ductus venosus: An additional ultrasound finding in portal hypertention, 1983.
30. *Claire E. Bender, MD. Andreas Adam, MB. Oeter R. Mueller, MD. Eric vanSonnenberg, MD Johannes Lammer, MD. Steven K. Teplick, MD.* Robert Braden. Radiology 1998; 209: 317-319.
31. *Clautic-Engle T & Jeffrey RB Jr:* Renal hypoperfusion of power Doppler imaging AJR; 168:127, 1997.
32. *Collins T, Kumar V, Ramzi S, et al (1999):* pathologic Basis of disease, sixth ed. W.B Saunders Company Philadelphia London, Liver 877-879, 1999.
33. *Cowling MG, Belli AM, Buckenham TM.* Evaluation and complications of direct graft puncture in thrombolysis and other interventional techniques. Cardiovas Intervent Radiol 1996; 19:82-84.
34. *Crawford JM (1994):* The liver & biliary tract. In Catra R, Kumar V, Robbins S, Schoen F (eds.): Pathologic basis of disease. Philadelphia, WB Saunders, 1994 pp831-895.
35. *Croley GG.* Gangrenous cholecystitis: Five patients with intestinal obstruction. Am Surg 1992; 58:284-292.

36. *Dachman AH.* Primary biliary neoplasia. In Friedman AC, Dachman AH (eds.): radiology of the Liver, Biliary tract, and pancreas. St. Louis: Mosby; 1994:pp611-632.
37. *Danason L, Matrinz-noguera A, and Zidan A, et al (1989):* Papillary process of the caudate lobe of the liver: Sonographic appearance. Radiology, 1989; 173, 631-633.
38. *Desser TS, Jedrzejewicz & Haller MI.:* Colour & power Doppler Sonography: Techniques clinical applications & trade-offs for image optimization. Ultrasound quarterly; 14 (3):128, 1998.
39. *Dodd III GD, Miller WJ, Baron RL, Skolnick ML, Campbell WL.* Detection of malignant tumours in end stage cirrhotic livers; efficacy of Sonography as a screening technique. Am J Roentegenol 1992; 159:727-733.
40. *Drane WE:* Nuclear medicine techniques for the liver and biliary system. Update for the 1990s. Radiol Clin North Am 1991; 6:1129.
41. *Durham JD, Zwerdinger S.* Percutaneous embolization of bleeding varices. In LaBerge JM, Durham JD (eds.): Portal Hypertention: Options for diagnosis and treatment. San Francisco: society of Cardiovascular and interventional Radiology; 1995:pp143-154.
42. *Egbert RN; Braunstein P and Lyons KP:* Total bile obstruction: prompt diagnosis by hepatobiliary imaging. Arch Surg 1983; 709.
43. *Elaine M. Caoili. Erik K. Paulson. Laura E. Heynema M. Stanley Branch W. Steve Eubanks Rendon C. Nelson.* AJR;174: february 2000.
44. *El-Bolkainy MN. (1998):* In: El-Bolkainy MN. Tomographic pathology of cancer. Cairo: the national cancer institute: 1998:7-18.
45. *Elster AD:* Gradient-echo MR imaging: techniques and acronyms. Radiology 186. 1, 1993.

46. *England MA. (1983):* Color Atlas of life before birth: Normal fetal development. Chicago O, Year Book medical, 1983.
47. *Farzaneh F., Riederer SJ. & Pele NJ:* Analysis of T2 limitations and off resonance effects on spatial resolution and artifacts in echo-planar imaging. Magn Reson Med 14:123, 1990.
48. *Federle MP, Filly RA, Moss AA:* Cystic hepatic neoplasm complementary roles CT and Sonography. AJR: 136:345-348, 1981.
49. *Felmlee JP& Ehman RL:* Spatial presaturation: A method for suppressing flow artifacts and improving depiction of vascular anatomy in MR imaging. Radiology 146:559, 1987.
50. *Foley WD, Hoffman RG, Quiroz FA:* Hepatic helical CT contrast material injection protocol. Radiology; 192:367-371, 1994.
51. *Foley WD, Wilson GR, Quiroz FA:* Demonstration of extrahepatic biliary tract with CT. comput. Assist. Tomog; 4:48-52, 1980.
52. *Foulner D,* Granular cell tumour of the biliary tree : sonographic appearance. Clin radiol 1994;49:503-504.
53. *Freeny PC:* cavernous haemangioma of the liver. Radiology; 138:637-644, 1981.
54. *French AL, Beaudet LM, Benator DA, et al.* Cholecystectomy in patients with AIDS: Clinicopathologic correlation in 107 cases. Clin Infect Dis 1995; 21:852-858.
55. *Friedman AC, Sachs L:* Embryology, anatomy, histology and radiologic anatomy. In Friedman AC, Ed: Radiology of the liver, biliary tract, pancreas and spleen, Baltimore, 1987, Williams & Wilkins.
56. *Gallego JC, Suarez I, Soler R,* Multiple bile duct Hamartomas: US, CT and MRI findings. A case report. Acta Radiol 1995;165:309-313.

57. *Garber SJ, Donald JJ, Lees WR.* Cholangiocarcinoma: Ultrasound features and correlation of tumour position with survival. *Abdom Imaging* 1993;18:66-69.
58. *Glazer GM, Laing FC, Brown TW, et al (1980)* Sonographic demonstration of portal hypertension: The patent umbilical vein. *Radiology* 1980, 136:161-163.
59. *Goldsmith MA & Woodbrune RT (1957):* The surgical anatomy pertaining to liver resection. *Surg Gynaecol Obstet*; 141:429-437, 1957.
60. *Goodman ZD, Ishak KG, Langloss JM, et al.* Combined Hepatocellular-cholangiocarcinoma: a histologic and immunohistological study. *Cancer* 1985;55:124-135.
61. *Graif M, Manor A, Itzhaky (1983):* Sonographic difference of extra & intra hepatic masses. *AMJ Roentgenol*, 141:553-556, 1983.
62. *Gray SW, Skandalakis JE;* Embriology for surgeons, Philadelphia, 1982, WB Saunders.
63. *Greany GC, Reynolds TB, Donovan AS;* CT of amoebic liver abscess. *AJR*; 120:553-558, 1985.
64. *Greissler M, et al (1997):* Molecular mechanism of hepatocarcinogenesis. In Okuda, Tabor E (eds.): liver cancer: New York, Churchill living-stone, 1997, pp59-88.
65. *Guertud M; Mendoza S and Jaen D:* Endoscopic retrograde cholangiopancreatography in infants and children with jaundice due to common bile duct stones. *Gastrointest Endosc* 1992; 38:450-453.
66. *Guyton AC (1986):* Textbook of medical physiology, 7th ed. Philadelphia. WB Saunders, pp 780-790, 1986.
67. *Hagen-Ansert, Zweible W, Kwan OL (eds.) (1995):* Textbook of diagnostic US. 4th Ed vol 1 st. Lewis, CV. Mosby, pp 573-577, 1995.

68. *Hamper J & Perssini C.* Convergent colour Doppler. Acuson corporation application note ACU 1249-IOM1096. Mountain view, Acuson Corp, 1997.
69. *Harbin WP; Mueller PR and Ferrucci JT:* transhepatic cholangiography: complications and use patterns of fine needle technique. *Radiology* 1980; 135:15-22.
70. *Hean Horchen, Hong N. Young, San-Kan Lee and Jye-Wen Chai:* Evaluation of liver disease via MTC and contrast agents: *Journal of Magnetic Resonance Imaging* 9:237-265, 1999.
71. *Heiken JP. Brink JA., McClennan BL., Sagel SS., Forman HP:* Comparison of contrast material injection rates biphasic and uniphasic protocols. *Radiology*, 187:327-332, 1993.
72. *Heiken JP. Weyman PJ., Balfe DM., Brunt EM., Picus D:* Detection of focal hepatic masses with CT, delayed CT and CT during arterial portography. *Radiology*; 171:47-52, 1989.
73. *Heiken JP., Brink JA., sayel SS., McClennan BL., Crowe TM.,* hepatic enhancement. *Radiology*; 195:353-357, 1995.
74. *Helena M. aylor, MD, FRCR, and Pablo R. Ros, MD, FRCR .* *Radiologic clinics of north america* volume 36. number 2. march 1998.
75. *Helenon O, Correas JM, Chabriais J, et al.:* Renal vascular Doppler imaging: Clinical benefits of power mode. *Radiographics*; 18(6), 1998.
76. *Hodgson T, Foy S, Bayjoo P,* Case report: Extra-hepatic biliary cystadenoma in association with adenomyomatosis of the gallbladder. *Clin Radiol* 1991;43:210-212.
77. *Husband JE, Reznek RH, Mclean D, (1996):* Imaging in oncology vol 1, Philip roobinson, Liver ISIS Oxford 780-787, 1996.
78. *Joe Ariyama,MD.* *Diagnostic Imaging Asia Pacific* ;June 2001.

79. *John S, Virginia A, John T, Scott II*: National medical series for independent study, 2nd ed. John W. and sons: 241-284, 1993.
80. *Joseph V. Hajnal, Christine J. Baudouin, Angela Otridge, Ian R. Young and Graeme M. Bydder*: Design and implementation of magnetization transfer for clinical use. *Journal of Compu Assist Imogr* 16:7-18, 1992.
81. *Jukka I. Tantt, Raimo E. Sepponen, Martin J. Lipton and Timo Kuusela*: Synergistic enhancement of MRI with Gd-DTDA and magnetization transfer. *Journal of Computer Assisted Tomography*, 16:19-24, 1992.
82. *Kairaluoma M, Leinonen A, Stahlberg MM*; Percutaneous aspiration and alcohol sclerotherapy for symptomatic hepatic cysts. *Ann surg*, 210:208-215, 1989.
83. *Kane RA (1981)* Sonographic anatomy of the liver *Semin us*: 190-197, 1981.
84. *Kane RA, Hughes LA, Cua EJ et al.* The impact of intraoperative ultrasonography on surgery on surgery for liver neoplasms. *J Ultrasound Med* 1994; 13:1-6.
85. *Kane RA, Roizental M, Kruskal JB, et al.* preliminary investigation of liver and biliary imaging with a dedicted laparoscopic US system. *Radiology* 1994; 193(p):287.
86. *Kane RA.* US anatomy of liver & biliary tree *Semin us* 1980, 1:86-95.
87. *Khuroo MS, Dar MY, Yattoo GN, et al.* serial cholangiographic appearances in recurrent pyogenic cholangitis. *Gastrointestinal Endos* 1993; 39:674-679.
88. *Kim WS, Choi BI, Lee YS, et al.* Endodermal sinus tumour associated with benign teratoma of the common bile duct. *Pediatr radiol* 1993; 23:59-60.

89. *Kloiber R; Aucoin R and Hershfield NB*: Biliary obstruction after cholecystectomy: Diagnosis with qualitative cholescintigraphy. Radiology 1988; 169:643-647.
90. *Kruskal JR, Kane RA*. Intraoperative ultrasonography of the liver, Cru Rev Diagn. Imaging 1995; 36:175-226.
91. *Kumar L; Ihaa RR and Singh HS*: percutaneous transhepatic cholangiography using Chiba needle by blind method. J Id Med assoc 1989; 87:235-237.
92. *Kurtz AB, Middleton WD*, Ultrasound: The requisites. St. Louis: Mosby-Year Book, Inc.; 1996.
93. *Last PJ 1972*: Anatomy; regional and applied. 5th edn, the English language book society and Churchill Livingstone, Edinburgh, London, 1972.
94. *Lau W, Leung JWC, Li AKC*, Management of Hepatocellular carcinoma presenting as obstructive jaundice, Am J Surg 1990;160:280-282.
95. *Levine E, Cook LT, Grantham JJ*: Liver cysts in autosomal dominant polycystic kidney disease: Clinical and CT study. AJR; 145:229-233, 1985.
96. *Lim GY, Lee JM, Park JM, et al*. Mucin hypersecreting biliary neoplasms: two cases report . J Korean Radiol Soc 1995;33:395-398.
97. *Litwin DEM, Taybr BR, Greig P*: Nonparasitic cysts of the liver: the case for conservative surgical management. Ann surg; 205:45-48, 1989.
98. *Mack LA, Lee RA, Nyberg DA*. Intraoperative Sonography of the abdomen. In Rumack, Wilson, Charboneau (eds.): Diagnostic ultrasound. St. Louis: Mosby-year book Inc. 1991:pp492.
99. *Mariani AF, Bruneton JN, Pointreau CC*: Progressive enlargement of hepatic adenoma, gastroenterology; 77:1319-1324, 1989.

100. *Marieb EN*. Human anatomy & physiology red wood city, CA, Benjamin/Cumming, 1989.
101. *Marks WM, Filly RA and Callen PW*: ultrasonic anatomy of the liver: a review with new applications. J Clin Ultrasound; 7:137, 1979.
102. *Martinoli C, Derchi LE, Rizzatt L., et al.*: Power Doppler Sonography: General Principals, clinical applications and future prospects. Eur. Radiol.; 8:1224-1235, 1998.
103. *Martinoli C, Dretolesi F, Crespi G, et al.*: Power Doppler Sonography: Clinical applications. Eur J Radiol; 27 suppl 2:5133, 1998.
104. *Masayuki K., Takeyoshi L., Mizuno S., Yasuhiro S., Lidat*: value of 3-D spiral CT hepatic angiography. AJR; 166:585-591, 1996.
105. *Matsai O., Kadoya M., Kameyama T.*, Benign and malignant nodules in cirrhotic liver. Radiology; 178:493-498, 1991.
106. *Maurer AH and Malmud LS*: Radionuclide imaging: Basic principle. In: Grainger RG and Allison DJ (eds.): Diagnostic radiology. 2nd ed. Churchill Livingstone, 1992, p87.
107. *McDermott VG, Lawrance JAL, Paulson EK, et al.* CT during arterial portography: comparison of injection into the splenic versus superior mesenteric artery. Radiology 1996; 199:627-631.
108. *McDonald MI, Corey GR, Gallis HA*: Single and multiple liver abscesses. Medicine; 63:291-295, 1984.
109. *Mentzer RM Jr, Golden GT, Chandler JG, et al.* A comparative appraisal of emphysematous cholecystitis. Am J Surg 1975; 192:10-15.
110. *Miller WJ, Dodd GD, Federle MP*: Epithelioid Haemangioendothelioma of the liver. AJR; 159:53-57, 1992.

111. *Mir-Madlessi SH, Farmer RG, Sivak MV*, bile duct carcinoma in patients with ulcerative colitis. *Dig Dis Sci* 1987; 32:145-154.
112. *Molenda J and Brykaski D*: Usefulness of biliary scintigraphy using ^{99m}Tc mebofenin for detection of disorders of parenchyma of the bile ducts. (Abstract) *Pol Tyg Lek* 1992; 47:177-180.
113. *Moosman DA, Collier FA*: Prevention of traumatic injury to the bile ducts: a study of the structures of the cystohepatic angle encountered in cholecystectomy and supraduodenal choledochostomy, *Am J Surg* 82:132-143, 1981.
114. *Moser JJ, Baer HU, Glattli A, et al.* Mirizzi syndrome. A contraindication for laparoscopic surgery. *Helv Chi Acta* 1993; 59:577-580.
115. *Mukai JK, Stak CM, Turner DA, et al (1987)*: Imaging of surgically relevant hepatic vascular & segmental anatomy II; extent and respectability of hepatic neoplasm. *AJR*; 149:293, 1987.
116. *Murakami T, Kim T, Ohi, Nakamura H, Matsushita M*: Detectability of hypervascular Hepatocellular carcinoma by arterial phase imaging of MR and spiral CT. *Acta-radiol*; 36:372-376, 1995.
117. *Nahrwoid DL*: The Biliary system. In Sabiston DC, Ed; *Textbook of surgery*, Philadelphia, 1991, WB Saunders.
118. *Naidich DP.*, helical CT of the thorax (clinical application) *Radiologic clinics of North America* volume 32. Number 4 July 1994.
119. *Netter FH (1964)*: The CIBA collection of medical illustrations. Digestive system 2nd ed. Vol.3. Oppenheimer F (ed.) Summit, NJ: CIBA pharmaceutical Co. 1964.
120. *Okuda K, Peters RL, Simson IW (1984)*: Gross anatomic features of Hepatocellular carcinoma from three separate geographic areas. Proposal of new classification. *Cancer*; 54:2165-2173, 1984.

121. *Okuda K; tanikawa K and Emura T*: non surgical percutaneous transhepatic cholangiography Diagnostic significance in medical problems of the liver. Am J Dig Dis 1974; 19:21-26.
122. *Paranjpe and Bergin*, spiral CT of lungs: Optimal technique and resolution compared with conventional CT. AJR; 162:561-567, 1994.
123. *Parulekar SG*: ligaments and fissures of the liver: Sonographic anatomy. Radiology; 130:409, 1998.
124. *Patten RM and Freeny PC*: CT of hypervascular tumours AJR; 161:979-985, 1993.
125. *Pereiras R*: Special radiologic procedures in liver disease. In: Schiff L and Schiff E (eds.); disease of the liver. Lippincott co. 1982, p145.
126. *Peter F. sharp, Howard G. Gemmell and Francis W. Smith*. Oxford university press 1998.
127. *Polacin A., Kalander WA., marchal G*: evaluation of section sensitivity profiles in helical CT. Radiology; 185:29-33, 1992.
128. *Powers C, Ros P*: Hepatic mass lesion, CT and MRI of the whole body, third edition Mosby-year book, Inc: 896-938, 1994.
129. *Prando A., Wallace S., Bernadino ME., Lindell MM*: CT arteriography of the liver. Radiology; 130:697-701, 1997.
130. *Prassopoulos P, Raptopoulos V, Chuttani R, et al*. Development of virtual CT cholangiopancreatography. Radiology 1998; 209: 570-574.
131. *Radiologica* 41 (2000) 621-626.
132. *Ralls PW*: Hepatic section. In sarti DA (Ed): Diagnostic us. Text & cases, 2nd Ed Chicago, yearbook medical, 1987.
133. *Rappaport WD, Gordon P, Warneke JA, et al*. Contraindications and complications of laparoscopic cholecystectomy. Am Fam Physician 1994; 50:1707-1714.

134. *Rees CR, Niblett RL, Lee SP, Diamond NG, Crippin JS.* Use of carbon dioxide as a contrast medium for transjugular intrahepatic Portosystemic shunt procedures. *J Vasc Intervent Radiol* 1994; 5:383-386.
135. *Reinhold C., Hammers L., Taylor Cr., et al.:* Characterization of focal hepatic lesions with Duplex Sonography: findings in 198 patients *AJR*; 164:1131-1135, 1995.
136. *Roberts AC.* Preprocedure testing. *J Vasc Intervent Radiol* 1994; 5:59-65.
137. *Rolf A. Heckemann, MD. David O. Cosgrove, FRCR. Martin J. K. Blomley, FRCR. Robert J. Eckersley, PhD. Christopher J. Harvey, FRCR. Yoshitaka Mine, MS.* *Radiology* 2000; 216: 592-596.
138. *Rosen CB, Nagorney DM, Wiesner RH, et al.* Cholangiocarcinoma complicating primary sclerosing cholangitis *Ann surg* 1990; 213:21-25.
139. *Rubenstein WA, Auh YH, and Whalen JP:* The perihepatic spaces: Computed atomographic & ultrasound imaging. *Radiology.* 1983, 149: 231-239.
140. *Rubin GD., Dake MD., Napel SA:* Spiral CT of renal artery stenosis: Comparison of three dimentional rendering techniques. *Radiology,* 190:181-189, 1994.
141. *Rubin JM, Bude RO, Couson PL., et al.:* Power Doppler US a potentially useful alternative to mean-frequency-blood colour Doppler Sonography. *Radiology;* 190:855, 1994.
142. *Sacks BA; Calubran OV and Epstein HY:* Sepsis associated with transhepatic cholangiography. *J Hosp Infect* 1992; 20(1):43-50.
143. *Salvador Grande F, Saiz Monzon L, De la Torre P, et al.* Acalculous cholecystitis and intestinal cryptosporidiosis: Frequent association in HIV patients. *Revista Espanola de Enfermedades Digestivas* 1995; 87:593-596.

144. *Sanders RC*: Clinical Sonography: A practical guide, Little, Brown and Company, Boston/Toronto, 3rd edition, 1998.
145. *Sanders RC*: Doppler principles in clinical Sonography. A practical guide 2nd edition R. 25. Little, Brown and company, Toronto, London, 1991.
146. *Sato T., Katkura T., Suzuki K.*, review of system surface shape in helical CT. Acta-radiol;48:496-498, 1992.
147. *Schulte SJ, Baron RL, Teefy SA, et al*: CT of the extrahepatic ducts: wall thickness and contrast enhancement in normal and abnormal ducts, AJR 154:79-85, 1990.
148. *Schynder PA, Beachers OH, Straws DJ*: CT evaluation of echinococcal cyst of the liver. J. Comput. Assist. Tomog; 3:126-134, 1979.
149. *Scott G, Sanjay S, Peter RM*, Hepatobiliary and Pancreatic Radiol 1998; 6:561-673.
150. *Scott Gazelle, Sanjay S, Peter R, et al*. Hepatobiliary and pancreatic Radiology, New York, 1998; 24-36.
151. *Semelka RC, Brown ED, Ascher SM, et al*: Hepatic haemangiomas: A multi-institutional study of appearance on T2-weighted and serial gadolinium-enhanced gradient-echo MR images. Radiology 192:401, 1994.
152. *Semelka RC, Shoenut JP, Kroeker MA, et al*: Focal liver disease: Comparison of dynamic contrast-enhanced CT and T2-weighted fat-suppressed, FLASH, and dynamic gadolinium-enhanced MR imaging at 1.5T. Radiology 184:687, 1992.
153. *Shah KK; and Fink B*: Extrahepatic obstruction versus intrahepatic disorders. Differentiation with hepatobiliary scintigraphy and ultrasonography. J Clin Gastroenterol 1988; 10(2): 161-169.

154. *Shailendra Chopra, MD, MRCP, FRCR. Kedar N. Chintapalli, MD. Kalpana Ramakrishna, MD. Hyunchul Rhim, MD, PHD. Gerald D. Dodd III, MD, FRCR.* Radiology 2000; 214: 596-601.
155. *Shamsi K & De Schepper A (1994):* Medical imaging of focal liver lesions: A clinico-radiologic approach, 1st edn, Elsevier Science, Amsterdam, 1994.
156. *Shapiro HA:* Endoscopic diagnosis and treatment of biliary tract disease. Surg Clin N Am 1981; 61:843.
157. *Shapiro MJ, Luchtefeld WB, Kurzweil S, et al.* The increasing prevalence of acute acalculous cholecystitis in the critically ill. Am Surg 1994; 60:335-339.
158. *Shimamoto K., Sakuma S., Ishigaki T., et al.:* Hepatocellular carcinoma: evaluation with colour Doppler US and MR imaging radiology; 182:149-153, 1992.
159. *Shirai Z; Toriya H and Haeshiro K:* The usefulness of endoscopic retrograde cholangiopancreatography in infants and small children. Am J Gastroenterol 1993; 88:536-541.
160. *Siegelman ES, Outwater EK:* MR imaging techniques of the liver. Radiol Clin North Am 2:263, 1998.
161. *Siewert B, Muller MF, Foley M, et al:* Fast MR imaging of the liver. Qualitative comparison of techniques. Radiology 3:37, 1994.
162. *Silverman PM, Roberts S, Brown B:* Helical CT of the liver. AJR; 163:87-92, 1995.
163. *Silvis SE and Vennes JA:* Endoscopic retrograde sphincterotomy. In: Silvis SE (ed.): Gastrointestinal Endoscopy. New York, Tokyo, IGAKU-SHION, 1985, p 198.
164. *Simeone JF, Brink JA, Mueller PR, et al.* The sonographic diagnosis of acute gangrenous cholecystitis: Importance of the Murphy sign. AJR 1989; 152:289-290.

165. *Slot WB, Ooms HW, Van der Werf SD, et al.* Percutaneous gallbladder drainage in emphysematous cholecystitis. *Neth J Med* 1995; 46:86-89.
166. *Snell RS (1986):* Clinical anatomy for medical students. 3th edn, Little Brown Co, Boston, Toronto.
167. *Soyer P, Bluemk DA, Harban AH:* Primary malignant tumour of the liver. *Radiology*: 192:389-392, 1994.
168. *Soyer P, Bluemk DA, Zeiton G (1994):* Detection of liver metastases by spiral CT. *AJR*; 162:1327-1332, 1994.
169. *Soyer P, Bluemke DA & Rymer R:* MR imaging of the liver: Technique. *Meg reson Imaging Clin North Am* 5:205, 1997.
170. *Soyer P, Lacheheheb D, Levesque M.* CT arterial portography of the abdomen: Effect of injecting papaverine into the mesenteric artery on hepatic contrast enhancement. *Amer J Roentgenol* 1993; 160:1213-1215.
171. *Soyer P, Laissy JP, Sibert A, et al:* Hepatic metastases: Detection with multisection FLASHMR imaging during gadolinium chelate-enhanced arterial portography. *Radiology* 189:401, 1993.
172. *Stadalink RC and Matolo NM:* Radionuclide imaging of the biliary tree. *Surg Clin N Am* 1981; 61:827-841.
173. *Stadalnik RC and Hoffer PB:* Radiologic evaluation of biliary function. In: Way LW and Pellegrini CA (ed.): *Surgery of the gallbladder and bile ducts*. Philadelphia, WB Saunders, 1987, 203.
174. *Stephens DH, Mastsui O, Sample WF:* CT of the liver. *AJR*; 128:579-584, 1997.
175. *Stephens TD, Seely PR, Tatep.* *Anatomy & physiology at Louis*, Mosby college publishing, pp 554-556, 1989.
176. *Stephenson NJ. And Gibson RN,* Hepatic focal nodular hyperplasia: colour Doppler US can be diagnostic *Australas. Radiol*; 3a (3): 296-299, 1995.

177. *Stetter E*: Instrumentation. In Edelman RR, Hesselink JR & Zlatkin MB (eds.): Clinical Magnetic Resonance Imaging. Philadelphia, W.B. Saunders, 435, 1996.
178. *Steven D. Wolff, John Eng, and Robert S. Balben*: Magnetization transfer contrast method for improving contrast in gradient-recalled-echo images. Radiology 179:133-137, 1991.
179. *Stockbrugger RW, Olsson R, Jaup B, et al.* Forty-six patients with primary sclerosing cholangitis: Radiological bile duct changes in relationship to clinical course and concomitant inflammatory bowel disease. Hepatogastroenterology 1988; 35:289-294.
180. *Takayosuk K, Mariyama N, Muramatusu Y et al.* The diagnosis of small HCC. Efficacy of various imaging procedures in 100 patients. AM J Roentgenol 1990; 155:495-497.
181. *Talmont CA*: Renal ultrasonography and adrenal glands. In: Taylor KJW, Jacobson P Talmont CA and Winters R (ed.) Manual ultrasonography. 1st ed. Churchill Livingstone New York, Edinburgh, London, 1980.
182. *Tanttu JI & Sepponen RE*: imaging methods for whole body imaging applications of magnetization transfer contrast at 0.5T. Radiology 177:245, 1990.
183. *Tanttu JI, Kahn CE, JR Sepponen RE, Holland EA, Tierala E & Lipton MJ*: Magnetization transfer contrast of body tissues in vivo in MR imaging. Radiology 177:245, 1990.
184. *Taupitz M, Speidel A, Hamm B, et al*: T2-weighted breath-hold MR imaging of the liver at 1.5T: Results with three-dimensional steady-state free precession sequence in 87 patients. Radiology 194:439, 1995.
185. *Taylor GJ, Anagnostikos NP (1987)*: Principle of anatomy & physiology, 5th Ed. New York, Harpen & Row, pp: 332-345, 1987.

186. *Teplick SK; Haskin PH and Matsumoto T:* Interventional Radiology of the biliary system and pancreas. *Surg Clin N Am* 1984; 64:87-119.
187. *Tilvis RS, Aro J, Strandberg TF, et al.* Lipid composition of bile and gallbladder mucosa in patients with acalculous cholesterolosis. *Gastroentology* 1982; 82:607-615.
188. *Todani T, Watanabe Y, Fujii M, et al.* carcinoma arising from the bile duct in choledochal cyst and anomalous arrangement of the pancreatobiliary ductal union. *Biliary Tract Pancreas* 1985;6:525-535.
189. *Todua FI; Danilov MV and Karmazamovki G:* Computerized tomography in the diagnosis and treatment of mechanical jaundice. (Abstract) *Vestn Khir* 1988; 14:39.
190. *Trreir F, Becker CD, Triller JK:* Morphologic aspects of hepatic abscesses at CT. *Acta. Radiol*; 24:129-133, 1983.
191. *Tweedle D:* Endoscopic procedures in biliary and pancreatic disease. *Surgery* 1985; 1:484-489.
192. *Vazsquez JL, Thorsen MK, Dobbs WJ, et al.* Evaluation and treatment of intra-abdominal Bilomas. *AJR* 1985; 144:933-938.
193. *Verginia A, Scott H, John S;* National medical series for independent study, 2nd ed. John W. and Sons: 241-187, 1993.
194. *Vinegrad L. Mogle BP, Lernau OZ, et al.* Diffuse intrahepatic bile duct abscesses-diagnosed by percutaneous transhepatic cholangiography. *Gastrointest Radiol* 1980; 5:245-247.
195. *Vitti RA and Malmud LS:* The biliary tract: radionuclide studies. In: Grainger RG and Allison DJ (ed.) *Diagnostic Radiology*. 2nd ed. Churchill Livingstone, 1992, p1077-1110.
196. *Walter J and Israel T:* General pathology, seventh ed. Churchill living stone: 353-385, 1996.

197. *Wang G. and vannier MW*: longitudinal resolution in volumetric X-ray CT-analytical comparison between conventional and helical CT. Medical physic: 429-433, 1994.
198. *Warshauer D, Hamman SM, Koehler RE, Paulson EK*: No sarcoidosis of liver and spleen. Radiology. 195:757-762, 1995.
199. *Werlin SL*: Endoscopic retrograde cholangiopancreatography in children. Gastrointest Endosc Clin N Am 1994; 4:161-178.
200. *Williams P.I, Warwick R, Dyson M (1989)*: Gray's anatomy New York: Churchill living stone 1989: 1243-1249
201. *Wolf SD, Chesnick S, frank JA, Limko KO, Balaban RS*: Magnetization transfer contrast: MR imaging of the knee. Radiology 179:623-628, 1991.
202. *Wood ML, Runge VM, Henkelman M*: Overcoming motion in abdominal MR imaging. AJR AM J Roentgenol 150:513, 1988.
203. *Young Sw., Turner RJ. Castellino RA.*: Strategy for the conventional enhancement of malignant tumours using CT. Radiology; 137-140, 1980.
204. *Zagzebski, J.* Essentials of Ultrasound Physics St. Louis: CV Mosby, 1998.
205. *Zeman RK.* Choledocholithiasis and cholecystitis. In Gore RM, Levine MS, Laufer 1 (eds.): textbook of gasterointestinal radiology, Philadelphia: WB Saunders: 1994; pp 1636-1659.

- في السنوات الماضية حدثت ثورة في مجال تقنية التصوير التي أتاحت المجال لتنظيم الخيارات للطبيب الذي يسعى لتشخيص أمراض الكبد و القنوات المرارية . وبالأخص التقدم في التصوير بالموجات فوق الصوتية والأشعة المقطعية والرنين المغناطيسي والتصوير بالومضات التي أدت الى تحديد التشخيص والوصف الدقيق لأمراض الكبد والقنوات المرارية والذي يتم دون أي تدخل جراحي . وقد شارك وساهم أطباء الأشعة التشخيصية في مجال التقنيات التداخلية مثل المنظار الارتجاعي لتصوير القنوات الصفراوية وقناة البنكرياس وتصوير المجاري الصفراوية عن طريق الجلد مروراً بالكبد والتي تستطيع التصوير المباشر للقنوات المرارية .

— وتعتبر الموجات فوق الصوتية هي الاختيار الأول في تصوير الكبد والقنوات المرارية لأنها بسيطة وسريعة وغير مكلفة ، لذلك فهي تلعب دور رئيسي في اكتشاف المرضى المصابين بأمراض الكبد والقنوات المرارية .

— ويعين الدوبلر الملون الطبيب في تقييم الأوعية الدموية للكبد وأيضا لأورام الكبد ولذلك يساعد في تمييز هذه الأورام .

— ومن الاستخدامات الأساسية للموجات فوق الصوتية أنها تعين على أخذ عينات من الكبد والمناطق المصابة . ولكن تعبر حساسية الموجات فوق الصوتية في تحديد بعض أورام الكبد منخفضة حيث تصل إلى ٢٠٪ في حالات أورام الكبد الثانوية التي حجمها أقل من ١ سم و الآتية من أورام الجهاز الهضمي .

— وتعتبر الأشعة المقطعية من أوائل الاختبارات المتاحة لدراسة مريض الكبد والقنوات المرارية وقد استحدثت الآن الأشعة المقطعية لتصوير القنوات المرارية التي تعتبر طريقة غير تداخلية لتصوير القنوات المرارية .

— إن الأشعة المقطعية باستخدام الصبغة لها حساسية تصل إلى ٩١٪ في اكتشاف أورام الكبد الثانوية الأكثر من ١ سم .

— ومن مميزات الأشعة المقطعية أيضا هي تصوير ليس فقط الكبد ولكن المناطق الأخرى خارج الكبد ولذلك يساعد على اكتشاف الأورام الأولية الآتية من الجهاز الهضمي . ولكن من عيوب الأشعة المقطعية هي كمية الإشعاع والآثار الجانبية للصبغة ، ولكن بالرغم من ذلك فهي تعتبر من أفضل الطرق لتشخيص أمراض الكبد بالنظر إلى السرعة والوضوح .

— تصوير القنوات المرارية والبنكرياس بالرنين المغناطيسي يعتبر طريقة غير تداخلية نستطيع بها أن نرى التشريح الطبيعي والمرضى للقنوات المرارية لأنه يعطى تصوير القنوات المرارية من عدة اتجاهات .

— ولكن الأساس في تصوير القنوات المرارية هي الطريقة المباشرة باستخدام الصبغة عن طريق المنظار الارتجاعى لتصوير القنوات المرارية وقناة البنكرياس وأيضا تصوير القنوات المرارية عن طريق الجلد إلا أنها تعتبر مكلفة و تداخلية مما يؤدي إلى أعراض جانبية كثيرة .

— أما التصوير بالومضات فيتم باستخدام مركبات الأحماض الأمينية ثنائية الأسيبتون المعلق عليها (التكنيشيوم ٩٩) الذي يستخدم لدراسة إفراز العصارة الصفراوية من الكبد وحتى الأمعاء الدقيقة .

جامعة الأزهر .
كلية الطب .
قسم الأشعة التشخيصية .

تصوير الكبد والقنوات المرارية

مقال

رسالة توطئة للحصول على شهادة الماجستير في الأشعة التشخيصية

مقدمة من

ط/السعيد محمود محمد القطري
بكالوريوس الطب و الجراحة

المشرفون

أ.د/ مصطفى فاضل سنبل

أستاذ الأشعة التشخيصية
مستشفى الحسين الجامعي
جامعة الأزهر

د/ محمد فاروق عجاج
أستاذ مساعد أشعة التشخيصية
مستشفى الحسين الجامعي
جامعة الأزهر

د/ حاتم محمد حافظ شريف
أستاذ مساعد أشعة التشخيصية
مستشفى الحسين الجامعي
جامعة الأزهر